Research Article *Open Access*

Journal of Modern Classical Physics & Quantum Neuroscience

ISSN: 3068-4196

DOI: *doi.org/10.63721/25JPQN0110*

Device, Electronic, Technology for A M.E.M.S which Allow the Extraction of Electrical Power from Vacuum Energy, and Conform to Emmy Noether Theorem

Patrick Sangouard

Researcher -Teacher- in the Department Micro-electronics engineering ESIEE, France

Citation: Patrick Sangouard (2025) Device, Electronic, Technology for A M.E.M.S which Allow the Extraction of Electrical Power from Vacuum Energy, and Conform to Emmy Noether Theorem . J.of Mod Phy & Quant Neuroscience 1(3), 01-51. WMJ/JPQN-110

Abstract

This theoretical work corresponds to the hope of extracting, without contradicting EMMY NOETHER's theorem, an energy present throughout the universe: that of the spatial quantum vacuum.

This article shows that it should be theoretically possible to maintain a continuous periodic vibration of a piezoelectric structure, which generates electrical power peaks during a fraction of the vibration period.

Electronics without any power supply then transform these alternating current signals into a usable direct voltage.

To manufacture these different structures, we also present an original microtechnology for producing the regulation and transformation electronics, as well as that necessary for controlling the very weak interfaces between the Casimir electrodes and that of the return electrodes.

These vibrations are obtained by controlling automatically and at appropriate instants the action of the attractive Casimir force by a repulsive Coulomb force applied to return electrodes.

The Casimir force appearing between the two electrodes of a reflector deforms a piezoelectric bridge, inducing a displacement of the barycenter of the ionic electric charges of the bridge.

This internal piezoelectric field attracts opposing moving charges, from the mass, on either side of the piezoelectric bridge .They are used – after their homogenization - by a Coulomb force opposed and greater than the Casimir force.

During the homogenization of the electric charges between the face 1 and the return electrode, periodic current peaks appear during a fraction of the vibration time of the device.

These current peaks crossing an inductance, spontaneously induce voltage peaks at the terminals of this device, which are transformed into a usable DC voltage thanks to proposed electronics without a power supply.

Casimir and Coulomb forces, vibrations, current, or voltage peaks appear spontaneously and without external energy input. Everything is only a consequence of the existence of the Casimir force due to the quantum fluctuations of the vacuum.

This set does not seem to contradict Thermodynamics' law and Emily Noether's theorem.Casimir and Coulomb forces, vibrations, current, or voltage peaks appear spontaneously and without external energy input. Everything is only a consequence of the existence of the Casimir force due to the quantum fluctuations of the vacuum.
This set does not seem to contradict Thermodynamics' law and Emily Noether's theorem.

***Corresponding author:** Patrick Sangouard, Researcher -Teacher- in the Department Micro-electronics engineering ESIEE, France.

Submitted: 05.06.2025 **Accepted:** 11.06.2025 **Published:** 17.07.2025

Keywords: Nuclear Magnetic Resonance (NMR), Spin- Spin Interaction, Energy States in NMR, Coupling Constants in NMR, Clebsch-Gordan Coefficients

Introduction

We know that the quantum vacuum, the energy vacuum, the absolutely nothing, does not exist.
This statement has been proven multiple times and noted in particular by:
• Lamb's shift (1947) of atomic emission frequencies.
(https://quantummechanics.ucsd.edu/ph130a/130_notes/node476.html)

• By the force of Van der Waals which plays a very important physicochemical role and had an interpretation quantum 1930 [London] when two atoms are coupled to the same fluctuations in vacuum.
https://culturesciences.chimie.ens.fr/thematiques/chimie-du-vivant/les-forces-de-van-der-waals-et-le-gecko
• By Hawking's radiation theory, predicted in 1974 and observed on September 7, 2016. Article Observation of quantum Hawking radiation and its entanglement in an analogue black hole :
https://www.nature.com/articles/nphys3863

• By the experimental verification (1958) of the existence of a force equated by Casimir in 1948. This so-called Casimir force was measured for the first time in 1997 https://arxiv.org/abs/quant-ph/9907076
https://en.wikipedia.org/wiki/Casimir_effect

The term *vacuum energy* is sometimes used by some scientists claiming that it is possible to extract energy from the vacuum - that is, mechanical work, heat…. . But these different hypotheses arouse great scepticism among many scientific researchers because they call into question a principle demonstrated mathematically by the theorem of the mathematician Emmy Noether in 1915.
This important mathematical theorem, which is accepted in physics and has never been faulted until now, stipulate that "Any invariance (of space-time as well as the physical laws used) according to a group of symmetries (continuous and global) is necessarily associated with a physical quantity preserved in all circumstances" .
It involves the conservation of energy.
https://fr.wikiversity.org/wiki/Outils_math%C3%A9matiques_pour_la_physique_(PCSI)/Th%C3%A9or%C3%A8me_d%27Emmy_N%C5%93ther#

But the aforementioned effects, the interpretation of which is indisputable, imply a source of energy coming from a sort of "nothing" or more precisely from the quantum vacuum.

Thus, it is certain that this source of energy causing unmistakable physical manifestations exists.

In what follows, we adopt a reference frame based on the four-dimensional spacetime continuum, extended by the still poorly understood properties of the quantum vacuum. Within this framework, we aim to show that a MEMS (Micro-Electro-Mechanical System) device may exhibit behavior akin to "perpetual motion," not in violation of thermodynamic principles, but as a result of a continuous energy contribution from the vacuum itself.

Brief Presentation of Casimir's force

The vacuum energy is the zero-point energy of all fields (tensorial and scalar) in space. In quantum field theory, this vacuum energy defined as zero, is the ground state of fields. It has been observed and shown theoretically that this so-called zero-point energy, is non-zero for a simple quantum harmonic oscillator, since its minimum energy is equal to $E = h \nu /2$ with ν the natural frequency of the oscillator, and h the Planck's constant.

Originally [1], the Casimir effect is derived from statistical fluctuations in total vacuum energy and is the attraction (in general) between two plates separated by a vacuum. In this approach, this Casimir energy is the part E_{CA} of the vacuum energy which is a function of the z_S separation of the Casimir plates.

$$E_{CA} = S\left(\frac{\pi^2 \hbar c}{740\ z_4^3}\right) \quad \text{(Eq.1)}$$

Thus, the Casimir force associated, is

$$F_{CA} = \frac{d(E_{CA})}{dz} = S\left(\frac{\pi^2 h c}{240\ z_4^4}\right) \quad \text{(Eq.(2))}$$

With ħ the reduced Planck constant ħ, c the speed of light and S the surface of the reflector, z_s the distance between the plates

The presence of the reflective plates excludes wavelengths of virtual particles longer than z. They thus induce a pressure difference of the virtual particles generated by the vacuum between the internal and external space of the 2 plates. This difference results in a force that pushes the plates together.

Figure 1: Casimir effect

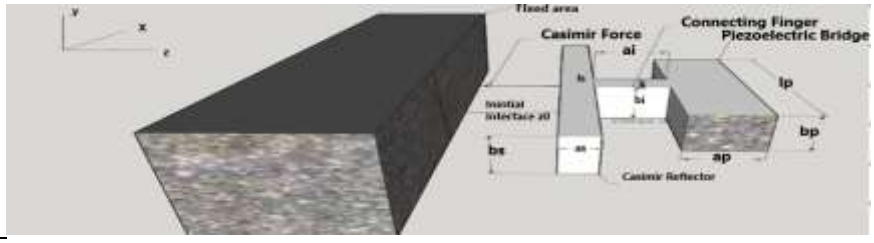

Figure 2: General representation of the structure

The famous physicist Evgueni Mikhaïlovitch Lifchits gave a general formula, which supplements that of Casimir because it considers the effect of temperature [3]. Indeed, when the temperature is no longer zero, the radiation of the black body must then be considered and the Casimir force at temperature T then becomes that of Lifchits [4]

$$F_{CA} = S\left(\frac{\pi^2 \hbar c}{240\, z_S^4} + \frac{\pi^2}{45}\frac{(k\,T)^4}{(\hbar\, c)^3} - \frac{kT\,\pi}{z_S^3}\exp\left(-\frac{\pi\hbar c}{k\,T\,z_S}\right)\right)$$ With k the Boltzmann constant and T the temperature.

We will use equation (2) to calculate and simulate the structure defined in the following diagram (Figure 2) because the effect of temperature is negligible and the formulation easier .

Description of the Principle Used to "Extract" Energy from the Vacuum

The term *vacuum energy* is sometimes used by some scientists claiming that it is possible to extract energy from the vacuum - that is, mechanical work, heat….. these different hypotheses arouse great scepticism among many scientific researchers because they call into question a principle demonstrated mathematically by the theorem of the mathematician Emmy Noether in 1915, which involves the conservation of energy .

This theorem is accepted in physics and has never been faulted until now.

In fact, the problem is less to extract energy from the vacuum than to extract it without spending more energy that we cannot hope to recover. Thus, in a cyclic system on the model of a piston engine going from a position n °1 to n ° 2 then from n ° 2 to n ° 1,the Casimir force in 1 /zs^4, therefore greater in position (2) than in (1), would then imply spending more energy to return to (1). Which would necessarily require an added energy.

This problem seems like that of perpetual movement. But, we know that in the case of a deformation perpendicular to the polarization of a piezoelectric layer, the fixed charges Q_F induced by the deformation of this piezoelectric layer are proportional to F_{CA} and are therefore in $1/z_s^4$. $Q_F = (d_{31}.F_{CA}.l_P)/a_P$ (Eq.(3)), [5] [6], with d_{31} = piezoelectric coefficient (CN^{-1}), l_p, a_p respectively length and thickness (m) of the piezoelectric bridge (figure 5). Q_F does not depend on the common width bp = bs = bi of the structures. This point is important and facilitates the technological realization of these structures since it limits the difficulties of a deep and straight engraving of the different structures.
These fixed electric charges on the two metallized faces of the piezoelectric bridge have opposite signs and attract mobile charges of opposite signs from the mass (figure 5). Thus, when it is effective, the Coulomb return force F_{CO} is in $1/z_s^{10}$ .with z_s = distance, time dependent, between Casimir

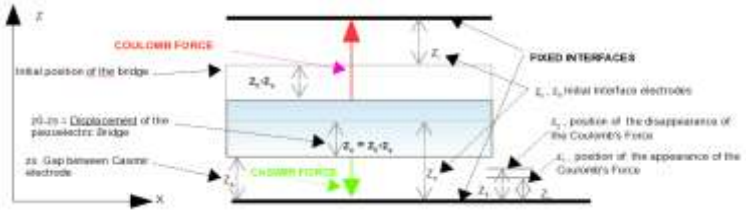

Figure 3: Nomenclature and Notations of the positions of electrodes for the device

The initials positions are z_r for the Coulomb's and z_0 for the Casimir intervals. Considering that the Coulomb force is null when the piezoelectric bridge has no deformation, the expression of the attractive Coulomb force of direction opposite to that of Casimir is with the same electric charge on both electrodes.

1. $$F_{CO} = \frac{Q_F^2}{4\pi\varepsilon_0\varepsilon_r}\left(\frac{1}{z_r + z_0 - z_s} - \frac{1}{z_r}\right)^2 = \left[\left(S_S \frac{\pi^2 \hbar c}{240}\right)\left(\frac{1}{z_s^4} - \frac{1}{z_0^4}\right)\frac{d_{31} l_p}{a_p}\right]^2 \left(\frac{1}{4\pi\varepsilon_0\varepsilon_r}\right)\left(\frac{1}{z_r + z_0 - z_s}\right)^2 \text{(Eq.(4))}$$

We note that $F_{CO} = 0$ when the bridge has no deflection ($zs = z_0$), so no electrical charges.

This Coulomb Force in $1/z_s^{10}$ can therefore become greater than that of Casimir which is in $1/z_s^4$.

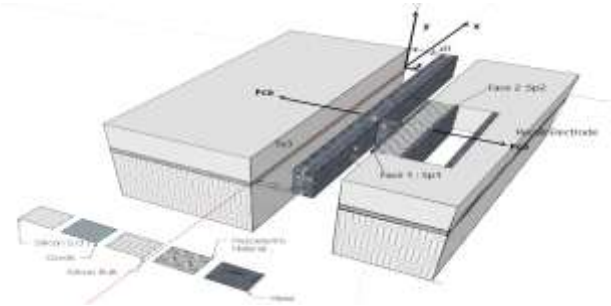

Figure 4: Different View of the device without

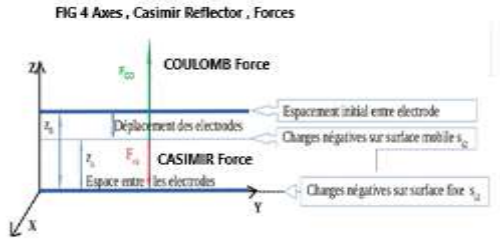

Figure 5: Axes, Forces, Casimir's Electrodes ectronics

As a preamble, we suppose that the events which induce the attractive force of Casimir are exerted in a universal, isotropic, perpetual, and immediate way, if the conditions of separation between reflecting Casimir plates are suitable.

Let therefore be a Casimir reflector device consisting of:

1 / a metallized and mobile parallelepiped electrode, of surface $S_{s1} = S_{s2}$ on its 2 lateral faces
2 / of a fixed metallized surface S_{s3} separated by a distance z_0 (figure 3, 4,5 and 6)

This parallelepipedic metallic Casimir reflector is rigidly linked by a metallic finger to a piezoelectric bridge embedded in its two ends. A displacement of the mobile Casimir electrode induces a deformation of the piezoelectric bridge and thus the appearance of ionic electric charges (Figure 4, 6).
Of course, it is also necessary that the movement of this moving plate S_{s2} of the Casimir reflector can be stopped at a chosen and predefined value before the collapse of the surfaces of the Casimir reflector occurs otherwise, no energy extraction is possible. Moreover, it is necessary that the mobile system returns to its initial position (or slightly exceeds it),

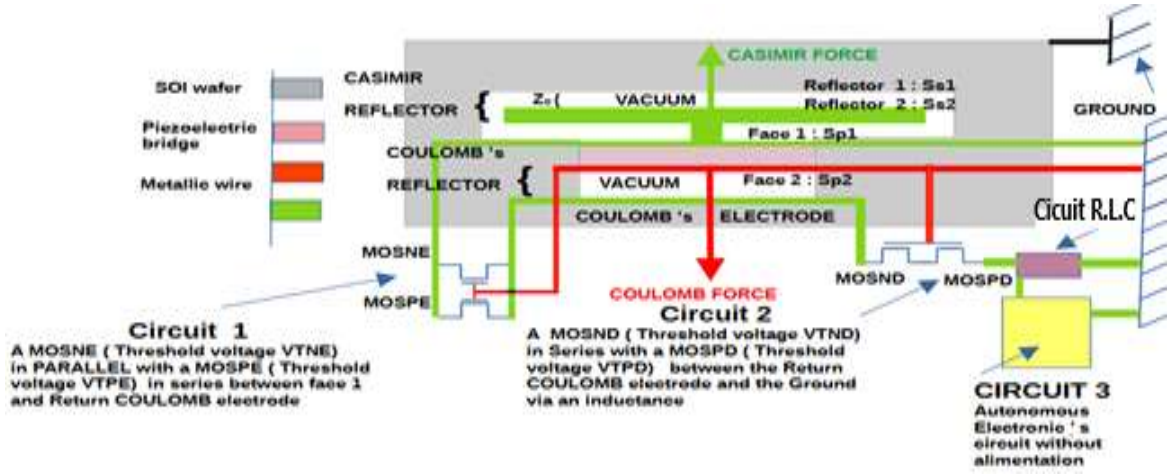

Figures 6: general configuration of the device: MOS grid connections (Face 2 of the piezoelectric bridge: red), Source connections (Face 1 of the piezoelectric bridge: green

We observe, in figures (6), that the surfaces (green and red) $Sp_1 = Sp_2 = b_p * l_p$, of the piezoelectric bridge, are connected :

1 / For the face n° 1 Sp_1, at the mobile electrode of the Casimir reflector through the metal finger (green). Thus, the metallic surfaces S_{p1} and the metallic parallelepiped $Ss_1 = S_{s2}$ are equipotential.

2 / For the face n ° 2 Sp_2, at the grids of the switch's circuits n°1 and n°2.

The deformations caused by the attractive force of Casimir, produce ionic electric charges for example $Q_{fn1} = - Q_{fp2}$, on the faces S_{p1} and S_{p2} of the metallic piezoelectric bridge. These fixed charges attract from the mass respectively mobiles electrics charges Q_{mp1} and Q_{mn2} on the metallics electrodes.
The different threshold voltages of the different transistors Thin Film Transistor Metal Oxide Semiconductor are:

The threshold voltage of the enriched transistors TFT MOSNE, MOSPE and depletion transistors TFT MOSND, MOSPD are technologically positioned as . $0 < VT_{PD} < VT_{NE}$ and $VT_{PE} < VT_{ND} < 0$

The figure 7 resume this configuration

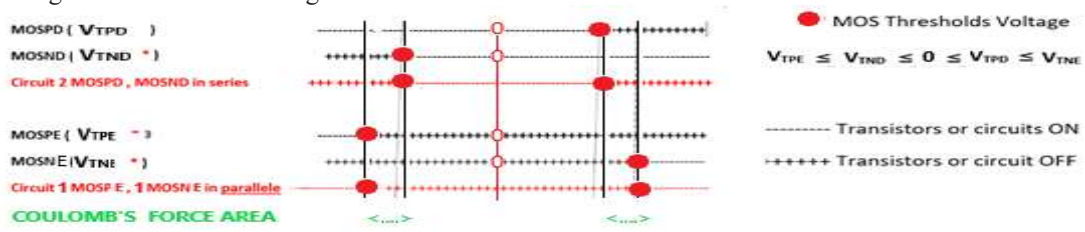

Figure 7: distribution of the threshold voltages of enriched and depleted N and P MOS switches.

The sign of the mobile's charges on the surfaces Sp1 and Sp2 depending on the polarization obtained during the realization of the piezoelectric material of this bridge, the voltage V_{GRIDS} can be positive or negative. So, the sign of the voltage appearing on the grids of the MOS depending on the sign of the polarization of piezoelectric material

1/ When $0 < V_{GRIDS} < VT_{ND} < VT_{NE}$, or $VT_{PE} < VT_{ND} < V_{GRIDS} < 0$ then switch 1 is OFF, and switch 2 is ON, so the Coulomb return electrode is grounded and isolated from piezoelectric bridge . There is no electric charges on the return electrode and no Coulomb's force Fco appears , the only force that deform the piezoelectric bridge is the Casimir force

2/ When $0 < VT_{ND} < V_{GRIDS} < VT_{NE}$, or $VT_{PE} < V_{GRIDS} < VT_{ND} < 0$, then switch 1 is OFF, and switch 2 is OFF, so the Coulomb return electrode is isolated from the mass and from piezoelectric bridge . There is no electric charges on the return electrode because the switch 1 is OFF. No electric charge move from the face 1 and no force F_{CO} appears , the only force that deform the piezoelectric bridge is the Casimir force .

3/ When $0 < VT_{ND} < VT_{NE} \leq V_{GRIDS}$, or $V_{GRIDS} \leq VT_{PE} < VT_{ND} < 0$, then switch 1 is ON, and switch 2 is OFF. Thus, the mobile electric charges pass through switch 1 and homogenize between the return Coulomb electrode. (See figure 6) .
Let $S_{p1} = S_{p2} = l_p * b_p$ be the surface area of the faces of the piezoelectric bridge, $S_r = S_{p2} = S_{p1}$ be the surface of the return electrode facing the metallized face S_{p2} of the piezoelectric bridge.

The mobiles charges for example negative Q_{mn1} , initially distributed on the metallic surfaces S_{p1} are distributed on the surfaces $S_{p1} + S_r$, so with a charge $Q_{mn} = Q_{mn1} /2 = F_{CA}\, d_{31}\, l_p /2\, a_p$ on only the return Coulomb's .
So, between the faces S_{p2} and S_r, with electric charges of opposite sign, appears an attractive force of Coulomb F_{CO} , parallel and opposite to the attractive force of Casimir.

$$F_{CO} = \left(\left(S_S \frac{\pi^2 \hbar c}{240}\right) \frac{d_{31}\, l_p}{a_p} \left(\frac{1}{z_s^4} - \frac{1}{z_0^4}\right)\right)^2 \left(\frac{1}{8\pi \varepsilon_0 \varepsilon_r}\right)\left(\frac{1}{z_r + z_0 - z_s}\right)^2 \quad \textit{Because } S_{p2} = S_r$$

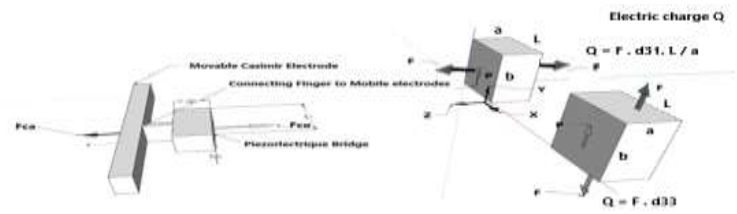

Figure 8: Polarization and applied force and load on a piezoelectric block

If, the threshold voltage of the MOSNE is adjusted so that the Coulomb force is triggered only when $F_{CO} = p\, F_{CA}$ with a chosen proportionality factor p, then the total repulsion force F_T variable in time and applied to the piezoelectric bridge becomes (figure 7, 8) $\overrightarrow{F_T} = \overrightarrow{F_{CA}} - \overrightarrow{F_{CO}} = (1-p)\overrightarrow{F_{TCA}}$. Becoming repulsive, this force F_T (dependent on time) induces a deformation of the piezoelectric bridge in the other opposite direction, and the piezoelectric bridge returns or slightly exceeds (because of inertia) its neutral position therefore towards its position without any electrical charge.

Calculation of the Electric Charges on the Coulomb's Electrode

When $0 < V_{GRIDS} < VT_{ND} < VT_{NE}$, or $VT_{PE} < VT_{ND} < V_{GRIDS} < 0$ then switch 1 is OFF, and switch 2 is ON, so the Coulomb electrode is grounded and isolated from piezoelectric bridge . The electric charges on the Coulomb electrode are zero . When $0 < VTND < VTNE \leq VGRIDS$, or $VGRIDS \leq VTPE < VTND < 0$, switch 1 is activated (ON), and switch 2 is deactivated (OFF). Consequently, Coulomb's electrode becomes isolated from the ground, allowing mobile electrical charges to pass through switch 1 and homogenize between the return Coulomb's electrode.

Following as a first approximation, a law of distribution of the charges on a short-circuited capacitor, the temporal variation of the charges on the Coulomb's electrode is given by the well-known exponential form of discharge of a capacitor according with the formula:

$$Q_{mn} = Q_{mn1}\left[1 - Exp\left(-\frac{t}{R_m C_S}\right)\right] \quad \text{(Eq. (5))}$$

This variation in mobile charges stops when the electrical charges Q_{mn} are uniformly distributed over the two electrodes ,face n°1 of the piezoelectric bridge and the Coulomb's electrode with the area S_{p1} and Sr and are equal to Q_{mn1} / 2 on the two electrodes. This equilibrium's time is $t_e = R_m C_s \ln(2)$ (Eq. (5)), with R_m the ohmic resistance of the metal track, C_s the capacitance formed by the electrodes S_{P2} and Sr.

• $R_m = \rho_m \cdot l_m / S_m$, with ρ_m the resistivity of the self between electrode, l_m its total length, S_m its section.
• $Cs = \varepsilon_0 . \varepsilon_{0m} l_p . b_p / z_r$, the inter-electrode return capacitance, with ε_0 the permittivity of vacuum, ε_{0m} the relative permittivity of the metal oxide, l_p and b_p the geometries of the return electrode. An estimation of the duration of the homogenization of the electric charges is $t_e \cong 10^{-9}$ s . We obtain at t_e the coulomb's electric charges $Q_{mn} = F_{CA}\, d_{31}\, l_p /(2\, a_p)$

4/ as long as $0 < VT_{ND} < V_{GRIDS} \leq VT_{NE}$, or $VT_{PE} \leq V_{GRIDS} < VT_{ND} < 0$ the Coulomb's force F_{CO} continue to exist. The deformation of the bridge and the voltage on the MOS grids fall down, so when:

5/ $0 < V_{GRIDS} \leq VT_{ND} < VT_{NE}$, or $VT_{PE} < VT_{ND} \leq V_{GRIDS} < 0$, the circuit n°2 commute ON. The return Coulomb's electrode is another time connected to the mass. So, Coulomb's force F_{CO} disappears. The bridge uses its kinetic energy through inertia to continue its ascent and slightly surpass its neutral position. At that point, Casimir's force becomes the predominant factor.

The force of Casimir F_{CA}, still present, again attracts the metallic surface S_{S2} against S_{S3} and the events described above are repeated. The consequence is that the structure made up of the piezoelectric bridge, the connecting finger, the metal block forming the mobile Casimir electrode starts to vibrate, with a frequency depending:

1/ Of the Casimir restoring force, and of the Coulomb return electrode Force therefore so with:
a/ the starting z_0 and z_r separation interface
b/ geometric dimensions of the different electrodes,
2/ Properties of the piezoelectric bridge,
3/ The choice of threshold voltages of the different MOS transistors
4/ The choice of conductive metal.

As we will see, this frequency is lower than the first resonant frequency of the mobile structure if the initial interface z_0 is not weak enough (< 150 A°) (see chapter V and X).
An AC voltage peak U_{IN} is therefore automatically recovered at the terminals of the solenoid L_{IN}. This AC voltage peak can then be rectified to a DC voltage of a few volts, by suitable electronics operating without power supply (see chapter VI).
In conclusions it seems that all the electro-physical phenomena leading to a vibration of the structure and so to the production of an electrical power peaks are only the consequence of a first phenomenon which is at the Force of Casimir controlled by a Coulomb's force.

Calculation of the Behaviour of the Structure

Let us calculate the evolution in time of the force of Casimir which is applied between the two electrodes separated by an initial distance z_0. We use the theorem of angular momentum to this vibrating structure.

$$\overrightarrow{\sigma^{S}_{Ax,y,z}(\ Structure)} = \overline{I^{S}_{A\,x,y,z}}\ \overrightarrow{\theta^{S}_{A\,x,y,z}} \quad \text{(Eq. (8))}$$

With σ^{S}_{Axyz} the angular momentum vector of the structure, I^{S}_{Axyz} the inertia matrix of the structure with respect to the reference (A, x,y,z) and θ^{S}_{Axyz} the rotation vector of the piezoelectric bridge with respect to the axis Ay with α the low angle of rotation along the y axis of the piezoelectric bridge

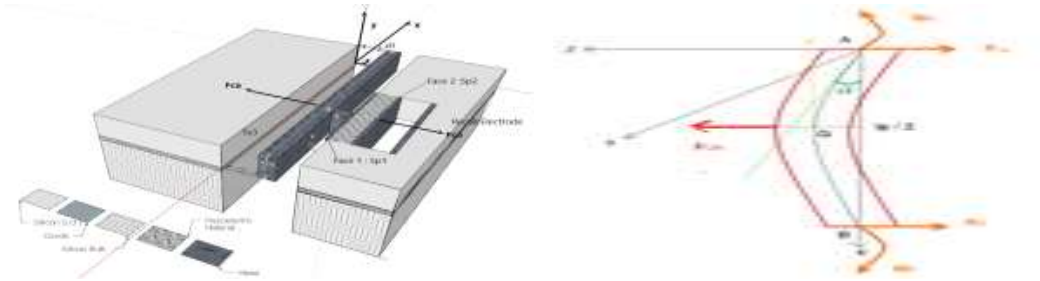

Figure 9: Piezoelectric bridge Cutting Reactions and Bending Moment, Deflection

We have $\overrightarrow{\theta^{S}_{A}} = \begin{pmatrix} 0 \\ d\alpha/dt \\ 0 \end{pmatrix}$ with $d\alpha/dt \approx \frac{2}{l_p}\frac{dz}{dt}$ because $\sin(\alpha) = \sin\left(\frac{2z_s}{l_p}\right) \approx \frac{2z_s}{l_p}$ because $z << l_p$

Let (Gp, x, y, z), (Gi, x, y, z), (Gs, x, y, z) be the barycentric points respectively of the piezoelectric bridge, of the metal connecting finger and of the metal block constituting the sole mobile of the Casimir reflector. We have (fig 5):

$$\overrightarrow{AG_{P,x,y,z}} = \frac{1}{2}\begin{pmatrix} l_p \\ b_p \\ a_p \end{pmatrix} \quad \overrightarrow{AG_{I,x,y,z}} = \frac{1}{2}\begin{pmatrix} l_p + l_i \\ b_p + b_i \\ a_p + a_i \end{pmatrix} \quad \overrightarrow{AG_{S,x,y,z}} = \frac{1}{2}\begin{pmatrix} l_p + l_i + l_S \\ b_p + b_i + b_S \\ a_p + a_i + a_S \end{pmatrix}$$

The inertia matrix of the bridge, in the frame of reference (Gp, x, y, z) is:

$$I^{P}_{GP} = \frac{m_p}{12}\begin{pmatrix} a^2_p + b^2_p & 0 & 0 \\ & l^2_p + b^2_p & 0 \\ 0 & 0 & a^2_p + l^2_p \end{pmatrix}$$

Taking Huygens' theorem into account, this inertia matrix becomes

$$I^{P}_{A,x,y,z} = m_p\begin{pmatrix} \frac{a^2_p + b^2_p}{3} & -\frac{l_p b_p}{4} & -\frac{l_p a_p}{4} \\ -\frac{l_p b_p}{4} & \frac{a^2_p + l^2_p}{3} & -\frac{a_p b_p}{4} \\ -\frac{l_p b a}{4} & -\frac{a_p b_p}{4} & \frac{l^2_p + b^2_p}{3} \end{pmatrix} \text{(Eq (9)):}$$

The inertia matrix of the finger is, in the frame of reference (Gi, x, y, z) is:

$$I^{I}_{GI} = \frac{m_i}{12}\begin{pmatrix} a^2_i + b^2_i & 0 & 0 \\ 0 & a^2_i + l^2_i & 0 \\ 0 & 0 & l^2_i + b^2_i \end{pmatrix}$$

Taking Huygens' theorem into account, this inertia matrix becomes:

$$I^{I}_{A,x,y,z} = \frac{m_i}{12}\begin{pmatrix} a_i^2 + b_i^2 & 0 & 0 \\ 0 & a_i^2 + l_i^2 & 0 \\ 0 & 0 & l_i^2 + b_i^2 \end{pmatrix} + m_i \begin{pmatrix} \frac{(b_p+b_i)^2+(a_p+a_i)^2}{4} & -\frac{(b_p+b_i)(l_p+l_i)}{4} & -\frac{(a_p+a_i)(l_p+l_i)}{4} \\ -\frac{(b_p+b_i)(l_p+l_i)}{4} & \frac{(l_p+l_i)^2+(a_p+a_i)^2}{4} & -\frac{(b_p+b_i)(a_p+a_i)}{4} \\ -\frac{(a_p+a_i)(l_p+l_i)}{4} & -\frac{(b_p+b_i)(a_p+a_i)}{4} & \frac{(b_p+b_i)^2+(l_p+l_i)^2}{4} \end{pmatrix}$$ (Eq. (10))

The inertia matrix of the reflector in the frame of reference (G_S, x,y,z) is

$$I^{C}_{GS} = \frac{m_s}{12}\begin{pmatrix} a_s^2 + b_s^2 & 0 & 0 \\ 0 & a_s^2 + l_s^2 & 0 \\ 0 & 0 & l_s^2 + b_S^2 \end{pmatrix}$$

Taking Huygens' theorem into account, this inertia matrix becomes:

$$I^{C}_{A,x,y,z} = \frac{m_s}{12}\begin{pmatrix} a_s^2 + b_s^2 & 0 & 0 \\ 0 & a_s^2 + l_s^2 & 0 \\ 0 & 0 & l_s^2 + b_S^2 \end{pmatrix} + m_s \begin{pmatrix} \frac{(b_p+b_i+b_s)^2+(a_p+a_i+a_s)^2}{4} & -\frac{(l_p+l_i+l_s)(b_p+b_i+b_s)}{4} & -\frac{(l_p+l_i+l_s)(a_p+a_i+as)}{4} \\ -\frac{(l_p+l_i+l_s)(b_p+b_i+b_s)}{4} & \frac{(l_p+l_i+l_s)^2+(a_p+a_i+a_s)^2}{4} & -\frac{(b_p+b_i+b_s)(a_p+a_i+as)}{4} \\ -\frac{(l_p+l_i+l_s)(a_p+a_i+as)}{4} & -\frac{(b_p+b_i+b_s)(a_p+a_i+as)}{4} & \frac{(b_p+b_i+b_s)^2+(l_p+l_i+l_s)^2}{4} \end{pmatrix}$$ (Eq. (11)) :

The total inertia of the structure becomes in the reference (A, x, y, z), $I^{s}_{A,x,y\,z} = I^{P}_{A,x,\,y,\,z} + I^{I}_{A,\,x,\,y,\,z} + I^{c}_{A,\,x,\,y,\,z}$ with A at the edge of the recessed piezoelectric bridge .The angular momentum theorem applied to the whole structure gives :

$$\frac{\overrightarrow{d(\sigma^{S}_{A,x,y,z})}}{dt} = \overline{I^{S}_{A,x,y,z}}\ \frac{\overrightarrow{d\theta^{s}_{A}}}{dt} \Rightarrow \overline{I^{S}_{A,x,y,z}}\ \frac{2}{l_P}\begin{pmatrix} 0 \\ \frac{d^2z}{dt^2} \\ 0 \end{pmatrix} = \sum_{A} \overrightarrow{Moments\ of\ the\ structure} =$$

(Eq. (12))

$$= \overrightarrow{M_A} + \overrightarrow{M_B} + \overrightarrow{F_{CA}} \wedge \begin{pmatrix} l_P/2 \\ 0 \\ 0 \end{pmatrix} with\ \overrightarrow{F_{CA}} = \begin{pmatrix} 0 \\ 0 \\ F_{CA} \end{pmatrix}$$

The structure rotates around the Ay axis. We know (see X), that the moments are: $M_{AY} = M_{BY} = -F_{CA}\ lp\ /8$, therefore: Σ Moments on the structure relative to the axe Ay = 1/4*lp * F_{CA} .

Any calculation done we obtain: $\overline{I^{s}_{y}}\ \frac{2}{l_P}\ \frac{d^2z}{dt^2} = \frac{l_P}{4} F_{CA} = \frac{l_P}{4} S_S \frac{\pi^2 \hbar c}{240\ z^4}$ (Eq. (13))

with I^{S}_{y} the inertia of the structure relatively to the axe Ay.

$$I^{S}_{Y} = \rho_P a_P b_P l_P \left(\frac{\left(l_P^2 + a_P^2\right)}{12} + \frac{\left(l_P^2 + a_P^2\right)}{4}\right) + \rho_i a_i b_i l_i \left(\frac{\left(l_i^2 + a_i^2\right)}{12} + \frac{\left(l_P + l_i\right)^2 + \left(a_P + a_i\right)^2}{4}\right) + \rho_s a_s b_s l_s \left(\frac{\left(l_s^2 + a_s^2\right)}{12} + \frac{\left(l_P + l_i + l_s\right)^2 + \left(a_P + a_i + a_S\right)^2}{4}\right)$$ (Eq. (14)

With ρ_P , ρ_i , ρ_S , respectively the densities of the piezoelectric bridge , the intermediate finger and the mobile electrode of the Casimir reflector

By equation 8, we obtain the differential equation which makes it possible to calculate the interval between the two electrodes of the Casimir reflector as a function of time during the "descent" phase when the Coulomb forces are not present

$$\frac{d^2z}{dt^2} = \frac{l_P^2}{8\,I_Y^S}\,S_S\,\frac{\pi^2\hbar c}{240}\,\frac{1}{z^4} = \frac{B}{z^4} \quad with\ B = \frac{l_P^2}{8\,I_Y^S}\,S_S\,\frac{\pi^2\hbar c}{240}$$ (Eq. (15))

This differential equation (15) unfortunately *does not have a literal solution and we programmed it on MATLAB* to calculate the duration of this "descent" of free Casimir electrode. This duration depending on the desired value of the coefficient of proportionality p. (See figures chapter IV) .

Just at the moment of closing circuit n°1, we have $F_{CO} = -\,p\,F_{CA}$ with p a coefficient of proportionality ≥ 2 defined by the threshold voltages of the MOS interrupters. The total force F_T exerted in the middle of the piezoelectric bridge just at the start of the charge transfer becomes: $F_T = F_{CA}-F_{CO} = F_{CA}\,(1-p)$

The "descent" time of the free Casimir electrode will therefore stop when $F_{CO} = -\,p\,F_{CA}$. However, we know that:

1 / The Casimir force is variable in time and its equation is (Eq. (1)): $F_{CA} = \frac{d(E_{CA})}{dz} = S\left(\frac{\pi^2\,\hbar\,c}{240\,z_4^4}\right)$

2 / The mobile charges transiting from side 1 to the Coulomb electrode through circuit 1 variable in time (Eq. (3)) are:

$$Q_{mn} \approx \frac{Q_{mn1}}{2} = \frac{d_{31}\,F_{CA}\,l_P}{2\,a_P}$$

3 / The Coulomb force (4), variable over time, acting in opposition to the Casimir force (Eq. (4)):

$$F_{CO} = \left(\frac{d_{31}\,l_P}{a_P}\,l_S\,b_S\,\frac{\pi^2\hbar c}{240}\left(\frac{1}{z_s^4} - \frac{1}{z_0^4}\right)\right)^2\left(\frac{1}{8\pi\varepsilon_0\varepsilon_r}\right)\left(\frac{1}{z_r+z_0-z_s}\right)^2 =$$

$$p\,F_{CA} = p\,l_s b_s\,\frac{\pi^2\hbar c}{240}\,\frac{1}{z_s^4}$$

The "descent" of the free Casimir electrode stops when the inter electrode interface z_s is such that:

$$z_S^4\left(\left(\frac{1}{z_R+z_0-z_S}\right)^2\left(\frac{1}{z_s^4} - \frac{1}{z_0^4}\right)^2\right) = \frac{1920\,p\,\varepsilon_0\,\varepsilon_r}{\pi\hbar c\,S_S}\left(\frac{a_P}{d_{31}\,l_P}\right)^2$$ (Eq. (16) See (Fig 68)

This programmable equation gives the time t_d of the "descent" of the structure submitted to the Casimir force and:

a/ depend on the coefficient of proportionality p,

$$F_T = (1-p)\,F_{CA} \Rightarrow (1-p)\,S_S\,\frac{\pi^2\hbar c}{240\,z_{sm}^4} < 0 \quad if\ p > 1$$

b/ is calculable and will stop when the inter-electrode interface z_s has a value z_e satisfying equation (16).
At this instant the total force is therefore:

$$F_T = (1-p)\,F_{CA} \Rightarrow (1-p)\,S_S\,\frac{\pi^2\hbar c}{240\,z_{sm}^4} < 0 \quad if\ p > 1$$

During all the phase where $0 < VT_{ND} < V_{GRIDS} \le VT_{NE}$, or $VT_{PE} \le V_{GRIDS} < VT_{ND} < 0$. The total force, variable over time and exerted at the center of the piezoelectric bridge, becomes:

$$F_T = F_{CA} - F_{CO} = S_S\,\frac{\pi^2\hbar c}{240\,z_S^4} - \frac{1}{2}\left[\frac{S_S\,\pi^2\hbar c}{240}\left(\frac{1}{z_s^4} - \frac{1}{z_0^4}\right)\left(\frac{d_{31}l_P}{a_P}\right)\right]^2\left(\frac{1}{4\pi\varepsilon_0\,\varepsilon_r}\right)\left(\frac{1}{z_r+z_0-z_s}\right)^2$$ Eq. (17)

The piezoelectric bridge subjected to this force then rises towards its neutral position. The Casimir inter electrode interval increases causing the Casimir force to decrease. As the deformations decrease, so does the electrical charge on the

piezoelectric faces, resulting in a decrease in the Coulomb force.

The F_T force therefore rapidly approaches the starting F_{CA} force, during the "ascent "of the Casimir electrodes.

Let us calculate an approximation of the duration of this "rise" of the mobile electrode of the Casimir reflector triggered when $F_{CO} = p * F_{CA}$. It is a maximisation of this time because in fact the Coulomb force F_{CO} stop when the circuit 2 close to ground another time. As we don't known the threshold voltage VT_{ND} or VT_{PD}, we made the calculation as they are null .

In these conditions, to know the time taken by the structure to "go back" to its neutral position, we must solve the following differential equation:

$$\frac{d^2z}{dt^2} = \frac{l_P^2}{8 I_S^Y}\left(F_{CA} - F_{CO}\right) = \frac{l_P^2}{8 I_S^Y}\left\{\left(l_S b_S \frac{\pi^2 \hbar c}{240 z_S^4}\right) - \frac{1}{2}\left[l_S b_S \frac{\pi^2 \hbar c}{240}\left(\frac{d_{31} l_P}{a_P}\right)\left(\frac{1}{z_s^4} - \frac{1}{z_0^4}\right)\right]^2\right\}\left(\frac{1}{4\pi\varepsilon_0\varepsilon_r}\right)\left(\frac{1}{z_r + z_0 - z_S}\right)^2$$

By posing $A_1 = \left\{\left(l_S b_S \frac{\pi^2 \hbar c}{240}\right)\right\}$ the differential equation (18) concerning the "ascent" of the bridge is written

$$\frac{d^2z}{dt^2} = \frac{l_P^2}{8 I_S^Y}\left(F_{CA} - F_{CO}\right) = \frac{l_P^2}{8 I_S^Y} A_1 \left\{\frac{1}{z_S^4} - A_1\left(\frac{d_{31} l_P}{a_P}\right)^2\right\}\left(\frac{1}{8\pi\varepsilon_0\varepsilon_r}\right)\left(\frac{1}{z_s^4} - \frac{1}{z_0^4}\right)^2\left(\frac{1}{z_r + z_0 - z_S}\right)^2 \quad \text{(Eq.(18))}$$

This differential equation (18) has no analytical solution and can only be solved numerically. We programmed it on MATLAB. The properties and dimensions of the different materials used in this simulation are as follows (Table 1).

Table 1: Table of Characteristics used for MATLAB and ANSYS Simulations

PHYSICAL PROPERTY	PZT	AlN	LiNbO3	PMN-PT :
Young Modulus (kg*m*s^{-2}) / m²)	Ep=8.9*10^{10}	Ep=32*10^{10}	Ep=2.45*10^{9}	Ep=150*10^9
Volumic mass (kg m^{-3})	dp =7600	dp=3255	dp=4700	dp=7920
Piezoelectric coefficient d31 of the beam (C / (kg* m* s^{-2})	d31=200*10^{-12}	d31=2.400*10^{-12}	d31=6*10^{-12}	d31= 1450*10^{-12}
Length piezoelectric beam: lp (m)	50 10^{-6}	50 10^{-6}	50 10^{-6}	50 10^{-6}
Width piezoelectric beam: bp (m)	150 10^{-6}	150 10^{-6}	150 10^{-6}	150 10^{-6}
Thickness piezoelectric: ap (m)	10 10^{-6}	10 10^{-6}	10 10^{-6}	10 10^{-6}
Connecting finger length: li (m)	10 10^{-6}	10 10^{-6}	10 10^{-6}	10 10^{-6}
Width finger connection: bi (m)	150 10^{-6}	150 10^{-6}	150 10^{-6}	150 10^{-6}
Thickness finger connection: ai (m)	10 10^{-6}	10 10^{-6}	10 10^{-6}	10 10^{-6}
Mobile Casimir electrode block length: ls (m)	500 10^{-6}	500 10^{-6}	500 10^{-6}	500 10^{-6}
Mobile Casimir electrode block width: bs (m)	150 10^{-6}	150 10^{-6}	150 10^{-6}	150 10^{-6}
Casimir mobile electrode block thickness: as (m)	10 10^{-6}	10 10^{-6}	10 10^{-6}	10 10^{-6}

In these MATLAB simulations we considered that the metal of the electrodes and metal block was oxidized over a thickness allowing to have an interface between Casimir electrodes of 200 A ° which modifies the mass and the inertia of the vibrating structure (See chapter 5).

It turns out that the choice of aluminium as the metal deposited on these electrodes is preferable given:

1 / The ratio between the thickness of the metal oxide obtained and of the metal attacked by the thermal oxidation (see chapter V)
2 / Its low density increases and optimise the vibration frequency of the structure by minimising the inertia of the Casimir reflector and the parallelepiped block that transfers the Casimir force.

The mass $M_{structure}$ of the vibrating structure is then: $M_{STRUCTURE} = d_{pm}(a_s b_s l_s + a_i b_i l_i) + 2 d_{om} z_{of} (a_{s0} b_{so} + b_{so} l_{so} + a_{so} l_{ost}) + d_p (a_p b_p l_p)$

With d_{pm} the density of the metal, a_s, b_s, l_s the geometries of the final metal part of the Casimir electrode sole, d_{om} the density of the metal oxide, a_{so}, b_{so}, l_{so} the geometries of the oxidized parts around the 6 faces of the metal block, d_p the density of the piezoelectric parallelepiped (see figure 10):

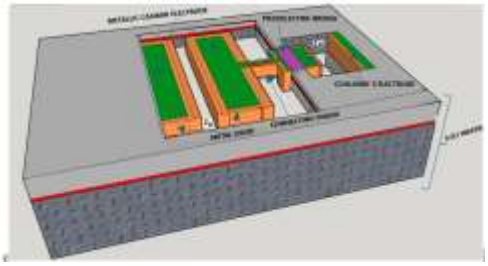

Figure 10: Final structure with the metal oxides surrounding the metal electrodes.

Simulation of Devices with different Piezoelectric Bridge

We present below the results of the MATLAB simulations carried out by numerically calculating the differential equations (15) and (18). These numerical calculations give the vibration frequency of the structure which, as we will see, vibrates at a frequency lower than its first resonant frequency (IV) .This vibration frequency depends on the characteristics of the structure (Nature of material, , geometric dimensions, coefficient of proportionality $p = F_{CO} / F_{CA}$…)). (See IV and Annex) .The metal used for the Casimir reflector block is Aluminium with a density of 2.7 g cm^{-3}

Piezoelectric Materials = PZT (Lead Zirconia Titanium)

Interface between Casimir Electrodes as a Function of Time for Different Trigger Values of Mos Transistors

For a starting interface between Casimir electrode of $z_0 = 200 * 10^{-10}$ (m) and a coefficient of proportionality $p = F_{CO} / F_{CA} = 2$, we obtain the following evolution in time of the Casimir interface:

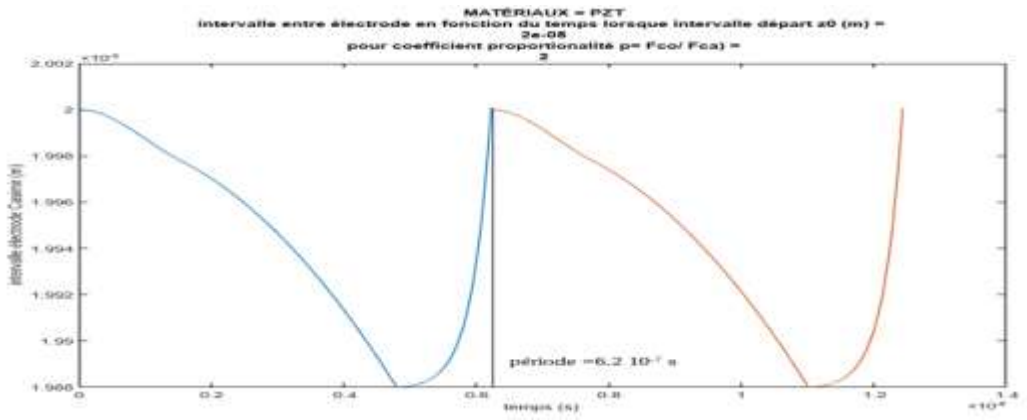

Figure 11: Interval between Casimir electrodes as a function of time for a proportionality coefficient FCO / FCA = 2: PZT

We notice a phase of rise of the Casimir electrode faster than that of descent. The period of vibrations is 6.18 10^{-7} s therefore with a vibration frequency of 1.613 10^6 Hertz , while the first resonant frequency of the same structure is 6.54 10^6 hertz. The moving electrode drops to z_s = 198.8 Angstroms from the fixed electrode S_{S3}. The current peak for this coefficient of proportionality p = 2 is 2.58 10^{-8} A. This current is obtained by adjusting the threshold voltage of the enriched and depleted MOS transistors to a value Vt = 0.6553V for a length L = width =W = 4 10^{-6} m and with a grid

oxide thickness SiO2 = tox of 250 10^{-10} m (See figure 27).

Let us simply change the coefficient p = F_{CO} / F_{CA} of proportionality to p = 200, then we get (See figure 12):

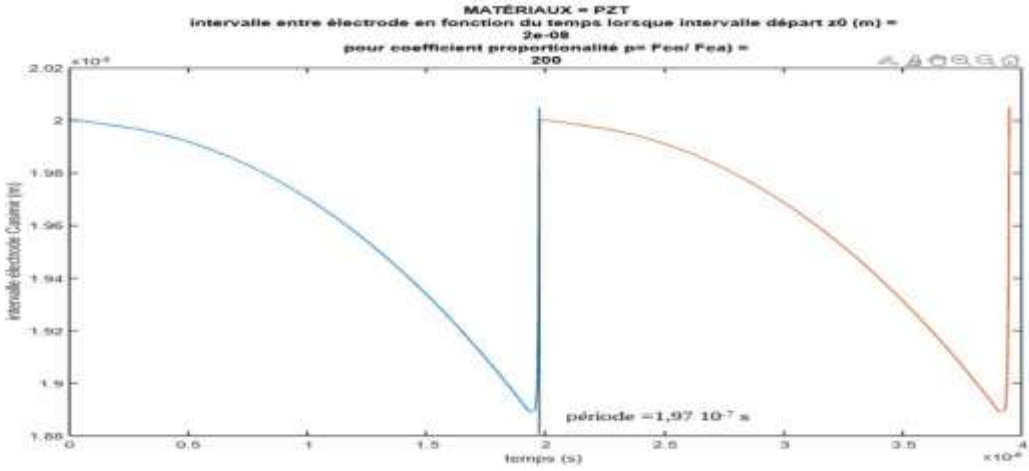

Figure 12: Vibrations of the structure for a coefficient of proportionality p = F_{CO} / F_{CA} = 200: PZT

We notice for the ratio p = F_{CA} / F_{CO} = 200 (figure 12), a phase of "rise" of the Casimir electrode also much more dynamic than for the ratio of previous p = 2 The vibration frequency of the device of 5.07 10^5 hertz, while the first resonant frequency of the structure is still 6.54 10^6 hertz.
The moving electrode is now approaching to z_s = 188.9A ° of the fixed electrode S_{S3}, so the vibration amplitude of the structure is 11.1 Angstroms.
The current is obtained by adjusting the threshold voltage of the enriched and depleted MOS transistors to a value Vt = 6.89 V for the same geometries as above (see figure 27).
We must therefore adjust the threshold voltages to precisely adjust the ratio p = F_{CO} / F_{CA} for which the Coulomb force is triggered. This is a point that can be easily obtained technologically (chapter VII)
As the vibration frequency of the structure depend on the coefficient of chosen coefficient of proportionality p, *the structure does not vibrate at its first resonant frequency.*

Spatial and temporal evolution of the Coulomb and Casimir force during an entire period

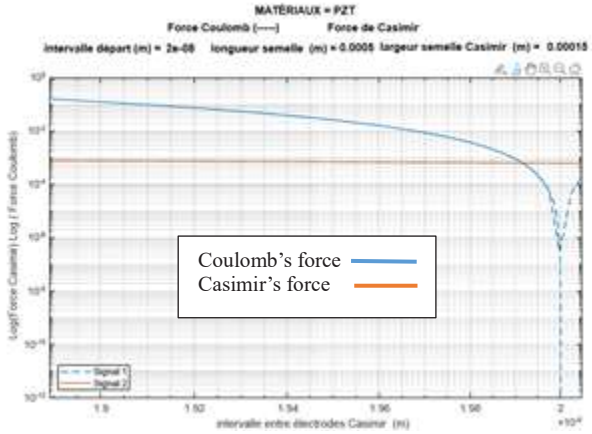

Figure 13: Casimir force and Coulomb force during a complete cycle)

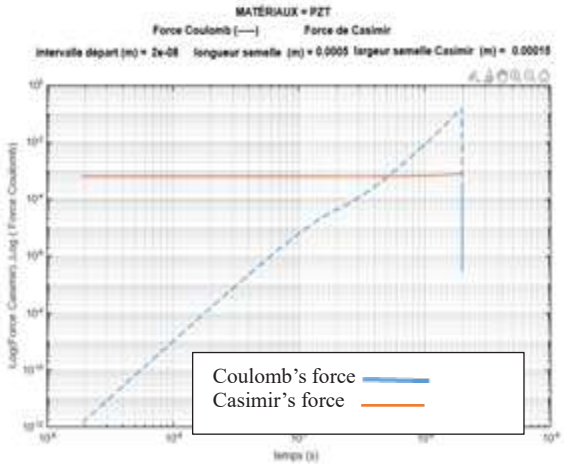

Figure 14: Casimir force and Coulomb force during a complete cycle) f (time)

Figure 13 illustrates for the same device the values of the forces of Casimir and Coulomb for an evolution of the Casimir's interface between electrodes from 189.5A ° to 200 A ° and during a complete cycle "descent + rise".

Figure 14 shows the evolution over time of the Casimir and Coulomb forces. Note that the Coulomb force is cancelled out during a complete structural vibration cycle at time t= 1.95 10^{-6} seconds.

We notice figure 15 that this ratio reaches the chosen ratio of 200 at time 1.95 * 10^{-6} seconds then plunges to zero during the "rise" of the structure.

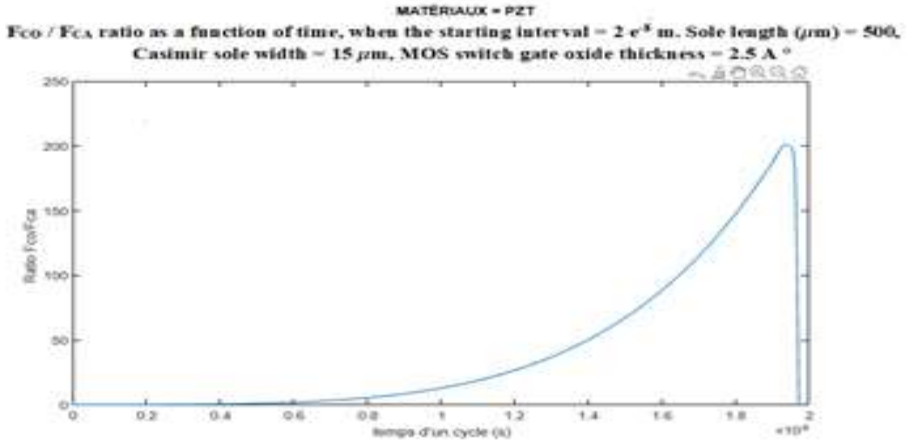

Figure 15 shows the ratio p = F_{CO} / F_{CA}= f(time) during a complete structural vibration cycle and with a choice of maximum ratio = 200

Variation of the starting Casimir's interface z_0 electrodes: PZT

Figure 16: Maximum Peak CURRENT = f (starting interface z0), Maximum selected F_{CO} / F_{CA} p ratio = 200

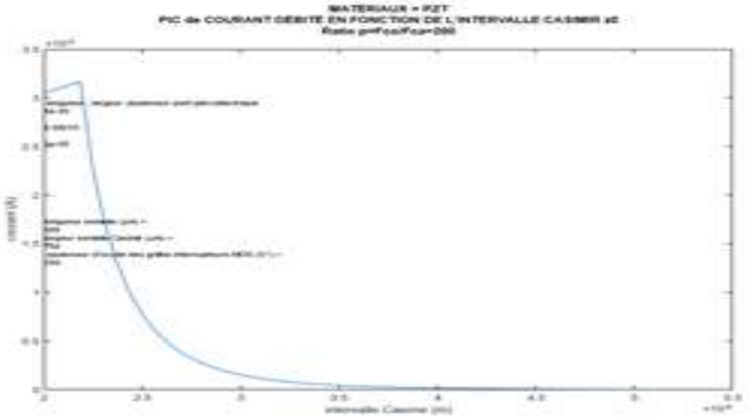

In order to have a significant current, it is necessary to use starting interfaces between the Casimir electrodes of less than 300 Angstroms. This low interface is difficult to obtain but is still possible with a technology that we present (see technology chapter VII).

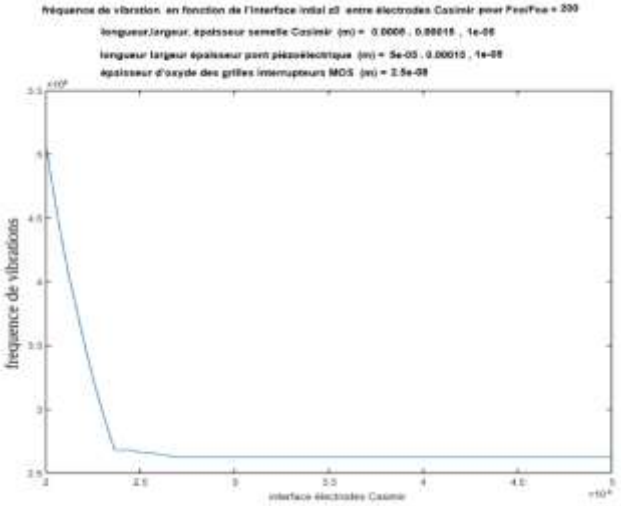

Figure 17: Structure vibration frequency = f (starting interface z_0): Fco / Fca chosen = 200: PZT

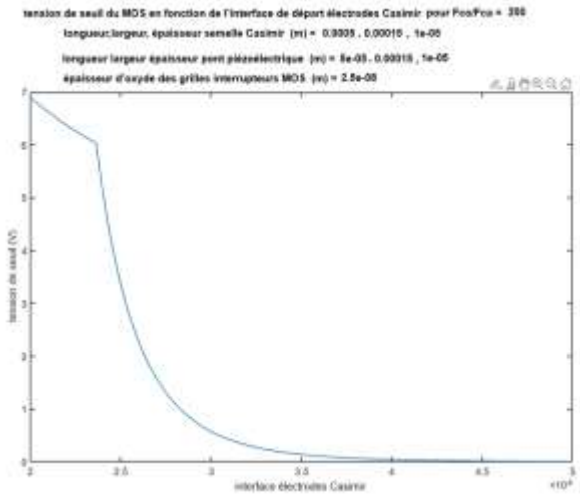

Figure 18: MOS threshold voltage = f (starting interface z0): Fco / Fca chosen = 200: PZT

We notice (Figure 17) that for a ratio F_{CO}/ F_{CA} of 200, the vibration frequency of the structure drops and stabilizes

around 2.6 MHz, when the initial space between the Casimir electrodes increases. It is related to a decrease in the Casimir Force. It is much lower than the first resonant frequency of the structure which is 6.85 Megahertz (for this structure). The vibration frequency approaches that of first resonance if the starting z_0 interface is less than 200 Angstroms.

The vibration frequency depends on the chosen F_{CO} / F_{CA} ratio.
We chose an initial interface of 200 A ° for reasons of technological feasibility (see VI).

It can be seen (Figure 18) that the threshold voltage of all MOS transistors in the switches increases with a decrease in the starting interface between the Casimir electrodes. As the Casimir force increases, so do the charges generated on its faces. It is therefore necessary that the threshold voltage of the MOS transistors is greater in order not to trigger with the increase in the V_{GRIDS}

Current and Threshold voltage function of the length ls of the Casimir electrode: PZT

We obtain (figure 19) a small decrease in the current, but a significant increase in the threshold voltage (figure 20), as the length of this electrode increases. This is correlated with an increase in the inertie of the structure.

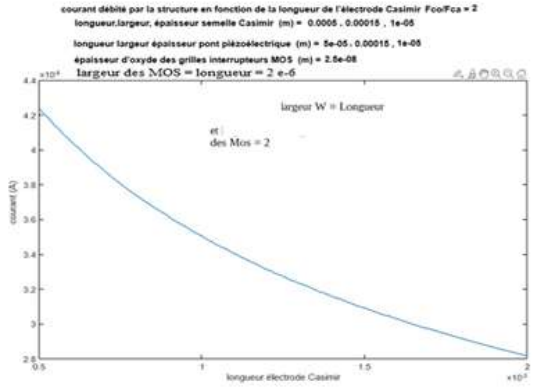

figure 19: maximum current = f (length of the Casimir electrode ls), starting interface = 200 A °, selected coefficient of proportionality p = Fco / Fca = 2

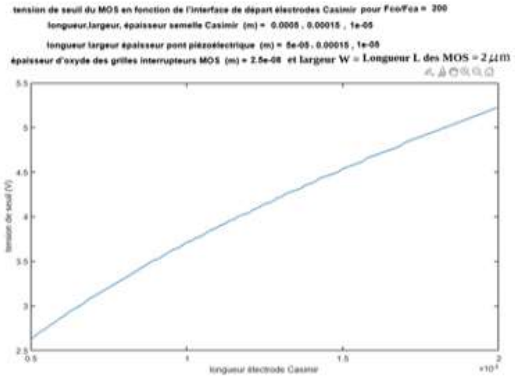

figure 20: Threshold Voltage = f (length of the Casimir electrode ls), starting interface = 200 A °, selected coefficient of proportionality p = Fco / Fca = 2

Variation of the Width Bp of the Piezoelectric Bridge: PZT

We vary the bp width of the piezoelectric bridge and obtain an increase in the threshold voltage of the MOS by increasing the bp width of the piezoelectric bridge (figure 21)
However, the current delivered by the structure varies little with the width of the piezoelectric bridge (figure 21)

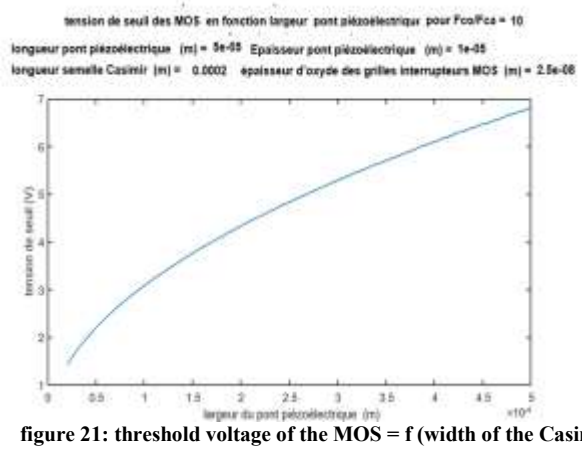

figure 21: threshold voltage of the MOS = f (width of the Casimir electrode b_p), starting interface = 200 A °, selected coefficient of proportionality = p = Fco / Fca = 10

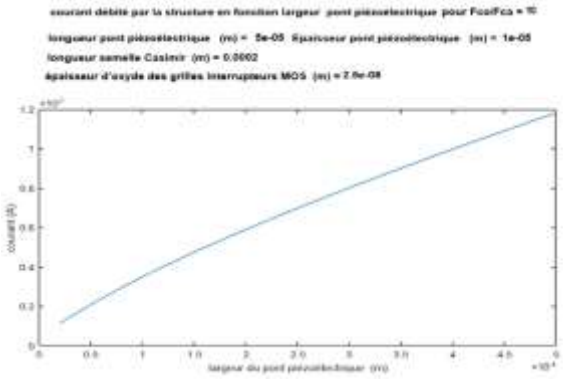

figure 22: Maximum current = f (width of the Casimir electrode b_p), starting interface = 200 A °, selected coefficient of proportionality = p = Fco / Fca = 10

These considerations give that: *For reasons of technological convenience, it will be preferable to choose a thickness of around 20 µm.*

Variation of the Thickness ap of the Piezoelectric Bridge: PZT

With an increase of the piezoelectric bridge thickness a_p, we obtain a decrease in the current (figure 23) and the threshold voltage of the MOS (figure 24) but an increase in the vibration frequency (figure 25)

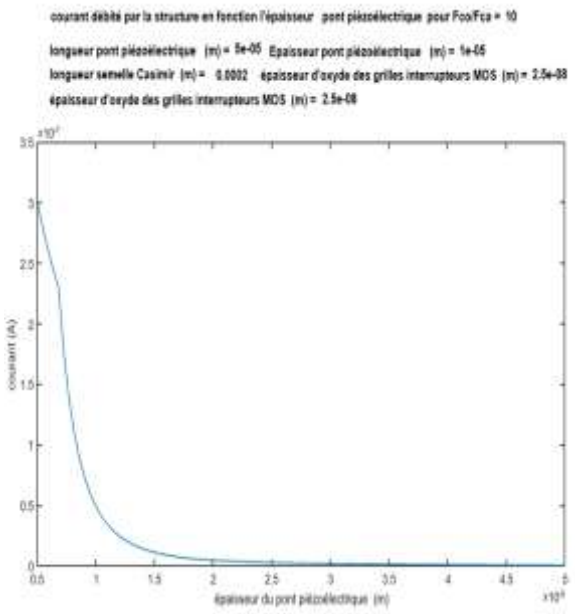

Figure 23: current of the MOS = f (Thickness of piezoelectric film a_p), start Interface = 200 A° with a choice Fco/Fca =10

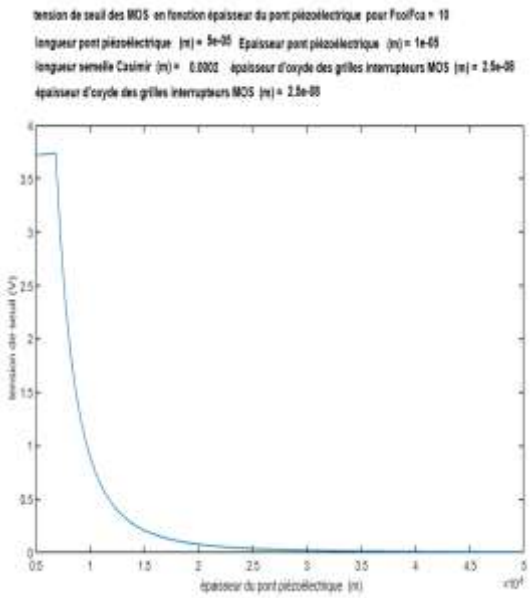

Figure 24: Threshold of the MOS = f (Thickness of piezoelectric film a_p), start Interface = 200 A° with a choice Fco/Fca =10

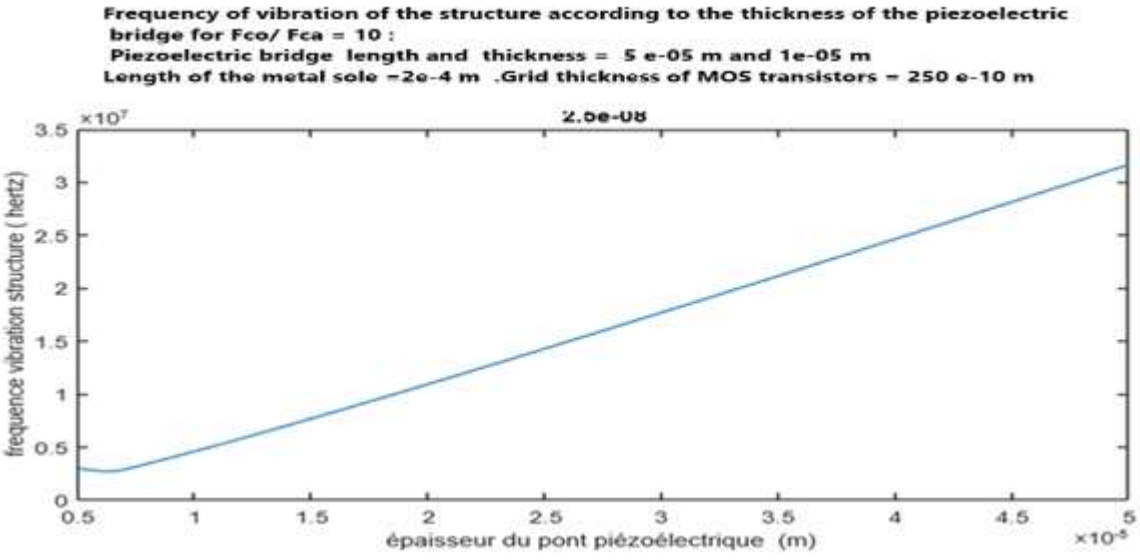

Figure 25: Structure vibration frequency as a function of the thickness ap of the piezoelectric bridge, starting interface z_0 to 200 A °, Ratio p = F_{CO} / F_{CA} = 10: PZT

Variation of the Proportionality ratio p = F_{CO} / $F_{CA:}$ PZT

In a non-intuitive way, the current simply increases linearly by a factor of 40 (figure 26) if we increase the proportionality ratio p = F_{CO} / F_{CA} by a factor of 500.

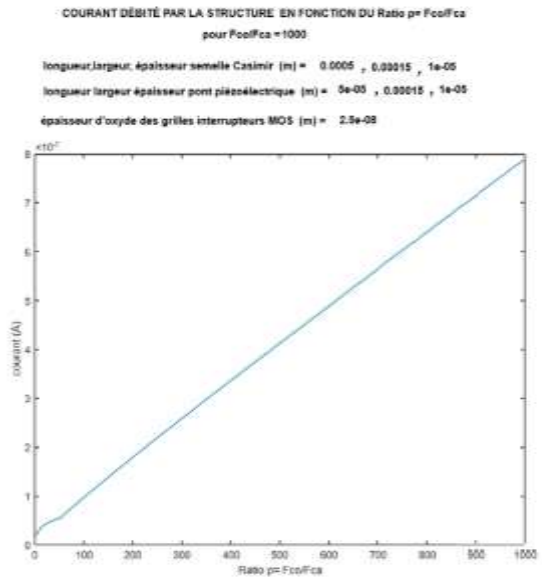

Figure 26: current of the MOS = f (ratio = Fco/Fca), start Interface = 200 A° piezoelectric material = PZT

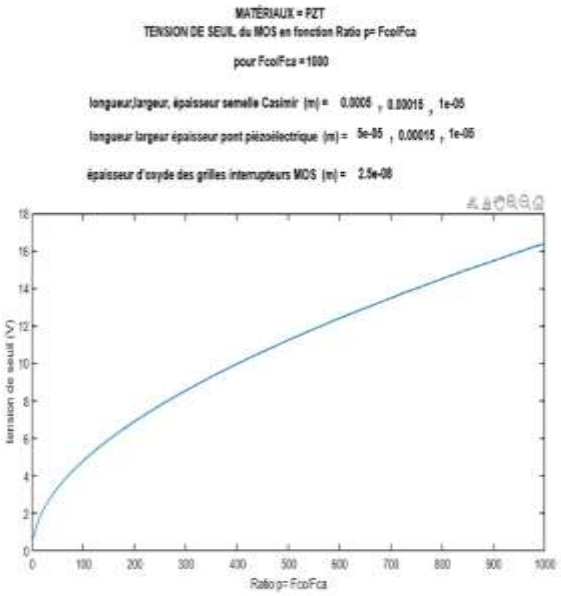

Figure 27: Threshold voltage of the MOS = f (ratio = Fco /Fca), start Interface = 200 A° piezoelectric material = PZT

On the other hand, the threshold voltage of the MOS switches increases by a factor 8 for the same variation of the interface (figure 27). The MOS N or P switch transistors enriched in parallel have the following geometries: Width W = 4 mm and length L = 4 mm

Use of other Piezoelectric Materials

In order to increase the density of electric charges at the terminals, piezoelectric material PMN-PT can be used. It can be deposited by RF-magnetron sputtering with a composition, for example:
PMN-PT= (1-x) Pb (Mg1 / 3 - Nb1 / 3) O3-xPbTiO3; d_{31} = 1450 .10^{-12} C / (kg .m .s^{-2}) and a Young's modulus of Ep = 150 .10^{9} Kg M^{-1} T^{-2} (Figure 1).

We will also simulate the results obtained with AlN (aluminium nitride) (d_{31}=2.4*10^{-12} C/ (Kg M T^{-2}) and Ep = Ep=32.10^{10} Kg M^{-1} T^{-2}, another piezoelectric material or AlN widely used in microelectronics because it is easily removable and lead-free.

Piezoelectric Material = PMN-PT

With the MATLAB simulation, for an interval between Casimir electrode z_0= 200 Angstroms, we obtain the evolution over time of the Casimir and Coulomb forces as well as the F_{CO} / F_{CA} ratio of figures 28 to 42 below. For a ratio of 1000, the maximum current delivered by the vibrating structure, the threshold voltage of the MOSE and the vibration frequency of the structure are respectively: 1.2 10^{-4} A, Vt = 3.2 V and 957000 Hertz

Evolution of the Casimir Interface as a Function of time during Two Periods: PMN-PT

For the F_{CO} / F_{CA} ratio = 10000 induces a period of 3.85 10^{-6} s and a rise time of 21.3 10^{-9} s with a deflection of the bridge of 105 A °. The structure vibrates at 259.7 kHz. Due to inertia, at the rise sequence, the structure exceeds the initial 200 A ° by 20 A ° (Fig 28).

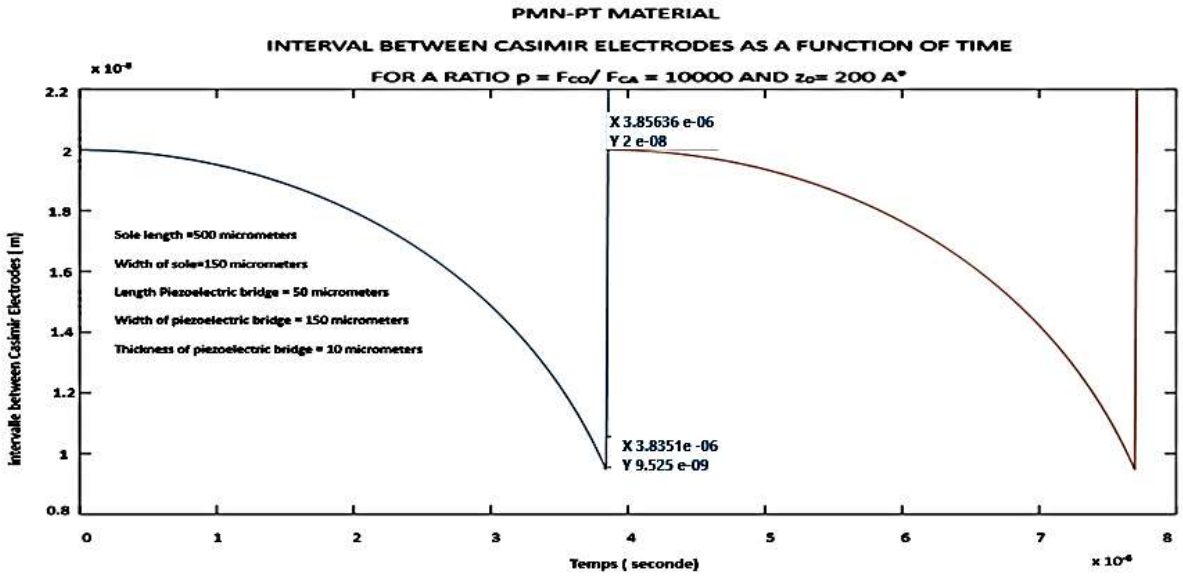

Figure 28: plot of the evolution of the Casimir inter-electrode interval as a function of time over two periods and an Fco / Fca Ratio = 10000: Casimir inter-electrode interface = 200 A°

A ratio F_{CO} / F_{CA} = 1000 induces a period of 2.96 10^{-6} s and a rise time of 44.5 10^{-9} s with a deflection of the bridge of 50 A ° The structure vibrates at 337.8 kHz: (fig 29). For this ratio of 1000 we notice a vibration amplitude of 50A ° , a period of 2.96 10^{-6} s, with the faster rise of the mobile electrode producing a slight rebound of 5A, because of the inertia of the structure.

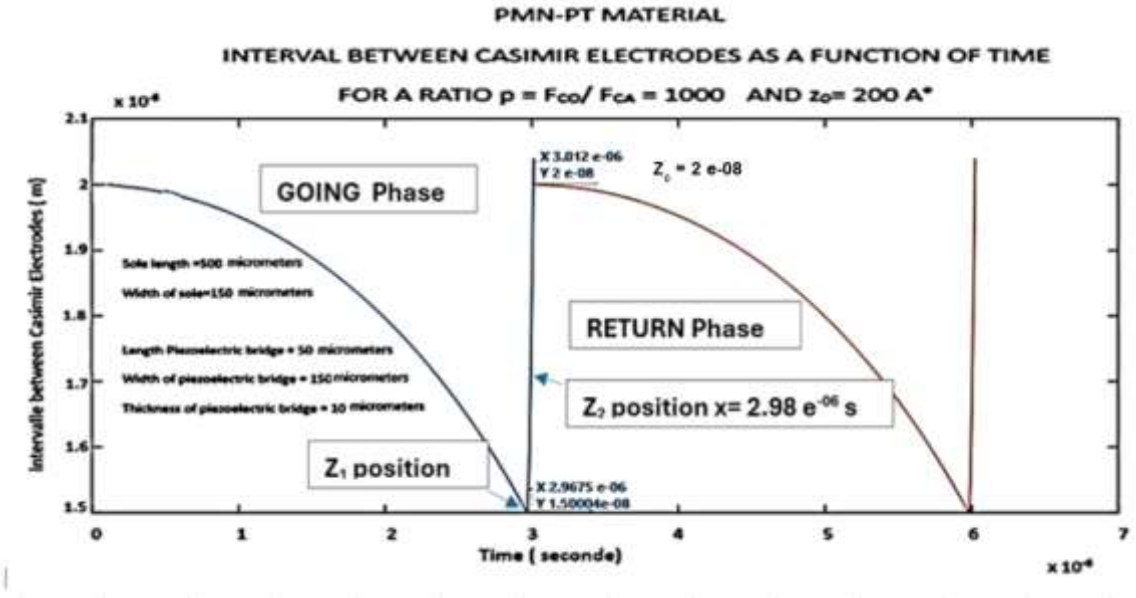

Figure 29: plot of the evolution of the Casimir inter-electrode interval as a function of time over two periods and an Fco / Fca Ratio = 1000: Casimir inter-electrode interface = 200 A°

For the ratio F_{CO} / F_{CA} = 2 (figure 30) a vibration amplitude of just 0.27 A ° and a period of 1.8610^{-7} s is obtained This low deformation of the PMN-PT piezoelectric bridge is mainly due to the extremely high piezoelectric coefficient d_{31} of 1450 (pC/N) of PMN-PT compared to 120 (pC/N) for PZT (Table 1).

We observe the weak overshoot of the initial interface.

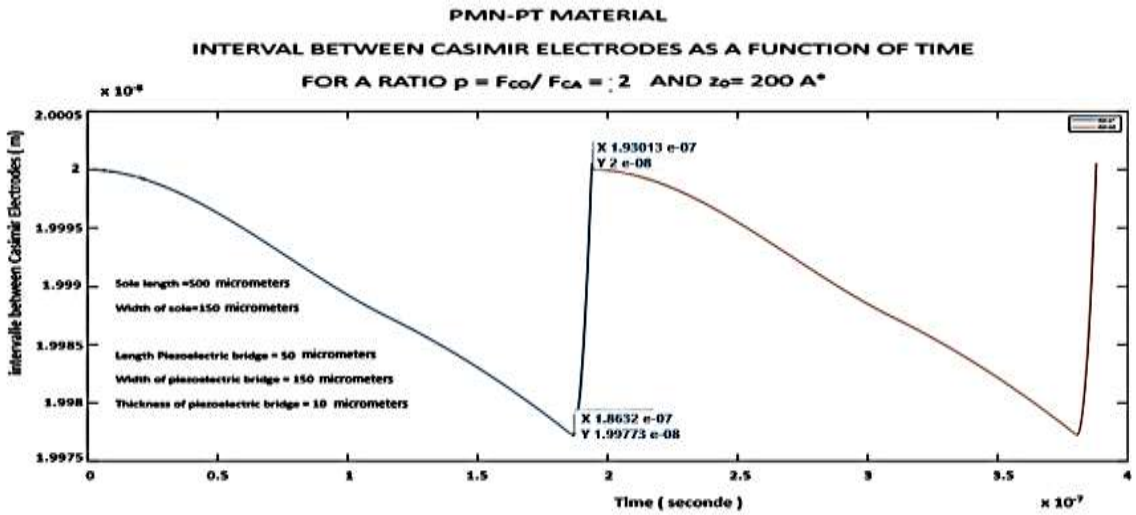

Figure 30: plot of the evolution of the Casimir inter-electrode interval as a function of time over two periods and a Ratio Fco / Fca = 2. Casimir inter-electrode interface = 200 A

IV-2-1-2 / Evolution of the forces of Casimir and Coulomb: PMN-PT

We obtain:
1/ The evolution of the Casimir and Coulomb forces as a function
a / of the inter-electrode interface (figure 31) and
b/ over time (figure 32)
2/ The F_{CO} / F_{CA} ratio as a function of time for an entire period (figures 33).

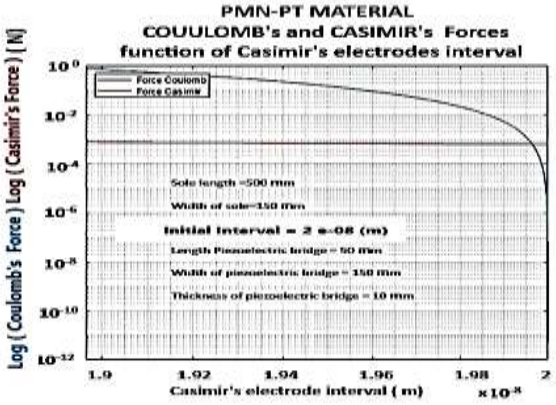

Figure 31: Materials = PMN-PT: Coulomb and Casimir force as a function of the inter-electrode interface. Start interface = 200A °

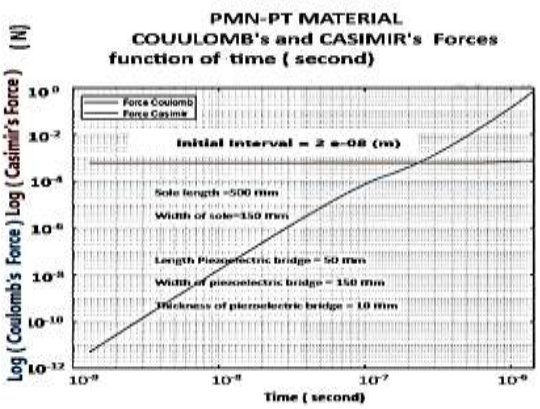

Figure 32: Materials = PMN-PT: Coulomb and Casimir force as a function of time. Start interface = 200A °

It is observed (Fig. 33) that the Coulomb return force is less important for an initial inter-electrode gap zr = 400A° than for z_r= 200A°.

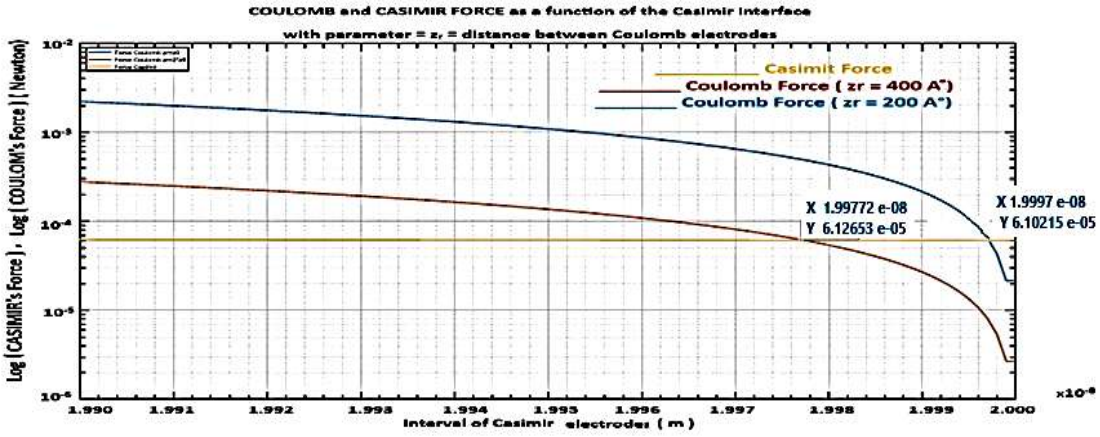

Figure 33: Materials = PMN-PT: Coulomb force for z_r = 200 A ° (Blue) and z_r = 400 A ° (Red) and Casimir force (Yellow, z0 =200 A°) as a function of the inter-electrode interface Starting interface = 200 A

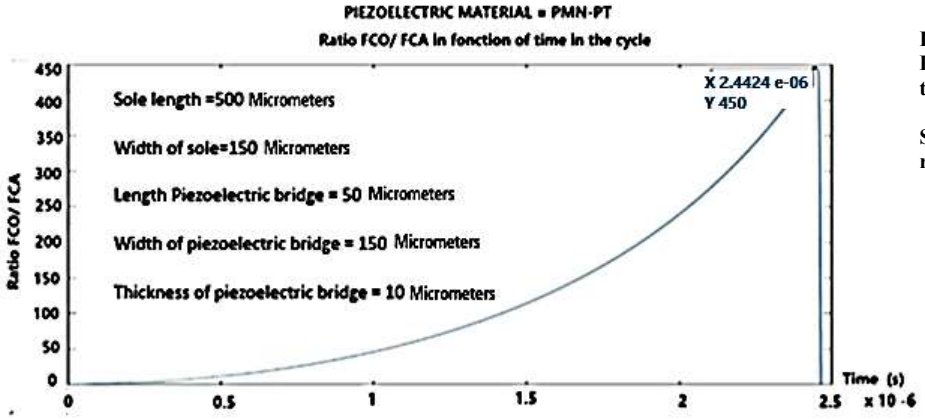

Figure 34: Materials = PMN-PT: Ratio p = F_{CO} / F_{CA} as a function of time, during a period of vibration.

Start interface = 200A °, Maximum ratio chosen = 450

The break circuits n°1 triggered at time t = 2.44 10^{-6} s suddenly induce a rise of the mobile electrode, therefore a sudden decrease in electric charges and grids voltages. We observe the gradual evolution towards the chosen ratio of 450 and then the sudden drop in this ratio as the electrodes regain their initial position (Fig. (34)).

Ratio F_{CO}/F_{CA} as a function of Casimir interval and current peak as a function of the ratio: PMN-PT

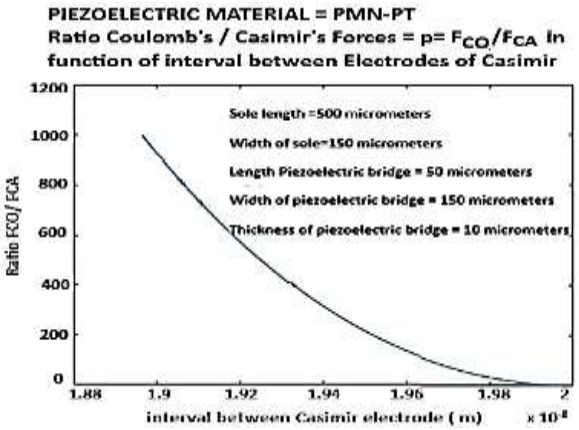

Figure 35: Materials = PMN-PT: Coulomb Force / Casimir Force ratio as a function of the Casimir inter-electrode interface. Start interface = 200A °

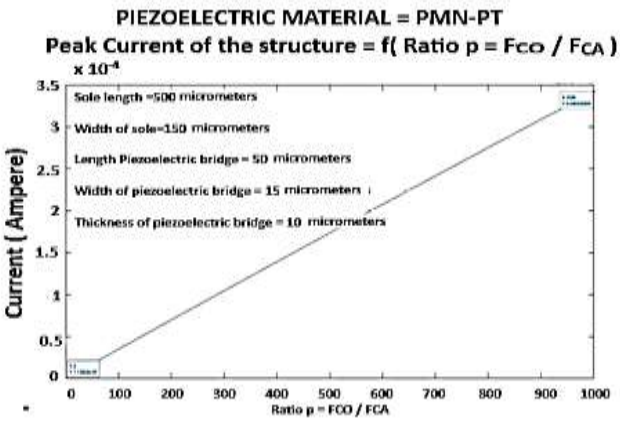

Figure 36: Materials = PMN-PT: Peak Current delivered by the structure as a function of the Fco / Fca Ratio. Start interface = 200A °

We observe (Fig 35) that for PMN-PT, a length of the piezoelectric bridge of 150 µm and a deformation of 10 A ° of piezoelectric bridge, is sufficient to have a ratio = 1000.
On Fig 36, we see that a ratio of 2 gives a peak current of 7 10^{-7} A, while a ratio of 1000 produces a peak current of about 3.25 10^{-4} A, for the same time of homogenization of the charges of about 10^{-9} s.

Peak Current as a Function of Time and Peak Voltage across the Inductance for 2 Periods: PMN-PT

The following figures illustrate the peak current generated by the automatic vibrating structure with an inserted magnification showing the shape of this peak as a function of time (figure 37) and its exponentially decrease during about 10^{-9} s. This current of about 1.2 10^{-4} A flowing through an inductor L_{IN} of 3 10^{-5} Henri naturally generates a voltage of 4 Volts (figure 38)

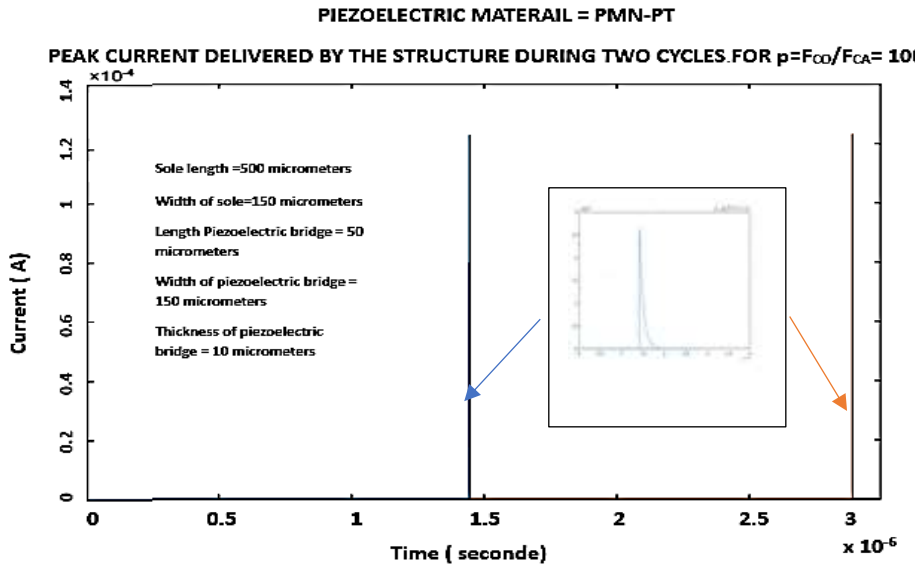

Note the exponential form of the current peak in each period.

Figure 37: Materials = PMN-PT: Current peak as a function of time obtained over 2 cycles. Starting interface = 200A ° Ratio p=Fco /Fca=1000

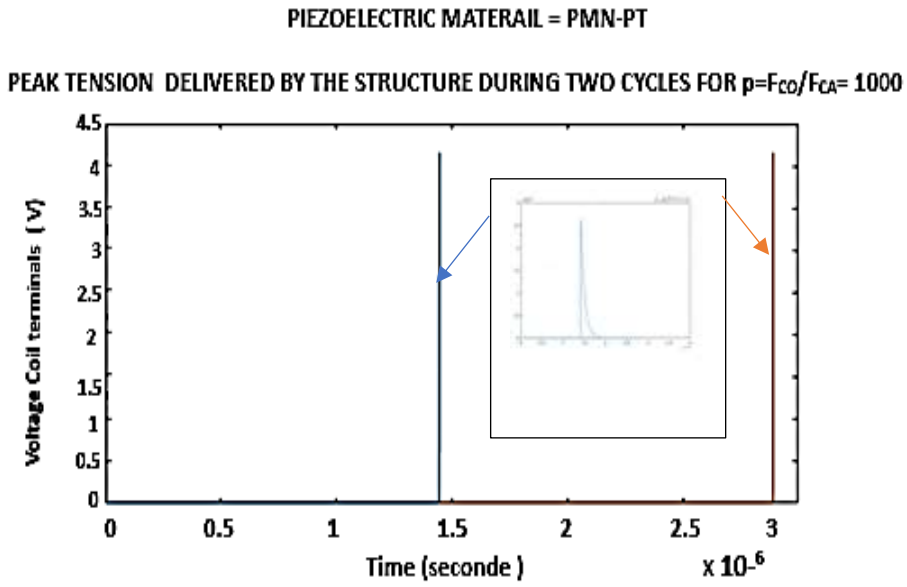

As this current peak cross an inductor, it induces by itself a voltage peak (fig 38)

Figure 38: Materials = PMN-PT: Voltage peak across the 4 . 10^{-5} H solenoid as a function of the time obtained over 2 cycles. Starting interface = 200A °, Ratio p=Fco /Fca=1000

Peak Voltage across the Inductance and Threshold Voltage According to the Desired Ratio F_{CO} / F_{CA}: PMN-PT

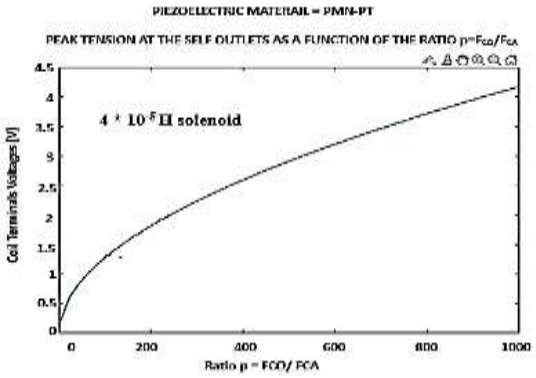

Figure 39: Materials = PMN-PT: Voltage peak across the 4 * 10^{-5} H solenoid as a function of the F_{CO} / F_{CA} Ratio. Start interface = 200A °

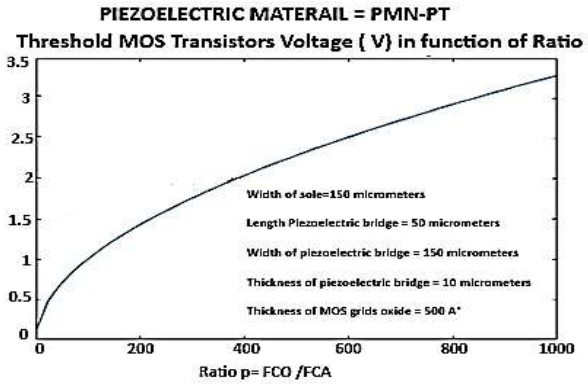

Figure 40: Materials = PMN-PT: Threshold voltage of the Enriched or Depleted MOS according to the F_{CO} / F_{CA} Ratio. Start interface = 200A °

It can be seen (Fig. 39) that the automatic peak voltage obtained without any energy expenditure increases by a factor of 16 from 0.25 V to 4 V, when the ratio p = FCA / FCO changes from 2 to 1000. Similarly, the MOSE and MOSD threshold voltage allowing these ratios increases from 0.2 V to 3.2 V (Fig 40).

Vibration frequency as a function of the F_{CO} / F_{CA} ratio and peak current as a function of the initial Casimir interval chosen: PMN-PT.

Note (fig 41), that for an initial interface z_0 = 200 A°, and for a ratio F_{CO} / F_{CA} = 2 , the maximum vibration frequency of the structure is 3.50 MHz . It falls to 750 kHz for a ratio of 1000. These frequencies are still lower than the first resonance of the structure, which is of the order of 7.94 Megahertz.

For a ratio F_{CO} / F_{CA} = 500, the maximum current delivered by the structure falls as a function of an increase in the initial Casimir interval (Fig 42).

This vibration frequency of the Casimir structure approaches that of the first resonance for weaker interfaces below 200 A°.
We are then unfortunately confronted with the technological possibility of controlling such a weak interface.
It seems that the piezoelectric material PMN-PT coupled with a conductor like aluminium is an interesting couple for our vacuum energy extraction structure.

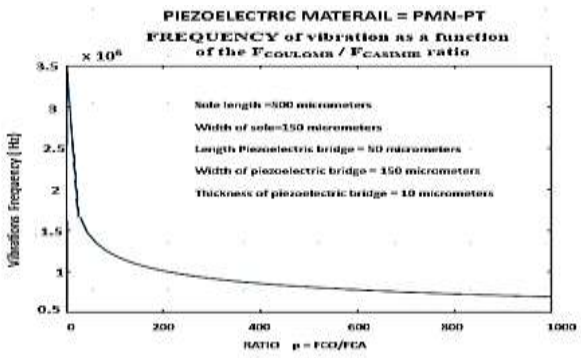

Figure 41: Materials = PMN-PT: Vibration frequency as a function of the F_{CO} / F_{CA} Ratio. Start interface = 200A ° Start interface = 200A °

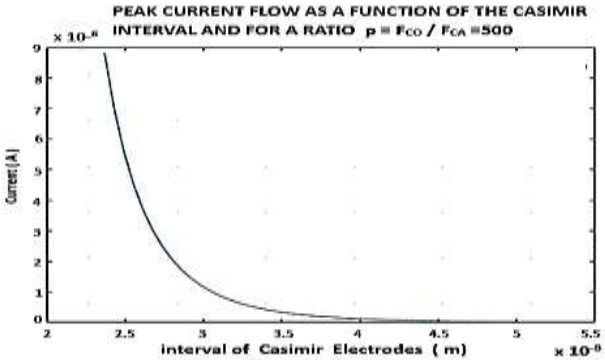

Figure 42: Materials = PMN-PT: Current peak across the 2 . 10^{-4} H inductance as a function of the starting interval between Casimir electrodes. Start interface = 200A °

Piezoelectric Material = AlN

We test with a MATLAB simulation of the behaviour of the structure make with piezoelectric Aluminium Nitride (AlN). We obtain the evolution with time of the Casimir and Coulomb forces on figures 43.

For a ratio of 10, the maximum current delivered by the vibrating structure, the threshold voltage of the MOS and the vibration frequency of the structure is respectively 1.85 10^{-7} A, Vt = 3.7 V and 667000 Hertz.

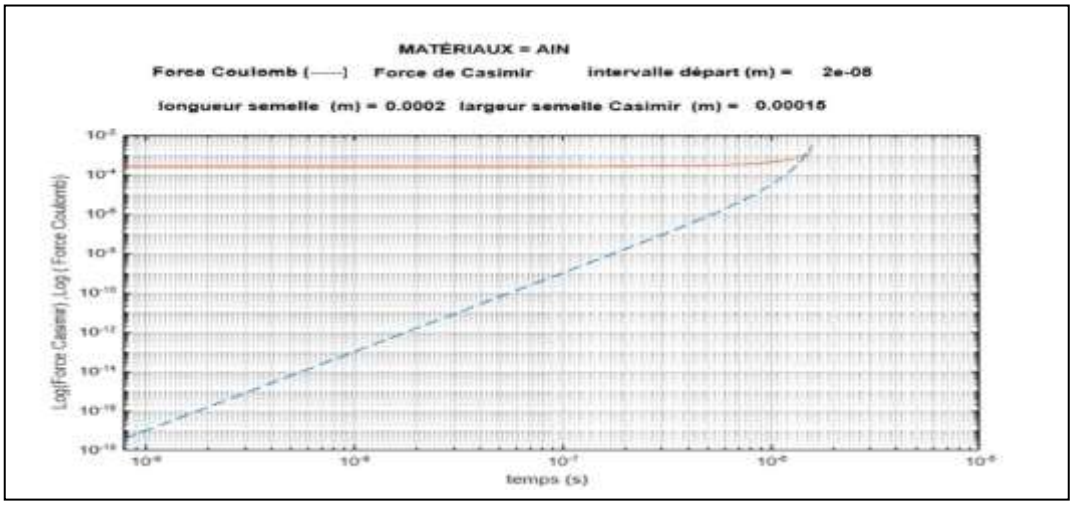

Figure 43: Piezoelectric Material = AlN Casimir, Coulomb Force = f (Time) starts Interface = 200 A°

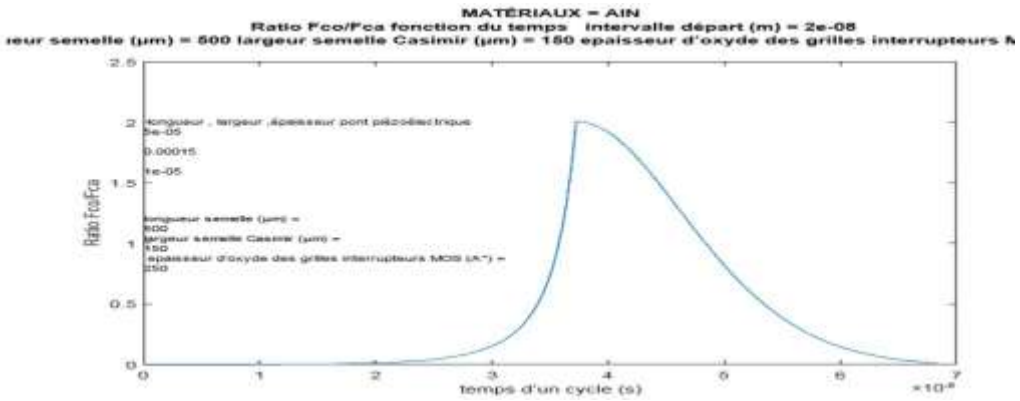

Figure 44: Piezoelectric Material = AlN. Ratio Fco/ Fca = f (Time) Start interface = 200A °

We observe (figure 44) that the ratio p = F_{CO} / F_{CA} barely equals 2

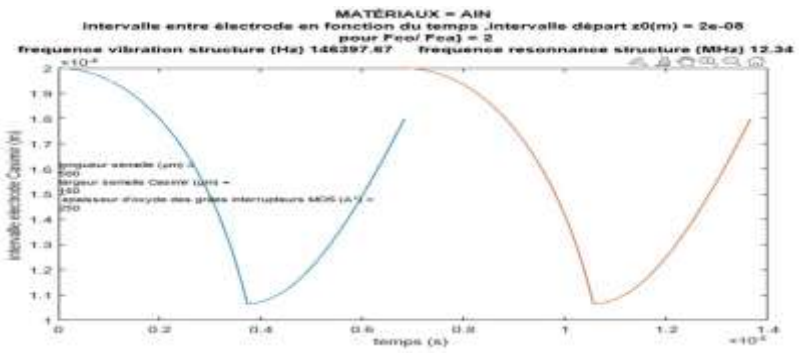

Figure 45: Material = AlN Interval between Casimir electrodes = f (time) during two complete cycles: Interface between starting electrodes = 200 A°

The time of "rise" of the mobile Casimir electrode is relatively slow , it is a consequence of the low value of the piezoelectric coefficient d_{31} of AlN.

In conclusion, the use of AlN does not seem suitable for this vacuum energy extraction application

Conclusions

It seems that the most suitable piezoelectric material for this vacuum energy extraction device is PMN-PT with a peak current more than 100µA (figures 28 to 42).

U_{IN} I_{IN} power peaks of nanosecond duration are converted into a DC voltage that can be used by electronics without a power supply

Electronic Transformation and Amplification without External Power Supply of a Periodic Signal of a Few Millivolts into a Dc Voltage of a Few Volts

U_{IN} . I_{IN} power peaks lasting a few nanoseconds are present at the input of an electronic circuit without any power supply (see fig 46).
We will describe these electronics designed and successfully tested with a simulator SPICE . This electronic gave very encouraging results and delivers in its output an exploitable direct voltage even if it has in its input an alternating and signal of some millivolts.

The principle used to amplify and transform a weak signal without power supply derives from that of the diode bridge rectifier of Graetz or the doubler of Schenkel and Marius Latour. The crippling problem is that the diodes of these rectifiers are conductive only with a minimum voltage of around 0.6 V at their terminals. As the alternating signal from the vacuum energy extraction device can be weaker, it is necessary to have switches that are triggered with a lower control voltage.

The principal diagram of this electronics is presented in figure (46)
In these SPICE simulations, the micro transformer of vacuum energy describe above was assimilated to a micro transformer delivering a power U_{IN} . I_{IN} limited to a few nW .

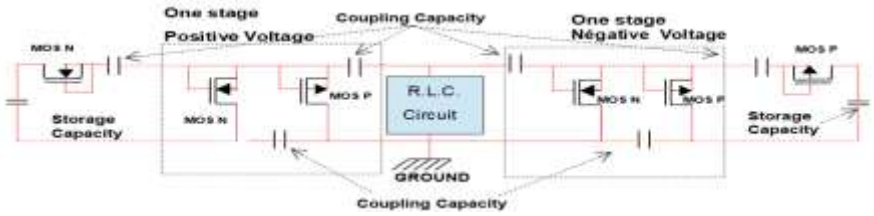

Figure 46 : Principle of the single-stage doubler without power supply electrical diagram. All the MOS are isolated from each other by etching on an S.O.I wafer and their threshold voltage is as close as possible to ground

The MOSE N and P transistors of this rectifier circuit must have a technologically defined threshold voltage as close as possible to zero. The precision of nullity of these threshold voltages will depend on the values of alternating voltages at the terminals of the inductor L_{IN} . In the circuit of figure 46, a micro transformer replaced the inductance L_{IN} . But this inductance plays the same role as this micro transformer since it delivers a limited power U_{IN} . I_{IN}

The left part of the micro-transformer takes care of the negative voltages of the input signal, while the right part takes care of the positive voltages. The circuit is composed of several stages without no power supply which rectify and amplify, on the one hand the negative parts of the weak input signal and on the other hand the positive parts.

The number of elementary stages depends on the desired DC voltage, but this DC voltage saturates with the number of stages in series (figure 49). The results obtained from SPICE simulation are shown in figures 47,48

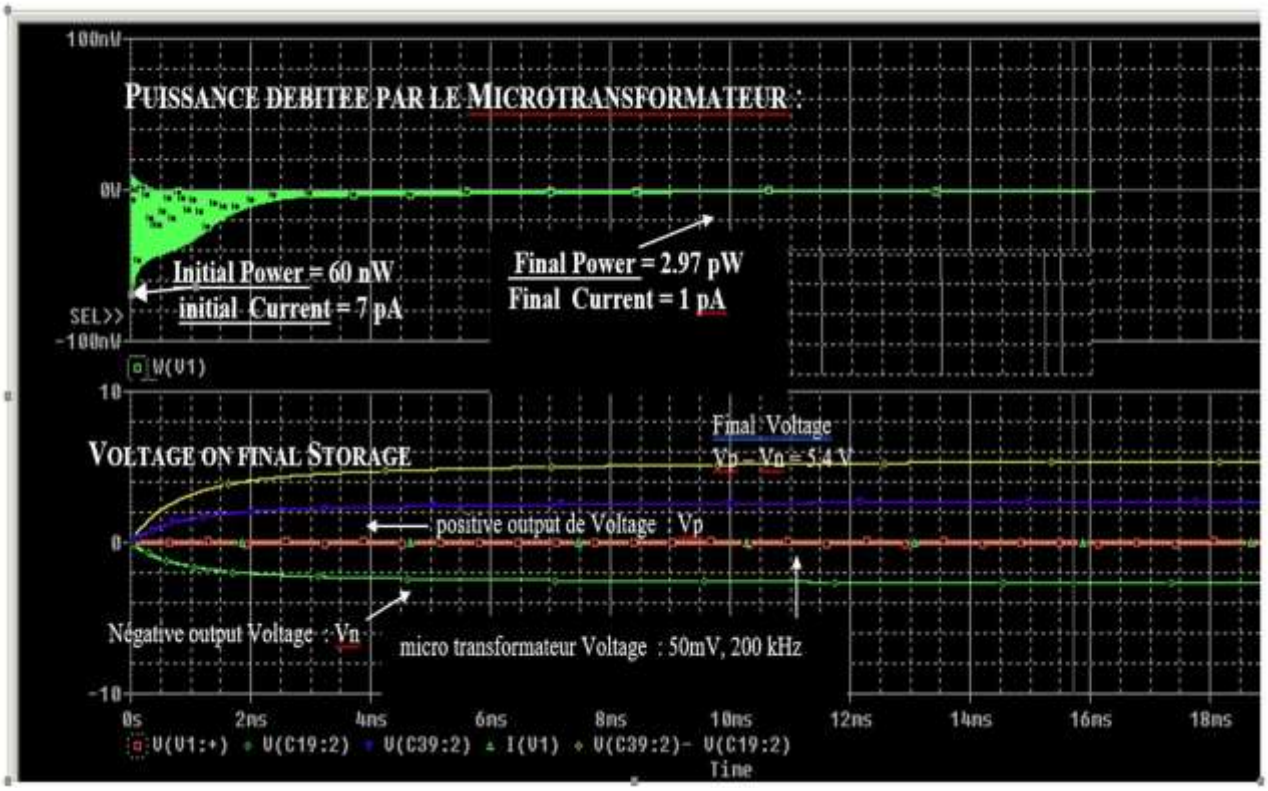

Figure 47: SPICE simulations of voltages, current, power consumed by the autonomous electronics for the transformation into direct voltage (5.4 V) of an alternating input signal of 50 mV, frequency = 150 kHz, number of stages = 14, coupling capacities = 20 pF, storage capacity = 10 nF.
We note the extreme weakness of the electrical power required at the start of the conversion of the power peaks (60 nW) and at the end (2 pW). This transformation require about 4 ms .

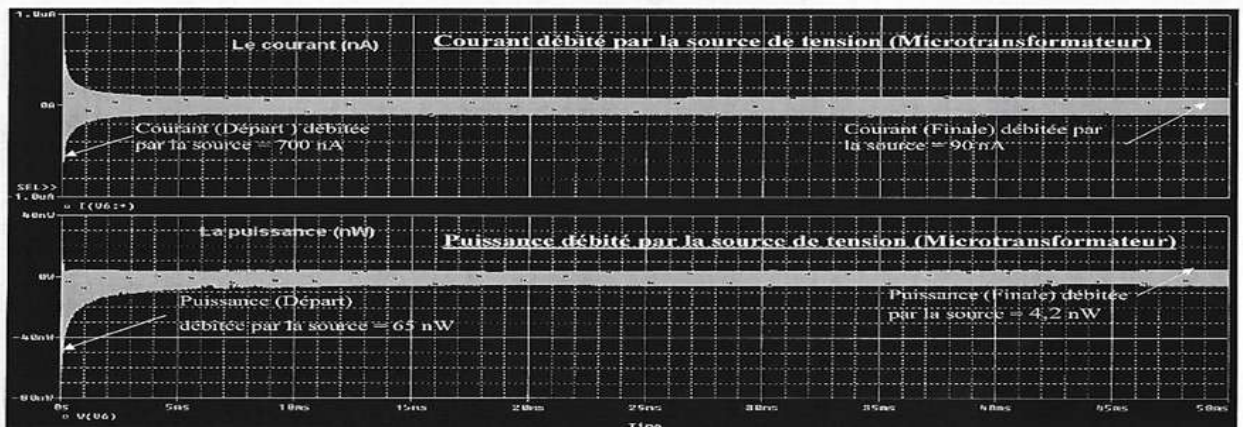

Figure 48: SPICE simulations of the currents drawn by the transformer and the power consumed by this transformer. Input signal = 100 mV, frequency= 150kHz, Number of stages =30, Coupling capacities = 20 pF, stocking capacity = 10 nF

Important points in figure 47 and 48, are the very low power and current consumption on the source since:

1 / In figure 47 the power delivered by the source begin at the start with 60 nW and ends at 2.97 pW for an input current starting at 7 pA and finishing at 1pA. The negative component of the alternating signal is transformed in 10 ns into a negative direct voltage of V_n = -2.7 V. Likewise the positive component the positive alternating part is transformed into a positive direct voltage of V_p = 2.7 V. We obtain therefore a direct voltage Vp -Vn = Vt = 5.4 V.

2 / In figure 48 the power delivered by the source begin at the start with 65 nW and ends at 4.2 nW for an input current starting at 700 nA and finishing at 90 nA. The negative component of the alternating signal is transformed in 10 ns into a negative direct voltage of V_n = -3.9 V. Likewise the positive component the positive alternating part is transformed into a positive direct voltage of Vp = 3.9V. We obtain therefore a direct voltage Vp -Vn = Vt = 7.8 V.

An important point is the need to have a high circuit output impedance of several Mega-ohms, so typically the input impedance of an operational amplifier.

The DC voltage obtained depends on the number of stages constituting these electronics without electrical power for transforming an AC signal of a few millivolts into a DC signal of a few volts. However, this transformation saturates with the number of floors, as shown in figure 49

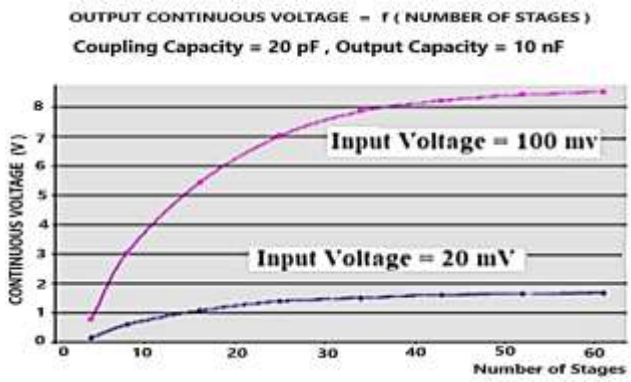

Figure 49: DC output voltages as a function of the number of elementary stages for AC input voltages of 20 mV and the other of 100 mV, Start interface = 200A °

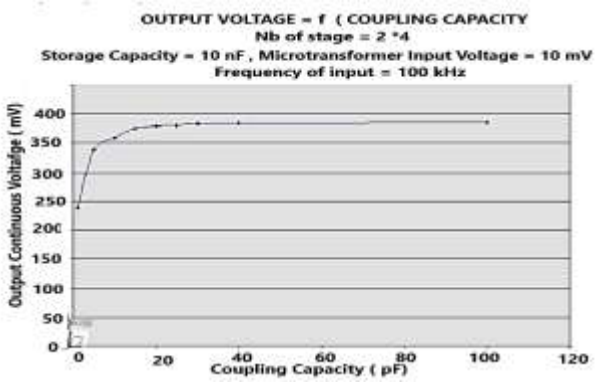

Figure 50: influence of the coupling capacitance on the amplification of the input signal. Start interface = 200A °

Note in Figure 49 that the DC output voltage saturates with the number of elementary stages and that the optimal number of stages is of the order of 40. We also looked at the influence of the coupling capacitance on the amplification of an input signal of 100mV with a storage capacity of 10nF. This amplification saturates and a coupling capacity of 20 pF which seems to be optimal signal (figure 50).

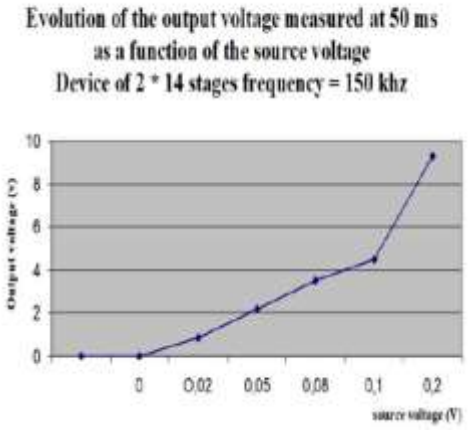

Figure 51 / Evolution of the DC output voltage as a function of the amplitude of the AC input signal for a frequency of 150 kHz Start interface = 200A °

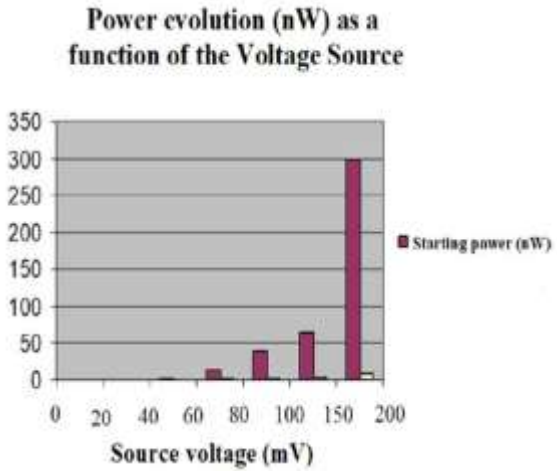

Figure 52 / Evolution of the power supplied in nW by the source as a function of the amplitude of the voltage supplied in mV. with 2 * 14 stages and a frequency of 150 kHz Start interface = 200A °

The following figure 51 shows the influence of the value of the input AC voltage, with a frequency of 150 kHz, on the DC voltage obtained at the output of a 2 * 14 stage device.

Figure 52 shows the power in nW delivered by the source at the start of the amplification.

A summary of the performance of this low "voltage doubler" device is shown in Figure 53 below

CHARACTERISTICS OF OUTPUT VOLTAGES (V), POWERS (nW) CURRENTS (nA)
AS A FUNCTION OF THE NUMBER OF STAGES
INPUT SIGNAL FREQUENCY = 150 kHz OUTPUT VOLTAGE MEASUREMENT FOR t = 50 ms

	Vg=50mV					Vg=100mV				
number of stages	Output Voltage	Current (nA) start	end	Power (nW) start	end	Output Voltage	Current (nA) start	end	Power (nW) start	end
2 ^3	550mV	300nA	26nA	15nW	1.3nW	1.1v	800nA	46nA	75nW	5nW
2 ^6	1	300nA	29nA	13nW	1.3nW	2V	700nA	67nA	60nW	6.5nW
2 ^14	2.2v	300nA	40nA	14nW	2.6nW	4,5v	700nA	50nA	65nW	4.8nW
2 ^21	2.8v	250nA	38nA	13nW	860pw	6v	600nA	80nA	60nW	2.7nW
2 ^30	3.3	250nA	43nA	12nW	1.2nW	6.5V	750nA	85nA	61nW	4nW
2 ^39	3.5v	250nA	45nA	12nW	900pW	7.5V	750nA	95nA	64nW	3.5nW
2 ^48	3.6v	250nA	46nA	12nW	1nW	7.6V	750nA	100nA	60nW	4.2nW
2 ^60	3.8	270nA	47nA	12nW	1.1nW	7.9V	700nA	90nA	65nW	4.2nW
2 ^61	3.8	270nA	48nA	12.1nW	1.3nW	8V	700nA	90nA	65nW	42nW

Figure 53; Summary of transformations from low alternating voltages to direct voltage frequency of 150 kHz . Start interface = 200A °

The interesting points for the presented electronics' device are:

1 / the low alternative input voltages required to obtain a continuous voltage of several volts at the output
2 / the low power and current consumed by this conversion and amplification circuit on the source which in this case is only an inductor supplied by the current peaks generated by the autonomous vibrations.
3 / the rapid time to reach the DC voltage (a few tens of milliseconds)

The technology used to fabricate the MOSNE and MOSPE transistors with the lowest possible threshold voltages is CMOS on intrinsic S.O.I. and the elements are isolated from each other on independent islands. This technology, represented in the following figure 54, strongly limits the leakage currents.

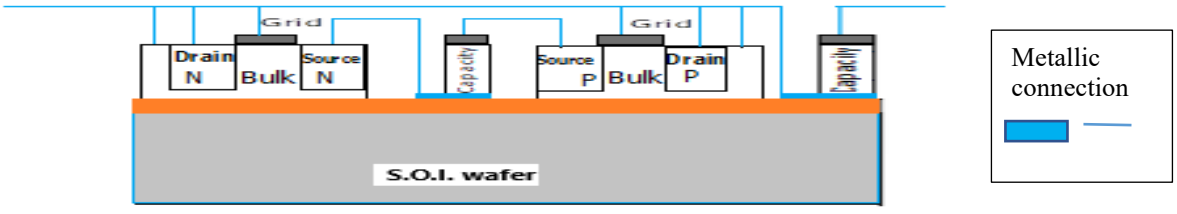

Figure 54: S.O.I technology for making the elements of the "doubler"

We note that, the coupling capacities of 20 pF of this electronic, like that of storage of the order of 10 nF, have relatively high values. In order to minimize the size of these capacitor we propose to use of titanium dioxide as insulator, with a relative permittivity of the order of 100 which is one of the most important for a metal oxide, then the size of the capacity passes to 33 µm for a thickness of TiO2 = 500 A °, which is more reasonable.

Technology of Realization of the Current Extractor Device Using the Forces of Casimir in a Vacuum

For the structures presented above, the space between the two surfaces of the reflectors must be of the order of 200 A °, …. which is not technologically feasible by engraving.

Yet it seems possible to be able to obtain this parallel space of the order of 200 A ° between Casimir reflectors, not by etching layers but by making them thermally grow.

Indeed, the S_{S3} and S_{S2} surfaces of the Casimir reflector must;

- be metallic to conduct the mobile charges
- insulating as stipulated by the expression of Casimir's law who established for surfaces without charges.
- This should be possible if we grow an insulator on the z direction of the structure, for example Al_2O_3 or TiO_2 or other oxide metal which is previously deposited and in considering the differences in molar mass between the oxides and the original materials.

For example, silicon has a molar mass of 28 g/mol and silicon dioxide SiO2 of 60 g/mol. It is well known that when a silicon dioxide SiO2 grows by one unit, a silicon depth of about 28/60 = 46.6% (figure 55)

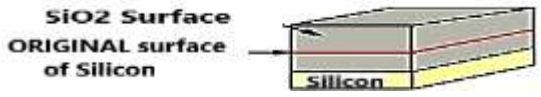

Figure 55: Growth of SiO2 oxide on silicon

This means that the fraction of oxide thickness "below" the initial surface is 46% of the total oxide thickness according to S.M. Sze. [9]

The same must happen, for example for thermal growth of alumina. The molecular masses of Alumina and aluminium are M_{Al2O3} = 102 g/mole and M_{Al} = 27 g/mole. We obtain an aluminium attack ratio of 27/102 = 26%, which implies that the original surface of this metal has shifted by 26% so that 74% of the alumina has grown out of the initial surface of the aluminium….

As regards the technological manufacture of electronics and structure, it therefore seems preferable:

1 / For electronics to choose Titanium Oxide because of its high relative permittivity ε_r =114 allowing to minimize the geometries required for the different capacities

2 / For the Casimir structure, the choice of aluminium, because its low density increases the resonant frequency of the structure and that 74% of the Alumina Al2O3 is outside the metal, allowing to reduce the interface between Casimir electrodes. A simple calculation shows for example that for aluminium gives : :

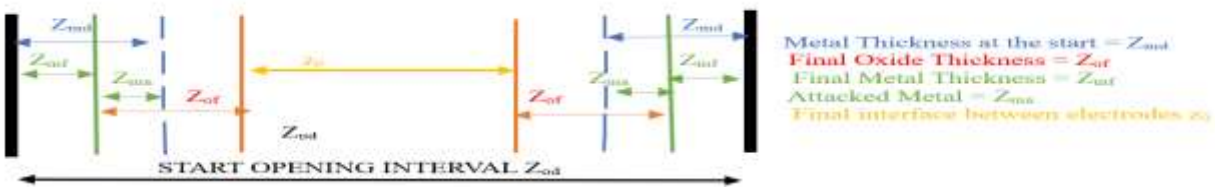

Figure 56 DISTRIBUTION OF THICKNESSES

$$z_{od} = 2\left(z_{md} + z_{of} - z_{ma}\right) + z_0 = 2\left(z_{md} + z_{of} \cdot (1 - 0.26)\right) + z_0$$

$$\Rightarrow z = z_{od} - 2\left(z_{md} + 0.74\, z_{of}\right)$$

For example, we start from an opening z_{od} = 3 µm. We deposit a metal layer of aluminium that is etched leaving a width

z_{md} = 1 µm on each side of the reflector. Then an Alumina Al_2O_3 can grow, the thickness of which is precisely adjusted, simply by considerations of time, temperature, and pressure to increase a necessary thickness to have the desired interface z_0..
For example, if z_0 = 200A °, z_{od} = 3 µm, z_{md} = 1 µm, then z_{of} = 0.662 µm. So, we obtain a Casimir interface of 200 A°. The final remaining metal thickness will be z_{mf} = 0.338 µm and will act as a conductor under the aluminium oxide.

Obviously, the growth of this metal oxide between the electrodes of the Casimir reflector modifies the composition of the dielectric present between these electrodes, therefore of the mean relative permittivity of the dielectric.

Let: ε_0 be the permittivity of vacuum and ε_0. ε_r the metal oxides one (ε_r = relative permittivity ≅ 8 in the case of Al_2O_3), z_{of} the final oxide thickness on one of the electrodes and z the thickness of the vacuum present between electrode, (initially we want z = z_0).

Then the average permittivity e_{0m} of the dielectric is:

$$\varepsilon_{0m} = \frac{z_{of}\,\varepsilon_0\,\varepsilon_r + z_0\,\varepsilon_0 + z_{of}\,\varepsilon_0\,\varepsilon_r}{\left(2\,z_{of} + z_0\right)} = \varepsilon_0\,\frac{\left(2\,z_{of}\,\varepsilon_r + z_0\right)}{\left(2\,z_{of} + z_0\right)} \simeq \varepsilon_0\,\varepsilon_r$$, because z_0 is << z_{of}...

For example, z_{of} = 6620 A° is large compared to z <= 200A ° therefore $\varepsilon_{0m} \cong 8 * \varepsilon_0$ in the case of Al_2O_3.

We have taken into account this change in permittivity in the preceding simulations.

Steps for the Realization of the Structure and its Electronics

We use an SOI wafer with an intrinsic silicon layer : The realisation start with voltage "doubler" is obtained by using CMOS technology with 8 ion implantations on an SOI wafer to make :

1 / The sources, drains of the MOSNE, MOSND of the "doubler" and of the Coulomb force trigger circuits and of the grounding

2 / The source, drains of the MOSPE, MOSPD of the "doubler" and of the Coulomb force trigger circuits

3 / The best adjust the zero-threshold voltage of the MOSNE of the "doubler" circuit

4 / The best adjust the zero-threshold voltage of the MOSPE of the "doubler" circuit

5 / To define the threshold voltage of the MOSNE of the circuit n°1

6 / To define the threshold voltage of the MOSPE of the circuit n°1

7 / To define the threshold voltage of the MOSND of the circuit n°2

8 / to define the MOSPD threshold voltage of the circuit n°2

This electronic done, we take care of the vibrating structure of CASIMIR

9 / engrave the S.O.I. silicon to the oxide to define the location of the Casimir structures (figure 57)

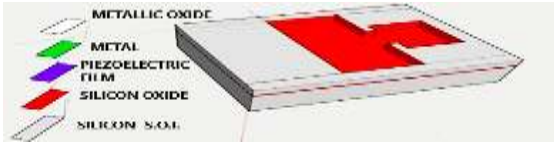

Figure 57 :
9/ etching of S.O.I silicon

10/ Place and engrave a protective metal film on the rear faces of the S.O.I wafer (figure 58)

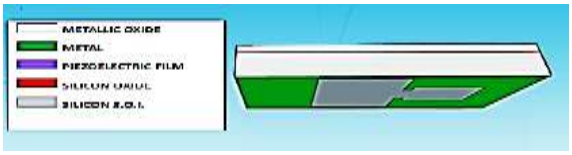

Figure 58:
10/ Engraving of the protective metal rear face of the S.O.I. silicon

11 / Deposit and engrave the piezoelectric layer (figure 59)

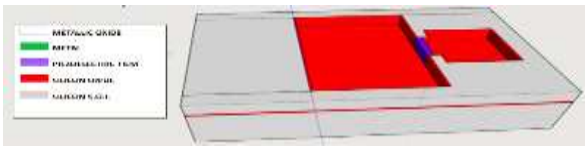

Figure 59:
11/deposition and etching of the piezoelectric layer e
61 deposition and etching of the piezoelectric layer

12/ Depose and etch the metal layer of aluminium (figure 60) .

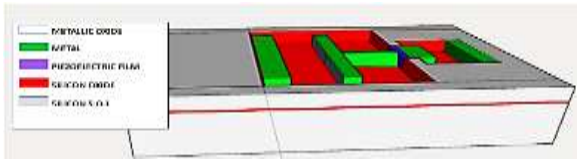

Figure 60:
12/ Metal deposit, Metal engraving
etching of the piezoelectric layer

13 / Plasma etching on the rear side the silicon of the Bulk and the oxide of the S.O.I wafer protected by the metal film to free the Casimir structure then very finely clean both sides (figure 61)

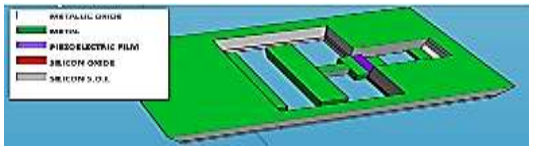

Figure 61:
13/ view of the Casimir device on the rear face, engraving on the rear face of the structures.

14 / Place the structure in a hermetic integrated circuit support box and carry out all the bonding necessary for the structure to function.

15 / Carry out the thermal growth of aluminium oxide Al_2O_3 with a measurement and control of the circuit under a box. The electronic circuit should generate a signal when the interface between the Casimir electrodes becomes weak enough for the device to vibrate ... and then stop the oxidation. (Figure 62)

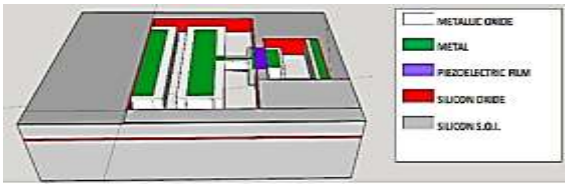

Figure 62:
14 /Adjusted growth of metal oxide under the electronic control, front view of the Casimir device

16 / Create a vacuum in the hermetic box

In the case where the 2 metal electrodes of Casimir, adhere to one another, they can be separated by the application of an electrical voltage on the Coulomb's electrodes.

In order to obtain a current peak greater in intensity, the Casimir cells can be positioned in a series and parallel network at the 2 terminals of a single inductance. For example, 20 Casimir cells can be placed in parallel and 10 in series. (Figure 63)

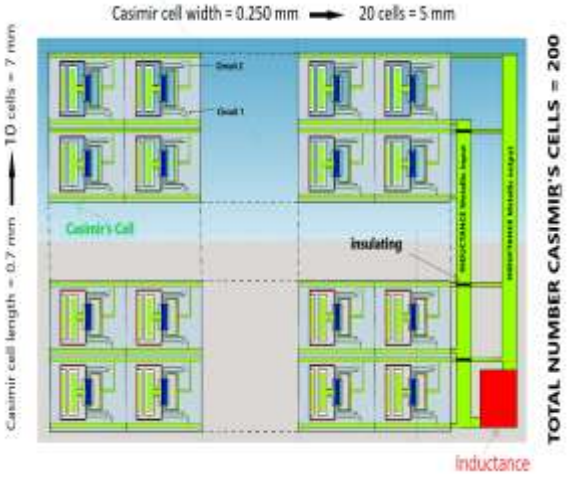

Figure 63: Positioning of 20 Casimir cells in parallel and 10 in series. Circuit 1 , Circuit 2 and Switches of circuit n°1 and n°2

Total of Casimir cells delivering a periodic current during a small part of the vibration frequency of the devices = 200.
Total des cellules = 200,
Width = 5mm, Length = 7 mm
Important increase in current intensity, time duration of the peak, as for the voltage peak

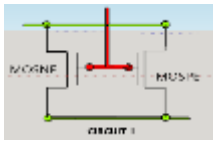

Circuit 1: parallel MOSPE and MOSNE; see Fig 6

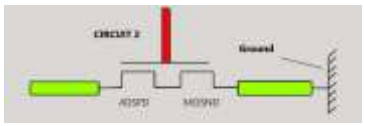

Circuit 2: serial MOSPD and MOSND; see Fig 6

Energy Balance

We will try to show that this physical repository makes it possible to explain, by a constant contribution of vacuum energy, an apparent "perpetual movement" of the MEMS device presented. In fact, the problem is less to extract energy from the vacuum than to extract it without spending more energy that we cannot hope to recover. For example, let us imagine a cyclic system on the model of a piston engine going from a spacing z_{s1} to the smaller spacing z_{s2}, then from z_{s2} to z_{s1}.

The attractive Casimir force is $F_{CA} = S\,\frac{\pi^2\, c\, \hbar}{240\, {z_s}^4}$ (Eq.2),ref [1],[2] ,[3] With S the surface of Casimir's electrodes , $\hbar = h/2\pi$ the reduce Planck constant and c the speed of light . This in $1/z_s^4$, would imply that a larger opposing force is provided to return the piston to z_{s1}.

The Coulomb's force can play this role with an energy balance satisfying Emmy Noether's theorem, because this force will be in $1/z_s^{10}$:

In fact, and in the case of a deformation perpendicular to the polarization of a piezoelectric film, by a Casimir force Fca, we know that the fixed charges Q_F induced by the deformation of this piezoelectric layer are proportional to the Casimir force FCA and are therefore in $1/z_s^4$.

We have $Q_F = \frac{d_{31}\, l_p}{a_p}\, F_{CA} \Rightarrow Q_F = \frac{d_{31}\, l_p}{a_p}\, S\, \frac{\pi^2\, c\, \hbar}{240} \left(\frac{1}{z_s^4} - \frac{1}{z_0^4} \right)$ (Eq. (3)),ref [4] [5] [6]. In this expression when z_s=z_0 the electric charge is null, with piezoelectric coefficient d_{31} (CN^{-1}), l_p, a_p respectively length and thickness (m) of the piezoelectric bridge. It does not depend on the common width bp = bs = bi of the structures (figure 1,2,3,4,5,6,5,6). This point is important and facilitates the technological realization of these structures since it limits the difficulties of their deep and straight engraving. These fixed electric charges inside the piezoelectric bridge have opposite signs and attract mobile charges of opposite signs from the mass on the two metallized faces of this bridge. The mobile charges of one of the faces of the bridge activate the insulating gates of the enriched transistors T.F.T. M.O.S N and P in parallel of switch n°1 (Fig 2).

It generates on these transistors a gate voltage V_G with the expression $V_g = \frac{Q_F}{C_{ox}}$ (Eq.19) . Cox the capacity of the grid's transistors $C_{ox} = \frac{\varepsilon_0 \varepsilon_{ox}}{t_{ox}} L_T W_T$ (Eq.20) with ε_o the permittivity of vacuum, ε_{ox} the relative permittivity of silicon oxide , L_T, W_T , and t_{ox} the length, width and thickness of the grid of the TFT MOS .

The mobile charges of the other face of the bridge supply the sources of the T.F.T. M.O.S. N and P and can circulate to homogenize on a so-called Coulomb electrode, if the threshold voltage of the switch is exceeded.
Before closing switch N°1, this Coulomb electrode was grounded by closing switch N°2 consisting of N and P M.O.S. T.F.T's in depletion and in series. (Fig 65). It is important to note that:

1/ The threshold voltage values of these switches are V_{T1} for switch n°1 and V_{T2} for switch n°2, with abs(V_{T1}) very slightly above abs(V_{T2}).
2/ If the voltage on the insulating gates of the MOS TFTs is above their threshold voltage, then: Switch n°1, changes from OFF to ON but conversely switch n°2 changes from ON to OFF (Fig 7)

Description of Switches n°1 or n°2 and Autonomous Electronic

Switches Electronic Description

These switches are made with:
a/ Circuit n°1 (fig 64): with MOS P and MOS N transistors enriched and in parallel: Threshold voltage V_{TNE} and V_{TPE}
b/ Circuit n° 2 (fig 65): with MOS P and MOS N transistors in depletion and in series: Threshold voltage V_{TND} and V_{TPD}

An important point is that the threshold voltage values of these transistors are positioned as Figure 7.

We have, $V_{TPE} < V_{TND} < 0 < V_{TPD} < V_{TNE}$. For the functioning symmetry $|V_{TPE}|$ can equal $|V_{TNE}|$ and $|V_{TPD}|$ can equal $|V_{TND}|$ Consequently, as $|V_{TND}| < |V_{TPE}|$ and $|V_{TPD}| < |V_{TNE}|$, circuit switch n° 2 is open or closed *just before* circuit switch n° 1 is respectively closed or open (see figure n° 7).

Circuit n°1: Switch n° 1

Switch n°1 consists of an enriched N type TFT MOS in parallel with an enriched P type TFT MOS (see fig 7,64) with their threshold V_{TNE} or V_{TPE} voltage as positioned in fig 2. [11]

The common gates voltage of these enriched T.F.T. MOS N and P in parallel of switch n°1(figure 2), are controlled by the free charges appearing on face n°2 of the piezoelectric bridge. The N and P sources of these T.F.T. MOS are connected to face n° 1 of the bridge and the drains Coulomb's electrode. (Fig 4,6). The input of the R.L.C circuit is connected in series between the return Coulomb electrode and the ground, the autonomous electronic n°3 in parallel (figure 4,5).
This return Coulomb electrode is itself grounded via switch n°2 (Fig 6)

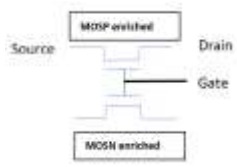

Switch n°1 (Fig. 64)

The switch n°1 is made with two types of enriched MOSPE or MOSNE transistors in parallel, to avoid the exact nature (holes or electrons) of the mobile electric charges appearing on the metal face n°1 of the piezoelectric bridge. Preferably, their threshold voltages are the same in absolute value $|V_{TNE}| = |V_{TPE}|$

VIII /1/4: Circuit 2: Switches n°2

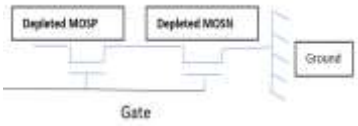

Switch n°2 (Fig. 65)

Switch n°2, consists of a P type depletion T.F.T. MOSPD in series with an N type depletion MOSND (see figure 6,7 ,65).
The common gates of these MOS switches are controlled by the free charges appearing on face n°2 of the piezoelectric bridge. (See figure 4,6)
The input of Switch n°2 is connected to the Coulomb electrode, and its output to the RLC circuit then to ground. Preferably, their threshold voltages are the same in absolute value $|V_{TND}| = |V_{TPD}|$. The values of $|V_{TND}| = |V_{TPD}|$ are lower but very close (90%) of $|V_{TNE}| = |V_{TPE}|$

Schematic and Comportment of the MEMS

Thus, when it is effective (switch n°1 closed), the Coulomb return force F_{CO} is (fig 4,5,6)

$$F_{CO} = \frac{Q_F^2}{4\,\pi\,\varepsilon_0\,\varepsilon_r}\left(\frac{1}{z_r + z_0 - z_s}\right)^2 = \left[\frac{d_{31}\,l_p}{a_p}\,S_S\,\frac{\pi^2\,c\,\hbar}{240}\left(\frac{1}{z_s^4} - \frac{1}{z_0^4}\right)\right]^2\left(\frac{1}{4\,\pi\,\varepsilon_0\,\varepsilon_r}\right)\left(\frac{1}{z_r + z_0 - z_s}\right)^2 \quad \text{(Eq. 4)}$$

We note that F_{CO} is in $1/z_s^{10}$, with z_s = distance (time dependent) between Casimir electrodes, and z_0 = initial distance between Casimir electrodes

The schematic of the sensor part of this MEMS is shown in figures (5 ,6). The perpetual, isotropic and timeless Casimir F_{CA} force, resulting from quantum vacuum fluctuations, causes the deformation of a microscopic piezoelectric bridge embedded in a silicon wafer.

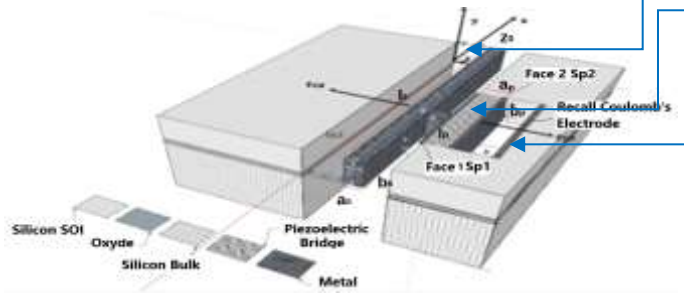

Casimir reflector electrodes
Piezoelectric Bridge
Recall Coulomb's electrode
a_p, b_p and l_p , are thickness, width, and length of the piezoelectric bridge.
a_s, b_s and l_s , are the thickness, width and length of the Casimir moving electrode .

Fig. 4 Vue of the top of device, Axes, Forces , Casimir's Electrodes

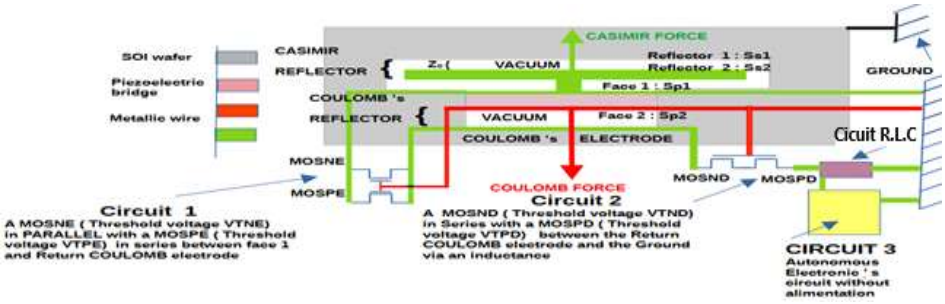

Figures 6: general configuration of the device: MOS grid connections (Face 2 of the piezoelectric bridge: red), Source connections (Face 1 of the piezoelectric bridge:

When the switch n°1 is OPEN the mobiles charges of face n°1 don't move and keep on this face n°1. When the switch n°1 is CLOSED and switch n°2 is OPEN, the free moving electric charges must homogenize between the metallic film of face n°1 and the metallic film of Coulombs electrode (Fig 4,5). Then, as the electrical nature of mobiles charges of faces n°1 and n°2 are opposite, Coulomb's force F_{CO} must appear between the two metallic electrodes.
The threshold voltages of the transistors of switch n°1, technologically predetermined, impose the intensity of Coulomb's forces which can be much greater than the force of Casimir F_{CA}.
The Coulomb force's lifespan is ephemeral, and its dissipated energy is determined by the threshold voltages of switch n°2, when it is close to ground (Fig 7,64,65). The resulting force F_{CO} - F_{CA}, applied to the center of the piezoelectric bridge changes direction or is zero.
The piezoelectric and elastic bridge having no force to keep it deformed, necessarily returns (by the stored deformation energy + the kinetic energy) to its initial position, therefore without any deformation or electrical charges. This ephemeral Coulomb force suppresses the collapse of the two very close electrodes of the Casimir reflector and reduces, then cancels the deformation of the piezoelectric bridge, and thus its electric charges. The structure returns to its initial state and is again deformed by the timeless and homogeneous Casimir force F_{CA} which always exists.
This cycle reproduce itself and the system vibrate (Fig 30) , with the vacuum energy transmitted by the F_{CA} force, as a continuous drive source for the deformation of the piezoelectric bridge and with the self-built Coulomb force F_{CO}, superior and opposed to F_{CA} as the counter-reaction force.

At each cycle, the automatic switching of the integrated switches of circuits n°1 and n°2 distributes differently the mobile electrical charges located on face n°1 of the bridge (Fig. 4, 6,7,64,65). When the switch n°1 return to OFF, immediately followed by the switching to ground of the switch n°2, then the mobile charges present on the electrode of Coulomb disappears by crossing an integrated R.L.C circuit . These peak of current ΔI, flowing through an integrated inductance to the ground induce a peak of voltage ΔU so a peak of power which supply autonomous electronics. (Fig 46 ;47)

The power peak ΔU. ΔI at the terminals of RLC circuit supplies electronics without any external power source and is automatically transformed into a direct voltage of several volts, usable on a high impedance.

Mems Energy Balance

In this part, we will try to make a detailed and exhaustive assessment of the behavior of the MEMS during one vibration. Firstly, we will focus on the first half of this vibration, which we will call the "go" phase. Secondly, we will focus on the second half of the vibration, which is to say the "return" phase.
Let us recall that, the piezoelectric bridge is perfectly elastic which implies, as with any elastic structure, that the energy expended by a mechanical deformation of the positions from 0 to 1 is integrally restored when returning without any permanent deformation, from the positions from 1 to 0. The conditions of use of it are in the purely elastic domain. We do not enter the domain of plasticity.
In the following we propose to put into equation the energy balance of «go» then in "return" steps. Voltage thresholds of the MOS are: **$0 < VT_{PD} < VT_{NE}$, and $VT_{PE} < VT_{ND} < 0$ and $F_{CO} / F_{CA} < p$** . With p the chosen amplification F_{CO} / F_{CA}. We note V_{T1}= abs (VT_{NE} or VT_{PE}) and V_{T2}= abs (VT_{ND} or VT_{PD}), and call V_G the voltage due to the mobiles charge on the face 2 of the piezoelectric bridge and appearing on the gate of all the TFT MOS transistors. [11]

MEMS energy balance during the phase "go" from z_0 to z_1

$0 < V_G <$ abs (V_{T2})< abs(V_{T1}). and $F_{CO} / F_{CA} < p$: switch n°1 OFF, Switch n°2 ON.

a/ At the start we are and, in the condition where At the beginning of the "go" phase we have very small deformations applied to the piezoelectric bridge. Consequently, very small electrical charges are present on it. The electrical voltages V_G on the grid of the enriched and parallel TFT MOS N and P of switch N°1 is lower than their threshold voltage V_{T1}, so this switch n°1 is open and in the OFF position. On the other hand, as $V_G < V_{T2}$, switch N°2 consisting of two TFT MOS N and P in series but operating in depletion mode is closed and in the ON position to ground. In these conditions the so-called Coulomb electrode is to the ground, thus eliminating the Coulomb force F_{CO}.

b/ **0 < abs (V_{T2})< V_G < abs (V_{T1}). and $F_{CO} / F_{CA} < p$: switch n°1 OFF, Switch n°2 OFF**.
No moving electric charge appears on the return side of the Coulomb electrode, which is connected to ground by switch 2, which is ON, and isolated from the piezoelectric bridge by switch 1, which is OFF. The Casimir force begins to deform the piezoelectric bridge more significantly. Consequently, the mobiles charge on face 1 and 2 of the piezoelectric bridge therefore the voltage V_G on the gates of transistors of switch n° 1 and n° 2 increases. This voltage V_G still lower than the threshold voltage V_{T1}, exceeds now V_{T2} of switch n°2 which opens and switches OFF.

The structure being assumed to be perfectly elastic and the amplitudes of the vibrations being extremely low, we will see that the mechanical energy losses by an increase of temperature in the device are negligible.
1/ Note also that the mobile parallelepiped metal electrodes of the Casimir electrodes remain parallel to each other and that the mobile metal Casimir electrode does not deform. It simply transmits its movement to the piezoelectric bridge which deforms but therefore does not heat up. (Fig 4,6)

2/ The expulsion of entropy ΔS from the vibrating structure of Casimir is transmitted to the piezoelectric bridge. It causes an extremely slight increase ΔT in its temperature and expels this heat to the outside. Let us calculate an order of this magnitude ΔT.
We note ΔQ_{vib} the heat transmitted by the vibrations of the piezoelectric bridge. In first approximation, we can use the well-known formula $\Delta Q_{vib} = \Delta S.\ \Delta T$, with ΔS= entropy variation (J °K^{-1}) and Δ T = temperature variation (° K)
However, we know that: $\Delta Q_{vib} = \frac{M_{Structure}\,[2\,\pi\,f_{vib}]^2}{2}\,z_1^2$ Eq. (21) [10] With: f_{vib}= Vibration frequencies of the piezoelectric bridge, $M_{Structure}$ = mass of this bridge, which is the only one to deform because the Casimir electrodes are simply in translations. We note z_1 the maximum deflection of the bridge (Fig 3)

This heat expended at the level of the piezoelectric bridge causes its temperature to increase. As a first approximation we can say: $\Delta Q_{vib} = M_{Structure}.\ C_{piezo}\ \Delta T$. With: C_{piezo} = Specific heat capacity of the piezoelectric bridge (J Kg^{-1} °K^{-1}), ΔT = Temperature variation (°K).

Consequently $\Delta T = \frac{2\,[\pi\,f_{vib}]^2}{C_{piezo}}\,z_1^2$ = Temperature variation of the bridge. Eq. (22)

For example, for a PMN-PT piezoelectric film: $C_{piezo} = C_{PMN\text{-}PT} = 310$ (J Kg^{-1} °K^{-1}), $f_{vib} \approx 10^6$ Hz, $z_e \approx 100*10^{-10}$ m, we

then obtain: $\Delta T \approx 10^{-3}$ °K. The expulsion of entropy from the vibrating Casimir Electrode is negligible. We note that simply half of this expended heat occurs in the "go", the second part occurs in the "return" phases of the vibration.

During a cycle from z_0 to z_1, to deform the ELASTIC PIEZOELECTRIC BRIDGE during the displacement " go " of the vibration , the quantum energy $E_{CASIMIR}$, given by the quantum vacuum , is used for four different energies:

1/ The mechanical energy for the deformation of the elastic bridge: W_{DEFCA}
2/ The energy to create the fixed Q_F charges in this piezoelectric structure : W_{BRIDGE}
3/ The energy for the simple displacement of the point of application of the Casimir force in the middle of the bridge : $W_{CASIMIR}$
4/ The expulsion of entropy $\Delta S/2$ energy, expended in heat due to the friction of the atoms in the half of the vibration of the bridge heat : $\Delta Q_{vib}/2$

We can write that: $E_{CASIMIR1} = W_{DEFCA} + W_{BRIDGE} + W_{CASIMIR1} + \Delta Q_{vib}/2$, (Eq 23).
This quantum vacuum energy $E_{CASIMIR1}$ is bigger than the simple translation energy $W_{CASIMIR1}$.

The energies W_{DEFCA} and also W_{BRIDGE} are store in the deformed piezoelectric bridge as a potential energy.
1/ The translation energy of the Casimir force is:

$$W_{CASIMIR1} = \int_{z_0}^{z_1} F_{CA}\, dz = \int_{z_0}^{z_1} S\, \frac{\pi^2\, \hbar\, c}{240\, z_s^4} dz_S = S\left(\frac{\pi^2\, \hbar\, c}{720}\right)\left[\frac{1}{z_1^3} - \frac{1}{z_0^3}\right] \text{.(Eq 23)}$$

This energy $W_{CASIMIR1}$ represents the translation of the point of application of Casimir force F_{CA} from z_0 and z_1, but absolutely does not consider that this force must also deform an elastic and piezoelectric structure from z_0 to z_1. Let us now calculate this deformation energy W_{DEFCA} of the piezoelectric bridge embedded at its two ends.
We know that the deformation energy of an elastic system is the energy that accumulates in the solid body during its elastic deformation. Yet, all Material Resistance book says that the deformation energy W_d of an embedded elastic bridge and for a constant force F is $W_d = \frac{1}{2}\, z_e\, F$ with $z_e = z_0 - z_s$, the deflection (arrow) acquired by the elastic bridge subjected to the constant force F .

In the case of our piezoelectric bride the force F being the Casimir force, varies in $1/z^4$, with the distance z. So, for a differential deflection dz of the bridge under the force F(z) we can write :

$$d(W_d) = 1/2\, F(z)\, dz\, . \Longrightarrow W_d = \frac{1}{2}\int_{z_0}^{z_s} F(z)dz \Longrightarrow W_{DFCA}(z_s) = \frac{1}{2} S\, \frac{\pi^2\, \hbar\, c}{240} \int_{z_0}^{z_s} \frac{1}{z^4}\, dz = \frac{1}{6}\, \frac{\pi^2\, \hbar\, c}{240} \left[\frac{1}{z_S^3} - \frac{1}{z_0^3}\right] \text{ (Eq. 24)}$$

This energy W_{DEFCA} is stored in the elastic bridge as a potential energy. The position of the mobile Casimir electrode reaches the limit z_1 when the grid voltage V_G on switch n°1 reaches its threshold voltage V_{T1} .
This position z1 reached is unstable because the Casimir force increases with the position. As a result, the mobile Casimir electrode can collapse (see annex). But, when the Casimir electrode is in position z_1 , the switch n°1 switches to ON . The charges present on the metallic face n°1 of the piezoelectric bridge must homogenize with the metallic Coulomb electrode, which was previously grounded by the closing of switch n°2 . Note that when switch n°1 switches, switch n°2 is still open because the voltage $V_G > V_{T2}$ (Fig 3,4,6,7) and the TFT MOS of switch n°2 are in depletion.

The energy stored in the bridge through its deformation is in z_1 , $W_{DFCA1} = \frac{1}{6}\, S\, \frac{\pi^2\, \hbar\, c}{240} \left[\frac{1}{z_1^3} - \frac{1}{z_0^3}\right]$.(Eq 25). Similarly when the structure reaches position z_2 , the memorized elastic energy is , $W_{DFCA2} = \frac{1}{6}\, S\, \frac{\pi^2\, \hbar\, c}{240} \left[\frac{1}{z_2^3} - \frac{1}{z_0^3}\right]$(Eq 26) .
We notice that $W_{DEFCA} > 0$ and that the numerical value of W_{DEFCA1} is a little smaller than the expression calculated when $F_{CA}(z_1)$ was constant: $Wd = \frac{1}{2}\, ze * F_{CA}(z_1)$.

2/ During the displacement " go " the energy $E_{CASIMIR}$ is also used to generates a potential energy W_{BRIDGE} accumulated in the capacity of this piezoelectric bridge which follows the equation:

$$d(W_{BRIDGE}) = Q_F\, d(V_{PIEZO}) \text{ with } V_{PIEZO}$$
$$= \text{voltage beetween the two metallic face of the piezoelectric bridge, with } Q_F = C_{PIEZO} V_{PIEZO} \Rightarrow$$

$$W_{BRIDGE1} = \int_0^{Q_1} \frac{Q_F}{C_{PIEZO}}\, d(Q_F) = \left[\frac{Q_F^2}{2\,C_{PIEZO}}\right]_0^{Q_1} = \frac{a_P}{2\ l_P b_P \epsilon_0\, \varepsilon_{PIEZO}} \left(\frac{d_{31}\, l_p}{2\, a_P}\right)^2 F_{CA}^2 =$$
$$\left(\frac{a_P}{2\ l_P b_P \epsilon_0\, \varepsilon_{PIEZO}}\right) \left(\frac{d_{31}\, l_p\, l_s b_s\, \pi^2 c\, \hbar}{480\, a_P}\right)^2 \left[\frac{1}{z_1^4} - \frac{1}{z_0^4}\right]^2 \text{ (Eq. 27)}$$

We notice that $W_{BRIDGE1} > 0$, similarly when the structure reaches position z_2 , the memorized elastic energy is

$$W_{BRIDGE2} = \int_0^{Q_2} \frac{Q_F}{C_{PIEZO}}\, d(Q_F) = \left[\frac{Q_F^2}{2\,C_{PIEZO}}\right]_0^{Q_2} = \frac{a_P}{2\ l_P b_P \epsilon_0\, \varepsilon_{PIEZO}} \left(\frac{d_{31}\, l_p}{2\, a_P}\right)^2 F_{CA}^2 =$$
$$\left(\frac{a_P}{2\ l_P b_P \epsilon_0\, \varepsilon_{PIEZO}}\right) \left(\frac{d_{31}\, l_p\, l_s b_s\, \pi^2 c\, \hbar}{480\, a_P}\right)^2 \left[\frac{1}{z_2^4} - \frac{1}{z_0^4}\right]^2 \quad \text{(Eq. 28)}$$

In these equations, we use $d(Q_F) = C_{PIEZO}\, d(V_{PIEZO})$, C_{PIEZO} = electrical capacity of the piezoelectric bridge, $C_{PIEZO} \frac{\epsilon_0\, \varepsilon_{PIEZO}}{a_P} b_P l_P$ (Eq 29) . Q_F the naturally creating fixed charges on this piezoelectric structure $Q_F = \frac{d_{31} l_P}{a_P} F_{CA}$ Eq. (3), and we have $Q_e = - Q_F$ = the accumulated mobile charges, coming from the mass, on the surface of the metallic film.This part W_{BRIDGE} of $E_{CASIMIR}$ is stored in the piezoelectric bridge as potential energy and contributes to the usable energy $W_{ELECTRIC}$ appearing during a cycle. So, during the phase "go" from z_0 to z_1 the total energy coming from the vacuum = $E_{CASIMIR}$ is used:

1/to deform the piezoelectric bridge W_{DEFCA},
2/ to produce the electrical charges as potential energy$W_{BRIDGE1}$,
3/Translate the point of application of the Casimir Force $W_{CASIMIR}$,
4/ produce a heat of the structure by the entropic transfer $\Delta Q_{vib}/2$.

We have: $\mathbf{E_{VACUUM} = W_{DFCA} + W_{CASIMIR} + W_{BRIDGE} + \Delta Q_{vib}/2 = W_{GOING}}$ (Eq 30)

W_{DEFCA} and W_{BRIDGE} are potential energies that will be used when the bridge returns to its equilibrium position, that is to say without deformation.

MEMS Energy Balance during the Phase "return" Phase from z_0 to z_1):

0 < abs (V_{T2}) < V_G < =abs (V_{T1}). and Ratio F_{CO} / F_{CA}> = p: switch n°1 ON, Switch n°2 OFF.

Figure 10 below shows the FCO/FCA ratio obtained by the value defined during the technological realization of the MEMS of the threshold voltage VT1 of operation of switch n°1 **.**

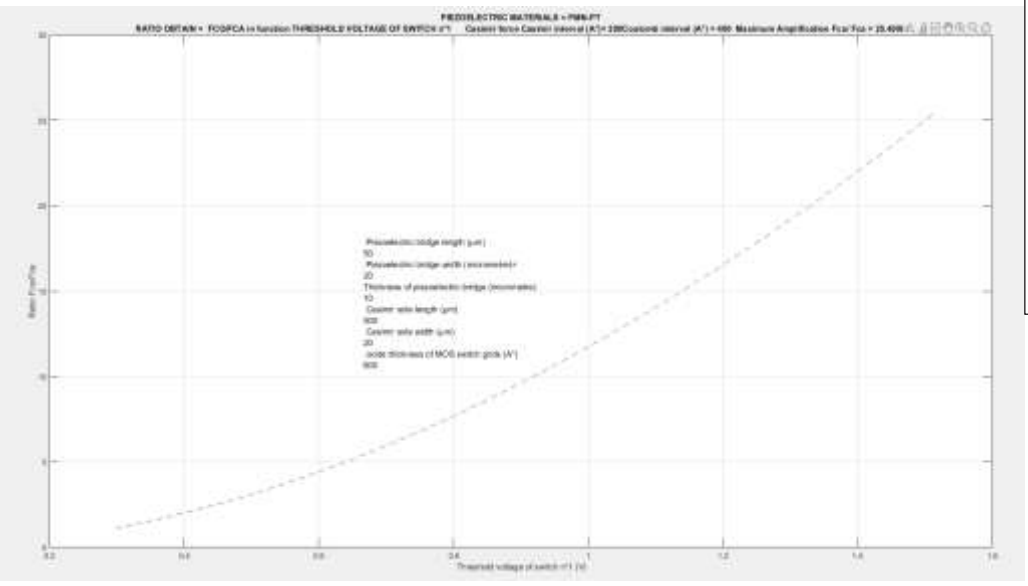

Fig 66. Ratio FCO/FCA obtain in function of the threshold voltage VT1

The voltage on the grids of switch n°1 exceed their threshold voltage. This switch commute ON. The switch n°2 is till OFF. The free charges Q_{m1}, stored on the metal electrodes of face 1(Fig 4 ,6), passing through one of the MOSE transistors, are uniformly distributed on the Coulomb metal electrode of the surface for example S_{C1} = lp*bp. This metallic Coulomb's electrode therefore has approximately a mobile charge Q_{mn} S_{C1}/ S_{P1} = Q_{mn}/2 if S_{C1} = S_{P1} . This homogenization is obligatory because there is no electric field in a perfect metallic conductor.

The free charges $Q_{m2,}$ stored on face 2 and on all isolated grids TFT MOS don't move. So, grids electrode and return electrode have opposite free charge. (Fig 4,5,66). A Coulomb force F_{CO} then appears between these two electrodes during the very short instant when switch no. 2 is still open, isolating the Coulomb electrode from the ground. Fig 10 .The resulting force F_R= F_{CO}-F_{CA} is now applied to the piezoelectric bridge. This force F_R, depending on the choice of the threshold voltage V_{T1} which condition the value of the amplification F_{CO} /F_{CA}, is opposite to the force F_{CA} or null. In presence of this null or opposite force the deformations of the bridge, its electrical charges, so the grids voltage are necessarily reduced.

Since the threshold voltage V_{T2} of switch n°2 is lower but very close to V_{T1} (we choose $V_{T1} - V_{T2}$ = 50 mV), the time duration during which this Coulomb force is exerted is very small (a few nanoseconds). But very quickly, the switch N°2 commutes from OFF to ON, grounding the Coulomb electrode via an R.L.C. circuit, (Fig 15). The Coulomb force vanishes after its appearance at position z_2. This position z_2 is very close to position z_1 of its appearance. The values of V_{T2} and V_{T1} impose that z_2 is very close to z1.

The energy $W_{COULOMB} = \int_{z_1}^{z_2} F_{CO}\,dz$ expended by the Coulomb force remains low, even if this force is several times that of Casimir in intensity. The time of existence of F_{CO} is of the order of a few tens of nanoseconds (fig 5, 10,11,18). The position z_1 of appearance of this force F_{CO} (fig. 10) is such that F_{CO} = p and is numerically calculated by MATLAB (fig. 12).

$$F_{CO}=pF_{CA} \Rightarrow \frac{Q_F\ Q_F}{8\,\pi\,\varepsilon_0\,\varepsilon_r}\left(\frac{1}{z_r+z_0-z_S}\right)^2 = \left[\frac{d_{31}\,lp}{a_p}\,S_S\,\frac{\pi^2\,c\,\hbar}{240}\left(\frac{1}{z_S^4}-\frac{1}{z_0^4}\right)\right]^2\left(\frac{1}{4\,\pi\,\varepsilon_0\,\varepsilon_r}\right)\left(\frac{1}{z_r+z_0-z_S}\right)^2 = p\,S\,\frac{\pi^2\,c\,\hbar}{240\,z_S^4} \quad \text{Eq 31}$$

We note that the position z_1 depends on the values of the interface's z_o of Casimir's electrodes and of Coulomb's electrodes z_r.

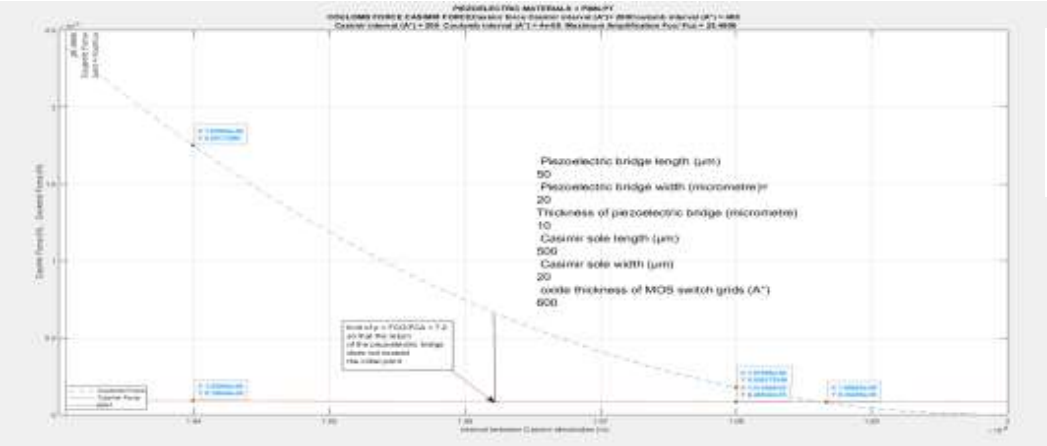

Fig. 67: Force of Casimir and Force of Coulomb

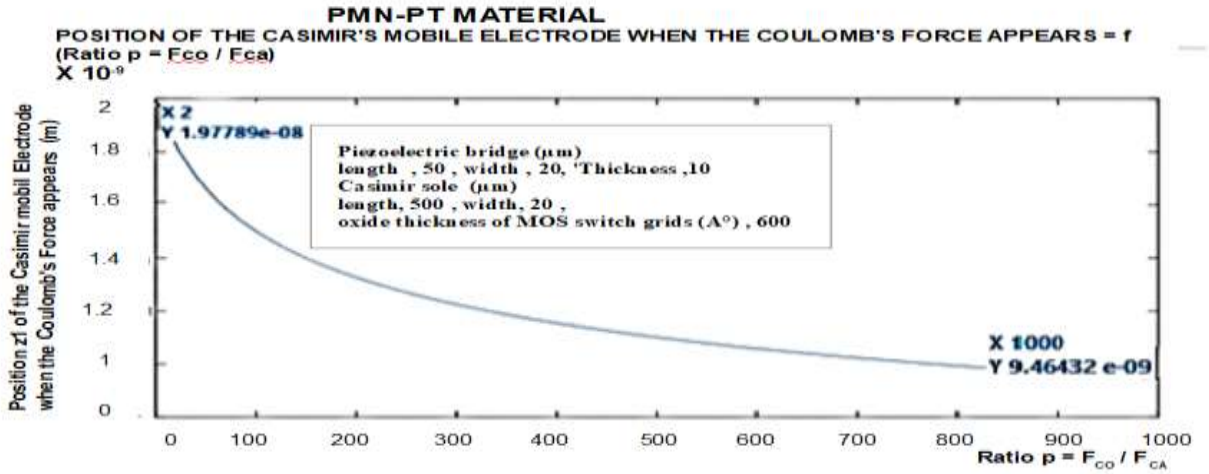

Fig. 68: Position of the mobile Casimir electrode z_1 where the Coulomb force occurs : $z_r = z_0$ =200A°,ls = 500 µm, bs = 20 µm, lp = 50µm, bp =20µm, ap = 10µm

The F_{CO}-F_{CA} force is now applied to the mobile structure. This resulting force is at least zero or of greater intensity than the Casimir force F_{CA}. It contributes with the energy stored in the elastic bridge to straighten the structure and to give it kinetic energy. This F_{CO} force exists as long as switch n°2 has not switched to ground, canceling its existence by the dispersion of charges on the Coulomb electrode. We describe below the energy dispensed in the cycle of the piezoelectric bridge positions.
We hope show that a usable energy $W_{ELECTRIC}$ is possible and not due to any electrical energy applied but by the dissipation of the mobile electric charges to the mass throw the switch n°2 and an R.L.C. circuit.(Fig 71)

From z1 to z0 (returning phase): There are two phases for this return to z0 :

1/from z_1 to z_2 where the Coulomb's force F_{CO} exist and contribute to straighten the elastic structure and to give it kinetic energy ,
2/ from z_2 to z_0 where this acquired kinetic energy, and the remaining energy still stored in the structure which will be dissipated by the energy spent by the Casimir force.

1/ Calculation of energies between z_1 and z_2. As soon as switch n°1 has switched to homogenize the electric charges between face 1 of the bridge and that on the Coulomb electrode, the resulting force FCO -FCA straightens this bridge and the electric charges drop. The electric voltage on the grids falls below the threshold voltage of this switch n°1 which switches again to The energy $W_{COULOMB}$ is write

$$W_{COULOMB} = W_{FC0} = \int_{Z_2}^{Z_1} F_{C0}\, dz = \left\{S_S \cdot \frac{\pi^2\ \hbar\ c}{240} \cdot \frac{d_{31}\ l_p}{a_p}\right\}^2 \left(\frac{1}{8\,\pi\epsilon_0\,\epsilon_r}\right) \cdot \int_{Z_2}^{Z_1} \left[\left(\frac{1}{z_s{}^4} - \frac{1}{z_0{}^4}\right)\left(\frac{1}{z_r+z_0-z_s}\right)\right]^2 dz_s \quad \text{Eq 32}$$

It only exists between the very close positions z_1 and z_2. The literal formulation of the $W_{COULOMB}$ energy is possible but its expression is not convenient because it is too complex. We have preferred to calculate its numerical value between the value z_1 and z_2 by MATLAB.

The position z_2 of commutation of switch n°2 is deduced from the chosen threshold value $V_{T2} = V_{T1}$-.05 (V) of switch n°2. We note that we can minimize the value of the energy spent by $W_{COULOMB}$, by choosing a value of the threshold voltage V_{T2} close but slightly lower than V_{T1} of switch n°1.For example, $V_{T2} = V_{T1}$- 0.05 (V).
We use MATLAB to find the position z_2 of commutation of circuit 2 to cancel the Coulomb's Force F_{CO}, see (Eq 16) and figure 11. Indeed, we have the electric charge in the TFT MOS , $Q_2 = \frac{d_{31}\ l_p}{a_p}\ S_S\ \frac{\pi^2\ c\ \hbar}{240}\left(\frac{1}{z_2^4} - \frac{1}{z_0^4}\right)$ with Q_2=Cox V_{T2} .

So , $z_2 = \frac{1}{\sqrt[4]{\left[\frac{240\ a_p\ C_{ox}}{d_{31}\ l_p\ \pi^2\ c\ \hbar\ S_S} V_{T2} + \frac{1}{z_0^4}\right]}}$ (Eq 33). We present in figure 68 the curve representing the translation energy of the Casimir force as well as the Coulombs force the time when the structure is between the positions z and z, which represents a few nanoseconds.

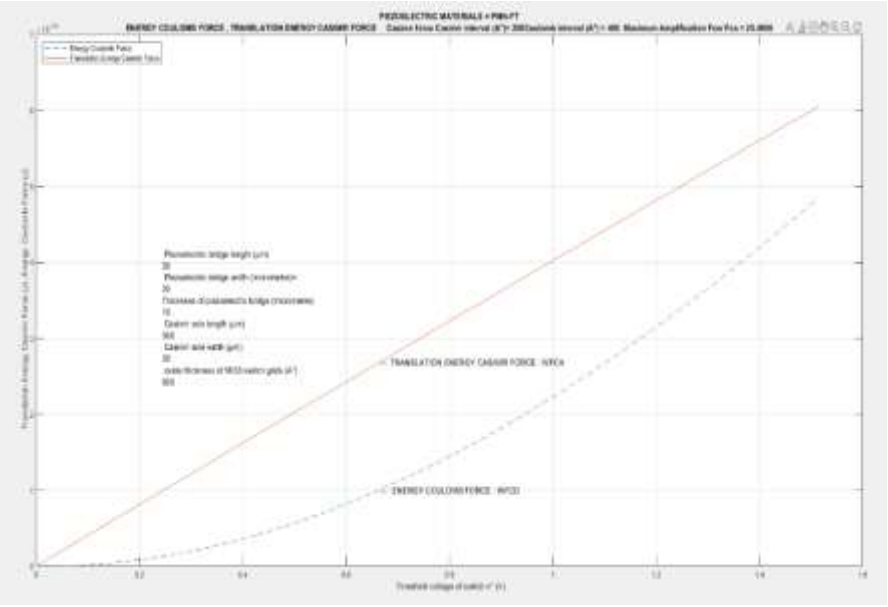

Fig 69 Energy of translation of Casimir Force and energy of Coulombs 'Force between its apparition in the position z_1 and its disappearance in position z_2

We can calculate the energy spent in the first part of return of the structure (from z_1 to z_2) Fig 3 , by simply calculating the kinetic energy W_{CIN} acquired by the structure when it reaches the position z_2 upon its return . We know that the variation of the kinetic energy W_{CIN} is equal to the sum of all the energies supplied or spent to the moving structure. Thus, as we know the numerical value of all these participants in the variation of this kinetic energy W_{CIN}, we can write

equation 34 which allows us to calculate W_{CIN} because all the terms are known.

$W_{CIN} = (W_{DFCA1} + W_{BRIDGE1}) - (W_{DFCA2} + W_{BRIDGE2}) + W_{COULOMB} - (W_{CASIMIR1} - W_{CASIMIR2})$ (Eq. 34) and fig 68.

We know the kinetic energy acquired in z1 and know that then the Coulomb force disappears. The structure must now spend this energy which gives it inertia. The braking energy provided by the Casimir force reduced by the stored elastic energy will cancel this inertia.
Let us calculate the final ascent position z_f of the structure. It has an inertia provided by the kinetic energy W_{CIN}, a stored elastic energy W_{DFCA} but is slowed down by the energy provided by the Casimir force.
We can write $W_{CIN} + \frac{1}{6} S \frac{\pi^2 \hbar c}{240}\left(\frac{1}{z_2^3} - \frac{1}{z_f^3}\right) = \frac{1}{3} S \frac{\pi^2 \hbar c}{240}\left(\frac{1}{z_2^3} - \frac{1}{z_f^3}\right) \Rightarrow W_{CIN} = \frac{1}{6} S \frac{\pi^2 \hbar c}{240}\left(\frac{1}{z_2^3} - \frac{1}{z_f^3}\right)$ Eq35
we deduce of this equation that the final position z_f of the bridge is $z_f = \frac{1}{\sqrt[3]{\left[\frac{1}{z_2^3} - \frac{6 W_{CIN}}{A} \frac{240}{\pi^2 \hbar c}\right]}}$ Eq 36 . We can see in Figure 17 that depending on the acquired inertia which depends on the energy provided by the Coulomb force, zf can slightly exceed its initial position. We will use this property at the end of this article in order to increase usable energy.

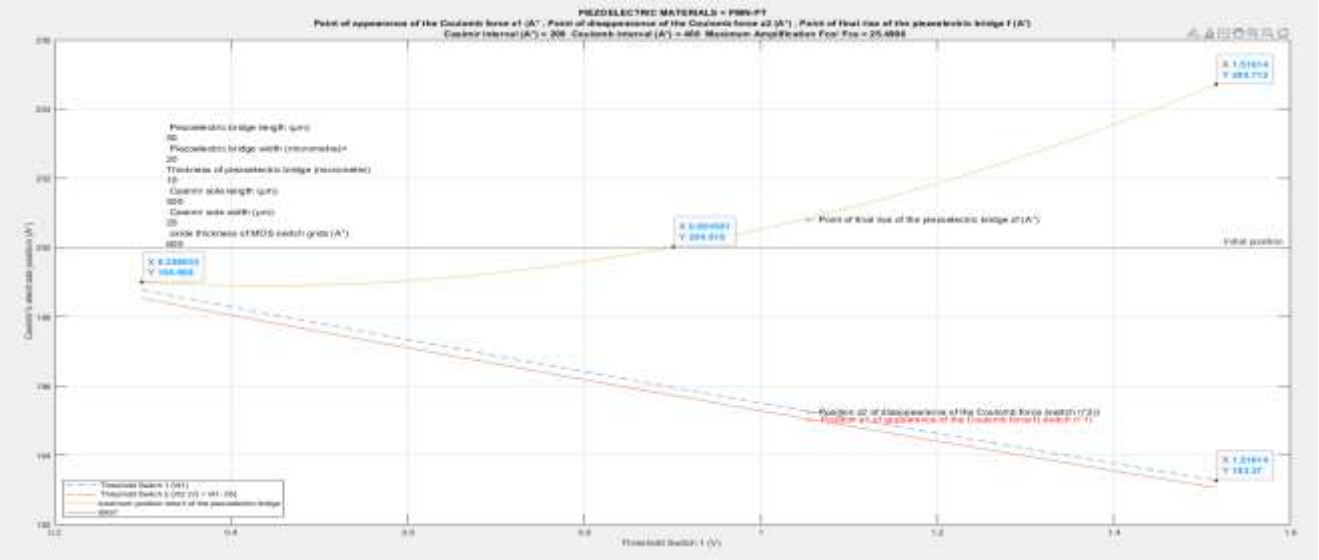

Fig 70: Positions of :
1/ The final rise z_f of the structure,
2/ of the point z_2 of disappearance of the Coulomb force depending on the threshold voltage V_{T2} of switch n°2
3/ of the point z_1 of appearance of the Coulomb force depending on the threshold voltage V_{T1} chosen for switch n°1

It is easy to calculate the damping energy $W_{CASIMIR2}$ that appears between the intermediate position z_2 and the final position z_f. We have $W_{CASIMIR2} = \int_{z_2}^{z_f} F_{CA}\, dz = \int_{z_2}^{z_f} S \frac{\pi^2 \hbar c}{240\, z_s^4} dz_S = S\left(\frac{\pi^2 \hbar c}{720}\right)\left[\frac{1}{z_f^3} - \frac{1}{z_2^3}\right]$ (Eq 37)

As, at position z_2 the switch n° 2 commutes to ON and puts the Coulomb electrode to ground through the RLC circuit below (Fig 71) . The electrical charges present on the Coulombs electrode flow towards the ground, creating a current and a power which remains to be evaluated.

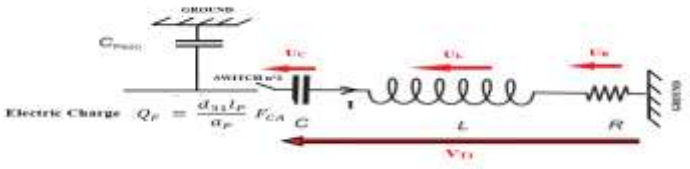

Fig 71 : RLC circuit to power the autonomous electronics for converting power peaks into direct voltage

We now evaluate this usable current flowing to ground. We put another capacitance C in the circuit which is an adjustment capacitance. We call $C_E = \frac{C_{PIEZO}\, C}{C_{PIEZO} + C}$ the equivalent capacity of the capacities in series.

When the switch n°1 commutes, we have the equation $U_C+U_L+U_R$, with U_R= R I, U_L=L dI /dt and $Q_F = U_C C_E$. with R a resistance, L an inductance and C a capacity. After rearranging we have the following equation

$\frac{d^2U_C}{dt^2} + \frac{R}{L}\frac{dU_C}{dt} + \frac{U_C}{L\,C} = 0$ Eq 38. This differential equation has solutions that depend on the value of its determinant.

We choose the values of R, L, C in such a way that the determinant $\Delta = \sqrt{\left(\frac{R}{L}\right)^2 - \frac{4}{LC}} = 0$ of this equation vanishes.

So, if $\Delta > 0$ the solution is : $x_1 = \frac{R}{2\,L}\left(-1 + \sqrt{1 - \frac{4\,L}{C\,R^2}}\right)$ *and* $x_2 = \frac{R}{2\,L}\left(-1 - \sqrt{1 - \frac{4\,L}{C\,R^2}}\right) < 0$ and if Δ=0 then we have $x_1 = x_2 = -\frac{R}{2\,L}$. Taking into account the initial conditions, we obtain $u_c = \frac{V_{T1}}{x_1 - x_2}\,[x_1 \exp(x_2 t) - x_2 \exp(x_1 t)]$Eq 36, and $i_c = C\frac{du_C}{dt} = C\frac{V_{T1}\;x_1 x_2}{x_1 - x_2}\,[\exp(x_2 t) - \exp(x_1 t)]$ (Eq 39) . The peak of current is given when d(i_c)/dt =0

so at the time $t_{imax} = \frac{Ln\left(\frac{x_2}{x_1}\right)}{x_1 - x_2} = \frac{Ln\left(\frac{1+\sqrt{1-\frac{4\,L}{C\,R^2}}}{1-\sqrt{1-\frac{4\,L}{C\,R^2}}}\right)}{\frac{R}{L}\sqrt{1-\frac{4\,L}{C\,R^2}}}$ Eq 40 Replacing t by t_{imax} in the equation 37 we obtain the expression for the maximum of current i_{cmax} ; and the maximum of the voltage is $u_{cmax} = V_{T1}$

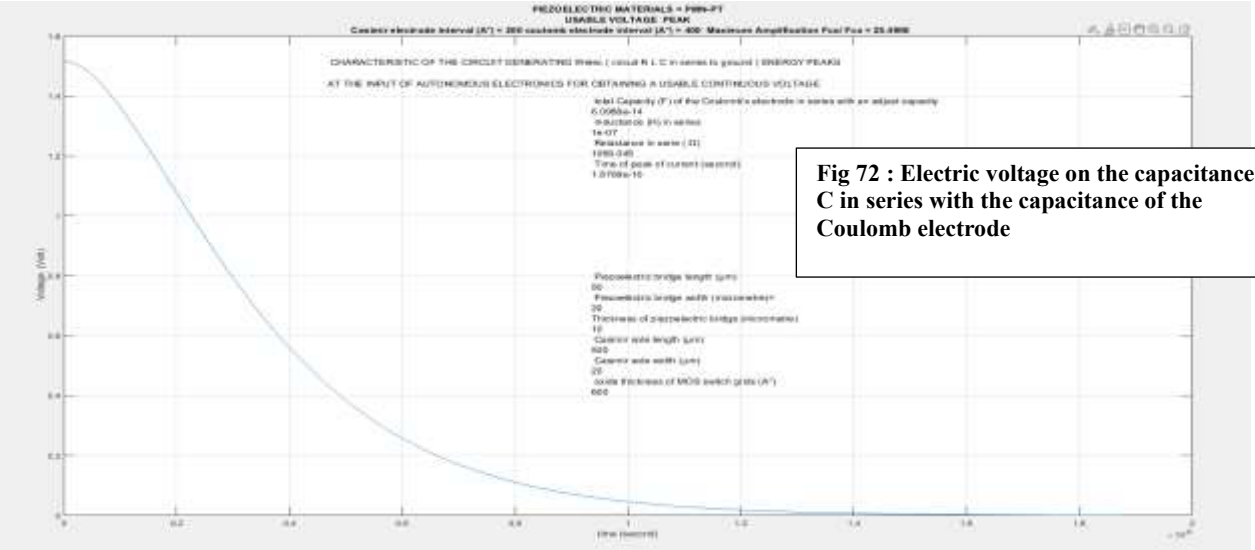

Fig 72 : Electric voltage on the capacitance C in series with the capacitance of the Coulomb electrode

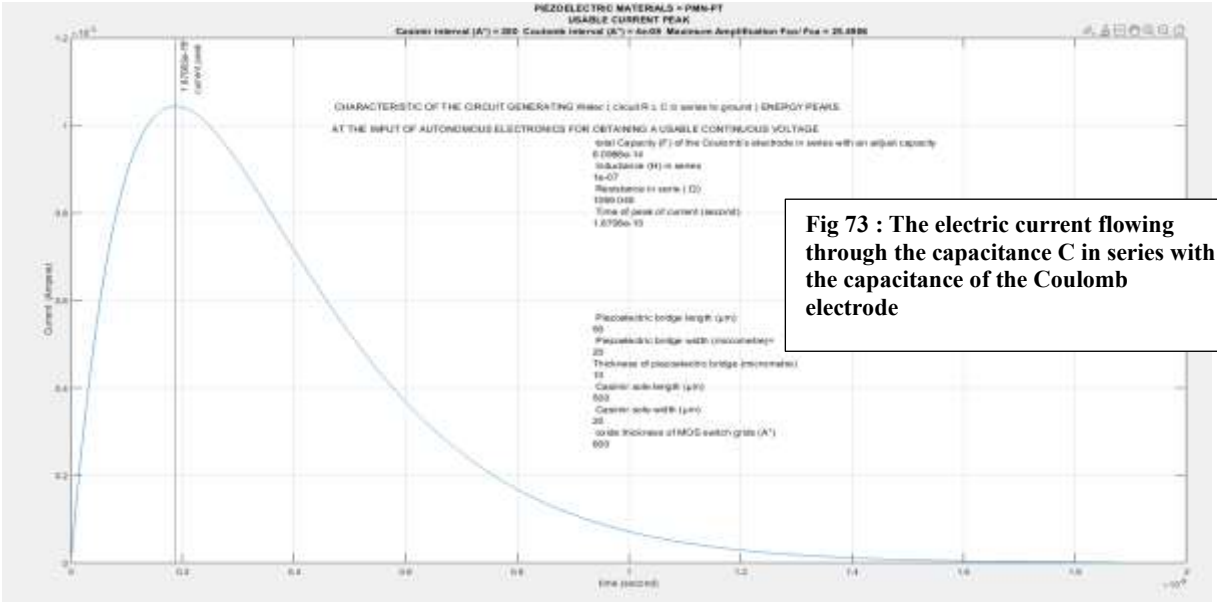

Fig 73 : The electric current flowing through the capacitance C in series with the capacitance of the Coulomb electrode

The electrical power of the signal is:

$$P(t) = u_c\, i_c = \left(\frac{V_{T1}}{x_1 - x_2}\right)^2 C\, x_1 x_2\, [\exp(x_2 t) - \exp(x_1 t)][x_1 \exp(x_2 t) - x_2 \exp(x_1 t)] \quad \text{Eq41}$$

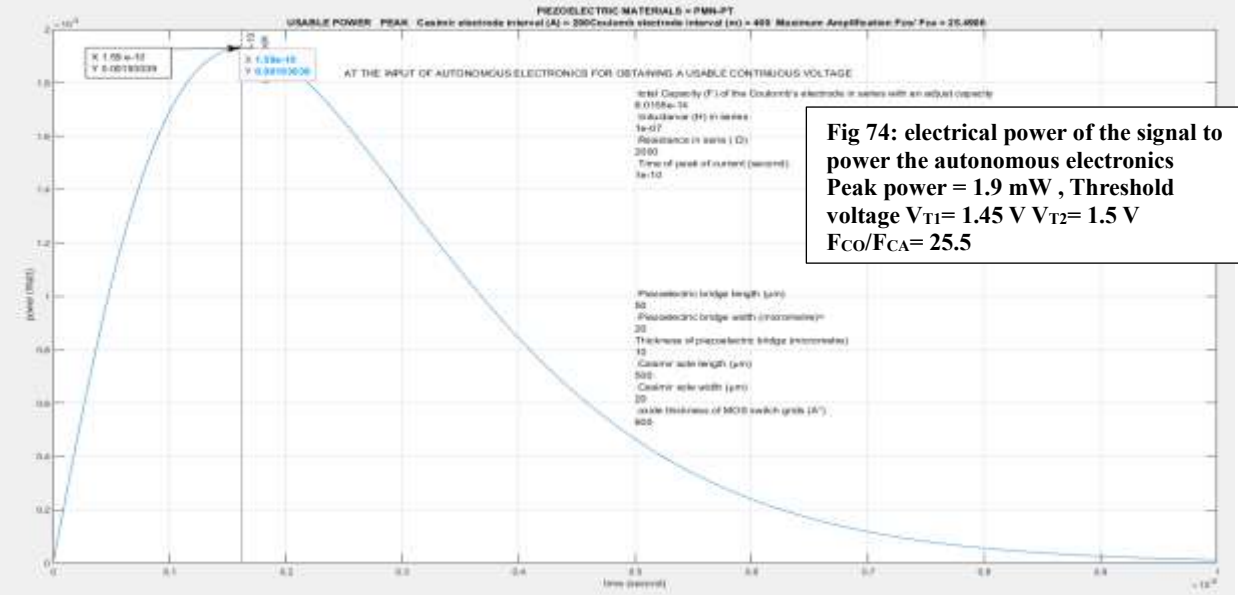

Fig 74: electrical power of the signal to power the autonomous electronics Peak power = 1.9 mW , Threshold voltage V_{T1}= 1.45 V V_{T2}= 1.5 V F_{CO}/F_{CA}= 25.5

We note on fig 73 and 74 that the maximum t_{imax} = 1.87 10^{-10} (s) for the peak current is different than those t_{pmax} = 3.03 10^{-10} for the peak power.

The peak power of 1.93 mW is sufficient to power the autonomous electronics of fig 46,47 and obtain a useful voltage of several volts in a few milliseconds. The period of a vibration being (fig 30) of 2 µs for an F_{CO} /F_{CA} of simply 2, the average power over a period is then approximately 1.93 10^{-3} * 3.03e^{-10} / 2e^{-6} ≈ 0.3 µW.
We deduce that the power provided by the system in 1 second is of the order of 3e-7 / 2e^{-6} ≈ 0.15 W.

Knowing the power P(time) we can numerically evaluate this finale and useable energy, by MATLAB. We obtain $W_{ELECTRIC}$ in fig 75 . Eq40

$$W_{ELECTRIC}(t) = \int_0^{10^* t_{max}} u_c\, i_c\, dt = \left(\frac{V_{T1}}{x_1 - x_2}\right)^2 C\, x_1 x_2 \int_0^{10^* t_{max}} [\exp(x_2 t) - \exp(x_1 t)][x_1 \exp(x_2 t) - x_2 \exp(x_1 t)]\, dt$$

The energy balance is completed for the "return" phase to its initial position of the structure.

We have $\mathbf{W_{RETURNING} = W_{CIN} + W_{ELECTRIC} + W_{DFCA2} + W_{BRIDGE2} - W_{CASIMIR2} + \Delta Q_{vib}/2}$ **(Eq 42)**

On Figure 75, we can make the energy balance of the energies provided by the quantum vacuum in the "going" and "returning" phases.

The constant energy provided by the quantum vacuum ocean in the "go" phase simply changes its nature and subdivides into other energies in the "return" phase of vibrations. One of these energies in this "return" phase can be used by creating a little electrical energy.
We note that the energy necessary for the perpetual maintenance of these vibrations is constantly provided by the isotropic and timeless energy of the quantum vacuum and that it is possible to extract from this gigantic ocean of energy of "nothing" a small electrical and exploitable energy.
Whatever the F_{CO}/F_{CA} amplification factor, we note that $W_{RETURNING}$ is always slightly lower than E_{VACUUM} , thanks to the choice of $W_{ELECTRIC}$ which can be modulated.

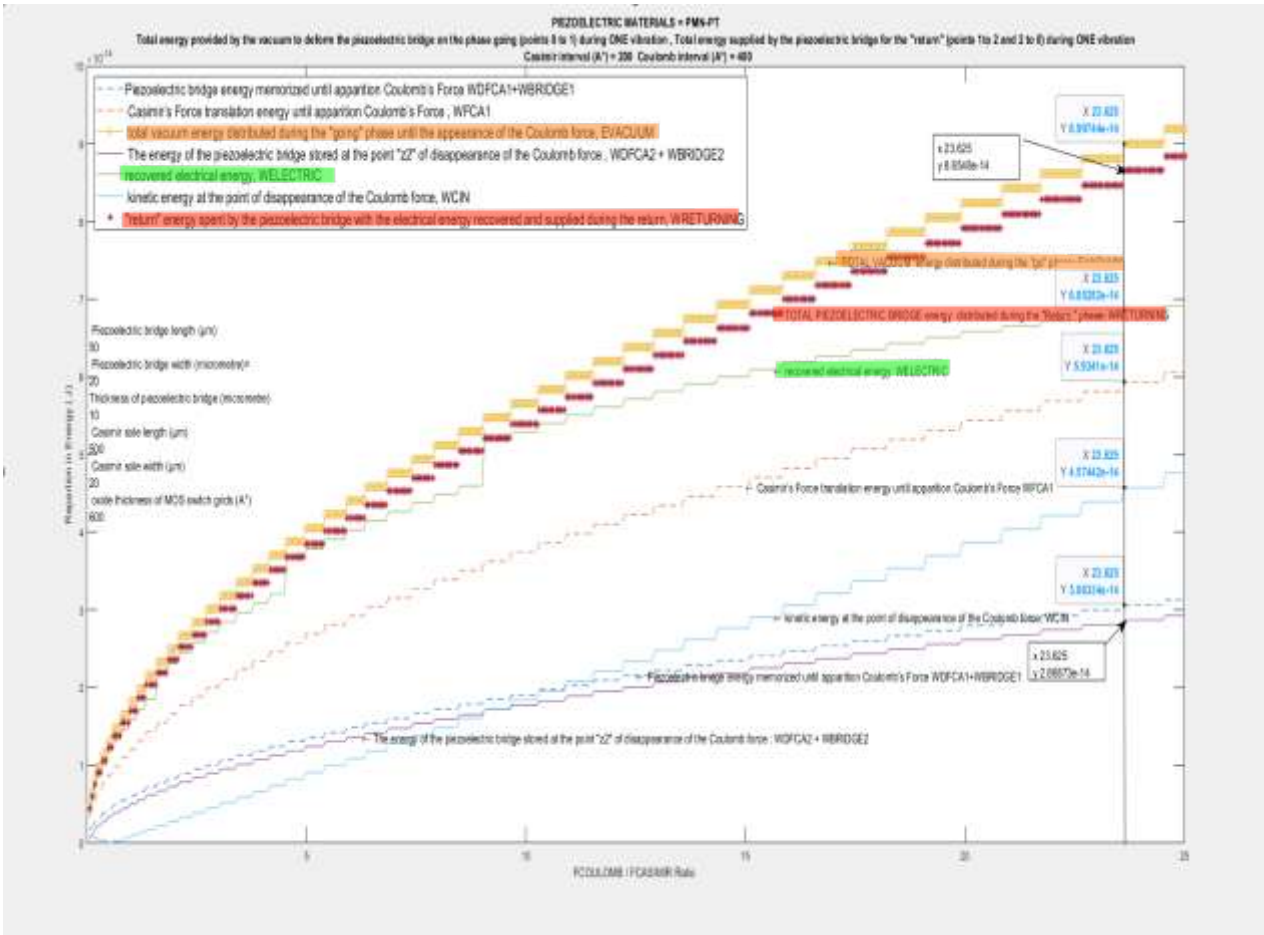

Fig 75: Balance of the energies of the "go" and "return" phases for the proposed MEMS which seems to be able to "extract energy from the quantum vacuum."

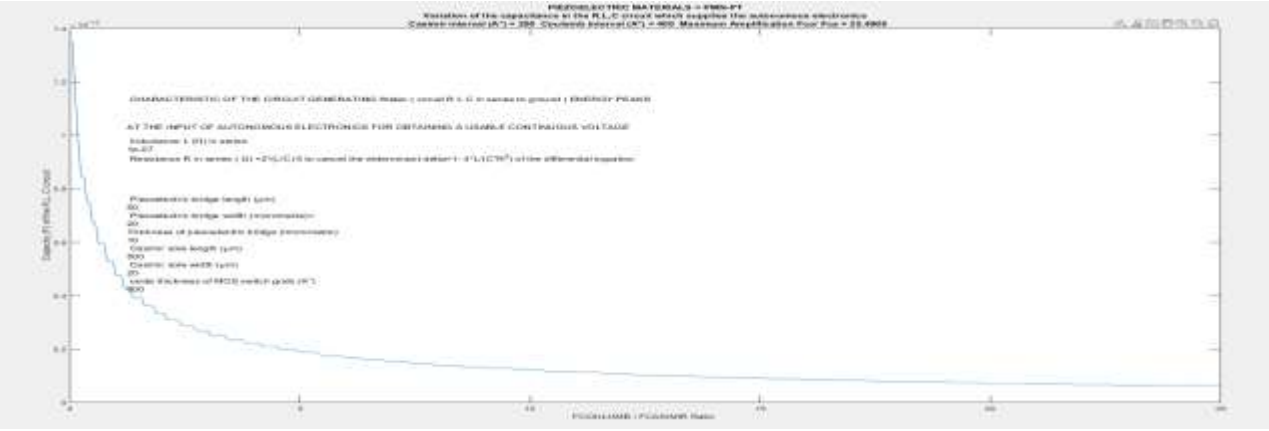

Fig 76 variation of the RLC circuit capacity as a function of the F_{CO}/ F_{CA} amplification used to adapt the usable electrical energy

We note that this energy balance seems to satisfy the fundamental theorem on invariants - of which energy is a part - of the mathematician EMMY NOETHER.

This very important theorem of 1905 explains why, as Monsieur de Lavoisier said, "Nothing is created, nothing is lost, everything is transformed."

We observed that in the referential of our 4 dimensions Space-Time plus the ocean of Quantic Vacuum, the energy is conserved which is consistent with EMMY NOETHER'S theorem. Remember that energy is defined as the "physical

quantity that is conserved during any transformation of an isolated system.
However, the system constituted by simply the MEMS device in space is not an isolated system while the system constituted by the MEMS device plus the space plus the energy vacuum seems an isolated system

We do not create energy ex nihilo, but we transform the energy of vacuum fluctuations, isotropic and timeless, present throughout the universe, to perpetually vibrate a structure on a very low amplitude and obtain usable energy from it.

The part of the MEMS energy sensor vibrates at frequencies depending on the size of the structure and operating conditions, but with an amplitude of just a few Angstroms. These vibrations should not be confused with an impossible perpetual motion, as the system can be continuously powered by the vacuum energy responsible for the Casimir force. The following diagram summarizes the operation of this presented MEMS (Fig77 and Fig 78)

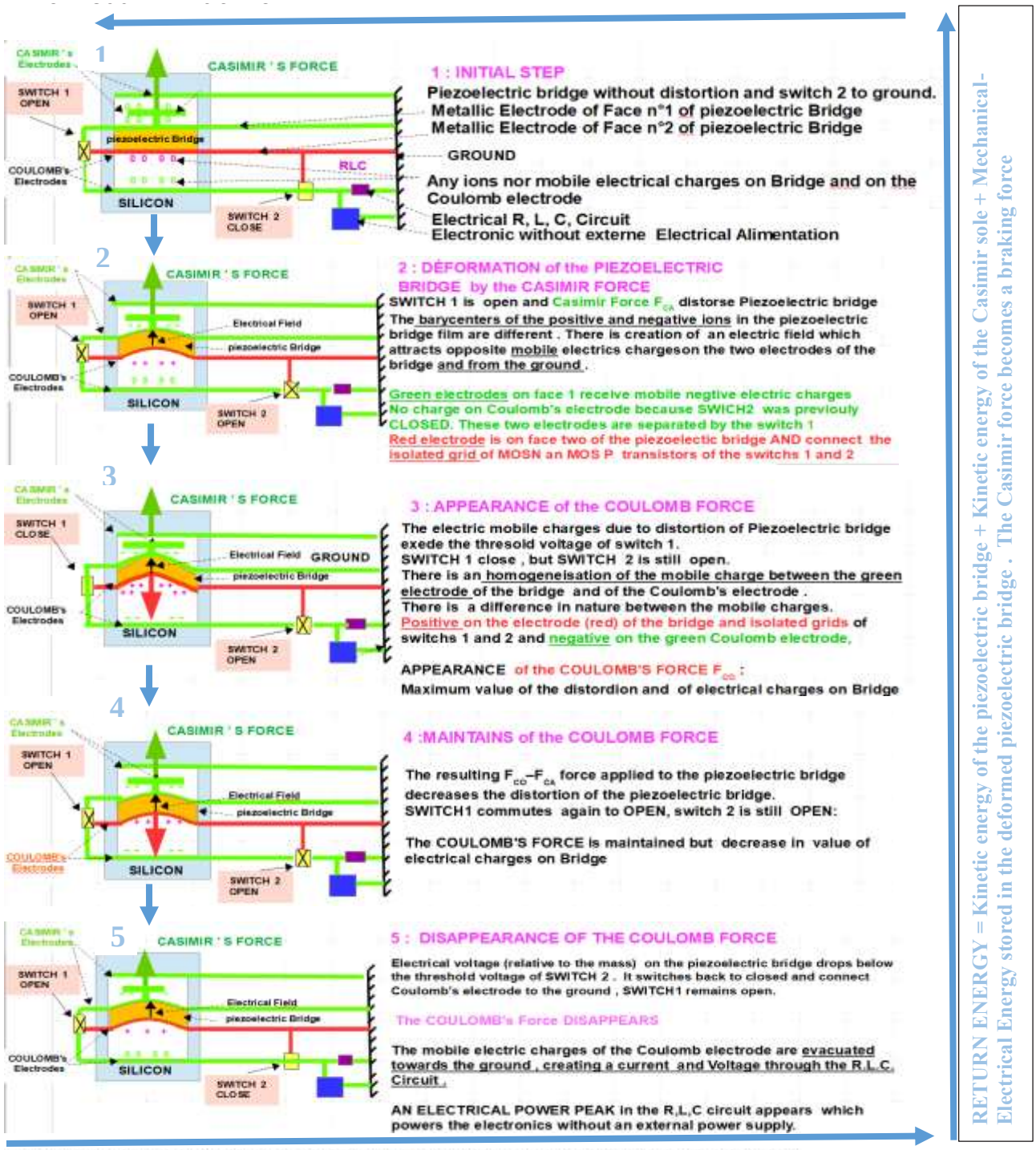

Fig 77: Overview of the 5 successive and repetitive steps of the M.E.M.S.

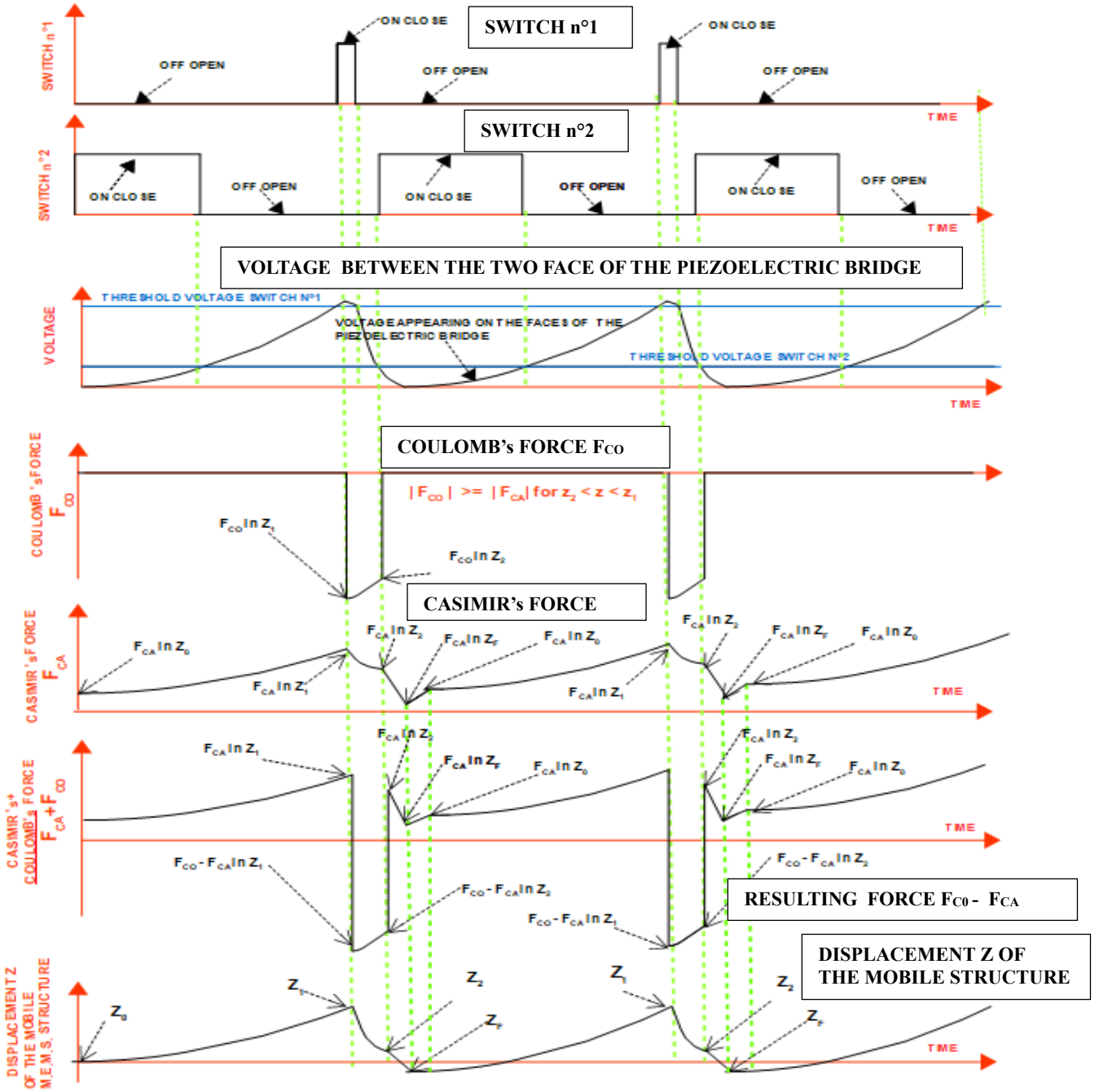

Fig 78: shape of the curves representing
1/ The switching of the two switches , 2/ The electrical voltage on face 1 of the piezoelectric bridge , 3/ The Casimir forces F_{CA} , 4/ The coulomb forces F_{CO} , 5/ the energies W_{FCO}, W_{FCA}, W_{FCO} -W_{FCA}, 6/ The maximum elevation z_f of the moving part

We notice in the previous pages that the piezoelectric bridge could reach a position z_f which exceeds its initial position z_0.

We can take advantage (fig 79) of this observation by modifying the moving part of this MEMS to provide the RLC circuit with the two signs of current peak and voltage emitted by the sensor. This modification should increase the continuous electrical voltage on the capacitive output of the autonomous electronic circuit whose role is to transform the signals from the quantum vacuum energy sensor series. (Figure 24)

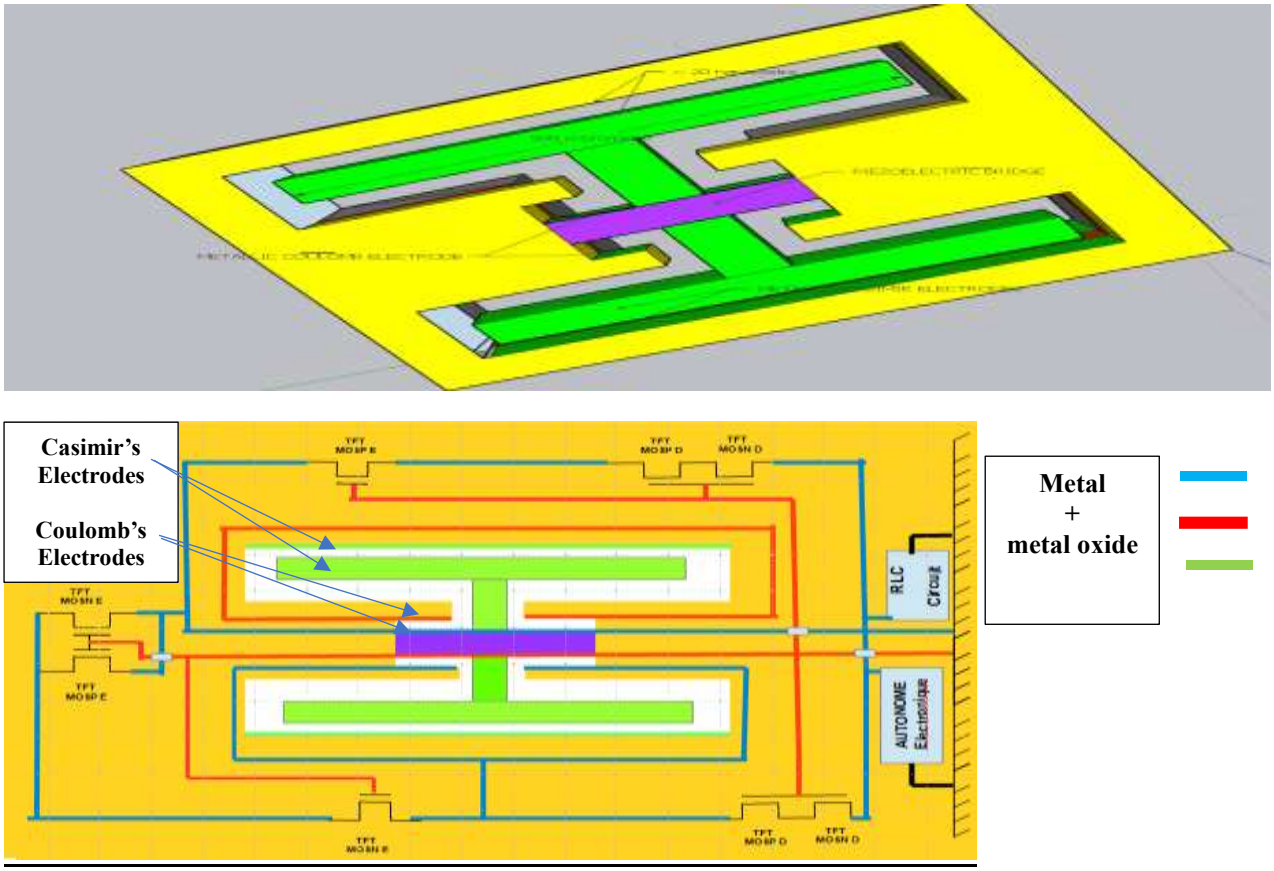

Fig 79: Shape of the MEMS circuit making it possible to double the direct voltage at the output of the autonomous electronic circuit, by providing it with consecutive voltage and current peaks of opposite sign.

This work on the energy balance of a M.E.M.S., which appears to be able to extract energy from a new, totally unexploited source, was carried out completely alone and without the help of any organization, by an old retiree. B

It seems that - unless there is always a possible error - the fundamental theorem of EMMY NOETHER from 1905 is not contradicted or the thermodynamics' law .

In the event of a theoretical confirmation by specialists, the supreme and definitive judgement will be the realization of a prototype and I will be happy to participate to this development .

Simple Remark and Resume

Remember that energy is defined as the "physical quantity that is conserved during any transformation of an isolated system".

However, the system constituted by simply the MEMS device in space is not an isolated system while the system constituted by the MEMS device plus the space plus the energy vacuum seems an isolated system.

The part of the MEMS energy sensor vibrates continuously at frequencies depending of the size of the structure and operating conditions, but with an amplitude of just a few tens of Angstroms.

These vibrations should not be confused with an impossible perpetual motion, as the system can be continuously powered by the vacuum energy responsible for the Casimir force.

Conclusions and Future Perspectives

This vacuum energy concept was carried out by an old retiree , completely alone and without the help of any organization We observed that in the referential of our 4 dimensions Space-Time plus the Quantic Vacuum, the energy seems to be conserved which is consistent with Noether's theorem and a perpetual small vibration exist.

I say it seems because , in this preliminary work , totally alone , I don't take the time to verify theoretically resume here :

- **Neglect of Nonlinearity**: The linear dynamic equations do not account for nonlinear electrostatic spring effects or nonlinear material responses, especially at small scales.
- **Idealized Joint and Surface Conditions**: The assumption of perfect pivoting and mirror-flat Casimir plates does not hold at the nanometer level.
- **Unvalidated Mechanical Model**: There is no comparison with experimental MEMS resonance data or full 3D FEM models (e.g., from COMSOL or high-fidelity ANSYS simulations).

1/ Piezoelectric Material Selection :

The simulations assume ideal material properties, without accounting for thin-film degradation, surface effects, or substrate interactions. No experimental validation or real deposition results are presented

1.1. PZT : Simulations show feasible behavior with moderate output (~10^{-6} to 10^{-4} A). However, PZT is lead-based, raising environmental and manufacturing concerns.

1.2. PMN–PT : Shows the highest theoretical performance due to a very high piezoelectric coefficient ($d_{31} \approx 1450$ pC/N).

However, film deposition at microscale with preserved d_{31} is technologically nontrivial. The required ~20 µm thick layers are difficult to deposit uniformly while maintaining crystalline orientation and domain structure.

2/ Electrical Conversion Circuit

The energy harvested from the piezo is routed through a MOSFET-controlled switching circuit and then rectified and multiplied using a passive voltage multiplier network. We remark that :

- **Efficiency Assumptions**: Simulations ignore MOSFET leakage, gate capacitance, threshold variability, and parasitic losses.
- **Timing Stability**: The concept relies on perfect triggering of MOSFETs based on charge thresholds that are sensitive to temperature and manufacturing variability.
- **Lack of Practical Data**: No load-line analysis, impedance matching, or power trace simulation is provided. No test circuit is presented or fabricated.

3. Technological Feasibility

The microfabrication scheme (using SOI wafers, etching, sputtering, etc.) is standard in concept, but several major issues are overlooked:

- **Surface Purity**: Any contamination layer (organic films) on Casimir plates suppresses the effect significantly.
- **Integration Complexity**: Combining PMN–PT films, metal contacts, and active electronics on a single substrate with tight thermal and mechanical tolerances is complex.
- **Switching Timing Precision**: The exact timing and response of the electrostatic reset stage relies on transistor thresholds differing by as little as tens of millivolts must be validated .

4. Physical Realism and Fundamental Objections

- **Can vacuum energy be truly extracted?** In mainstream quantum field theory, Casimir energy is a **potential well**, not a power source.
- **Stability of oscillations**: No analysis of long-term stability, phase noise, or stochastic behavior under vacuum fluctuations is provided.
- **Zero-point fluctuation limitations**: The model is deterministic and does not account for the inherently probabilistic nature of vacuum fields, thermal coupling, or quantum decoherence.
- **No empirical evidence**: All claims remain at the theoretical level. The absence of even a proof-of-concept MEMS prototype makes it impossible to assess feasibility

We believe that despite the verifications to be made cited above, this described concept merit further study. If confirmation the fabrication of a prototype would be the last judge. This work on the energy balance of a M.E.M.S., which appears to be able to extract electrical energy from is a new, totally unexploited source of energy :. The theoretical results of this project seem sufficiently encouraging to justify the development of prototypes.

Future Perspectives : Several directions may be explored to advance this work toward experimental realization:

1. **Fabrication of a MEMS prototype**: Using established SOI processes, the core Casimir-piezoelectric structure could be fabricated and tested for spontaneous oscillation and charge generation under high vacuum conditions.

2. **Optimization of the electrostatic tuning mechanism**
   Refining the design and control of the Coulombic counterforce could allow precise adjustment of the system's stability point, thereby enhancing energy output and frequency control

3. **Integration with ultra-low-threshold CMOS electronics**
   Coupling the system with high-impedance, low-power electronics would enable autonomous energy harvesting modules for use in nanoscale sensors or space applications.

4. **Extension to NEMS and 2D-material interfaces**
   Downscaling the architecture to NEMS and incorporating graphene or MoS_2 layers could dramatically enhance sensitivity to vacuum forces while reducing friction and energy losses.

5. **Experimental quantification of Casimir-induced energy transfer**
   Developing precision instrumentation to measure net energy extracted over time would help validate the theoretical model and quantify practical limits

This work opens a pathway for a new generation of self-powered microdevices operating at the edge of classical and quantum physics. While challenging, the experimental realization of such systems could lead to breakthroughs in autonomous electronics, quantum sensors, and fundamental vacuum physics.

As an inventor who has kept some important details confidential, I would like to collaborate in its development after signing a contract with the potential investor. If its theoretical predictions are confirmed, it will trigger a scientific, technical and human revolution, because the quantum vacuum can be used as a new source of energy both on Earth and in space with a considerable commercial market.

In the universe, everything is energy, everything is vibration, from the infinitely small to the infinitely large" Albert Einstein.

"A person who has never made mistakes has never tried to innovate." Albert Einstein

References

1. Fluctuations du vide quantique: Serge Reynaud Astrid Lambrecht (a), Marc Thierry Jaekel (b), a / Laboratoire Kastler Brossel UPMC case Jussieu F Paris Cedex 05, b / Laboratoire de Physique Théorique de l'ENS 24 rue Lhomond F 75231 Paris Cedex 05, Juin 2001.
2. On the Attraction Between Two Perfectly Conducting Plates (1948) H.B.G. Casimir, Proc. Kon. Nederl. Akad. Wet. 51 793.
3. Direct measurement of the molecular attraction of solid bodies (1957) 2. Method for measuring the gap. Results of experiments B.V. Deriagin(Moscow, Inst. Chem. Phys.), I.I. Abrikosova(Moscow, Inst. Chem. Phys.)Jul, 1956B.V. Deriagin and I.I. Abrikosova, Soviet Physics JETP 3 819.
4. Casimir force between metallic mirrors (1980) SpringerLink . E.M. Lifshitz, Sov. Phys. JETP 2 73 (1956); E.M. Lifshitz and L.P. Pitaevskii, Landau and Lifshitz Course of Theoretical Physics: Statistical Physics Part 2 Ch VIII (Butterworth-Heinemann.
5. Techniques de l'Ingénieur 14/12/2012 : l'expertise technique et scientifique de référence « Applications des éléments piézoélectriques en électronique de puissance » Dejan VASIC : Maître de conférences à l'université de Cergy-Pontoise, Chercheur au laboratoire SATIE ENS Cachan, François COSTA : Professeur à l'université de Paris Est Créteil, Chercheur au laboratoire SATIE ENS Cachan
6. Wachel JC, Bates CL (1970) Techniques for controlling piping vibration failures", ASME Paper, 76-Pet-18.
7. Jayalakshmi Parasuraman, Anand Summanwar, Frédéric Marty, Philippe Basset, Dan E Angelescu, et al. (2014) Deep reactive ion etching of sub-micrometer trenches with ultra-high aspect ratio Microelectronic Engineering 113: 35-39
8. F Marty, L Rousseau, B Saadanya, B Mercier, O Français, et al. (2005) Advanced etching of silicon based on deep reactive ion etching for silicon high aspect ratio microstructures and three-dimensional micro- and nanostructure. Microelectronics Journal 36: 673-677.
9. Semiconductor Devices, Physics' and Technology S. M. SZE Distinguished Chair Professor College of Electrical and Computer Engineering National Chiao University Hsinchu Taiwan, M.K. LEE Professor Department of Electrical Engineering, Kaohsiung Taiwan.
10. M Barthes, M Colas des Francs Solid Mechanical Vibrational physics, ESTP: (Special School of Public Works).
11. Modélisation de transistors polysilicium en couches minces sur isolants : conception et réalisation d'écrans plats à cristaux liquides et matrices actives, Auteur Patrick Sangouard , These de doctorat Paris 11 , Soutenance en 1987, president du jury René Castagné : https://theses.fr/1987PA112461.

Appendices a few Reminders from RDM

Calculation of the Deflection of a Bridge Recessed at its 2 Ends

Note: We take the case of pure bending, the shear force T is such that With M the bending moment applied to the piezoelectric bridge. The Casimir force in the z axis is applied in lp / 2 at the center of the bridge. (Figure 81)

Figure 80: general appearance a/ b/ of the device studied, forces and applied moments, c/ of the deformed bridge

a/ b/ c/

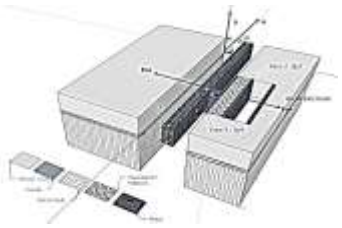

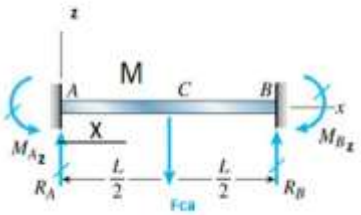

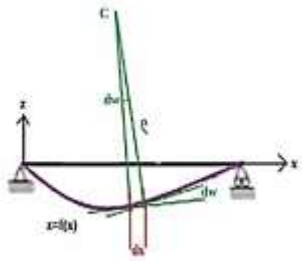

As stated in all RDM books, the equation of the distorted mean line is: $\frac{d^2(f(x))}{dx^2} = -\frac{M_z(x)}{E_P I_P(x)}$ Eq (42)

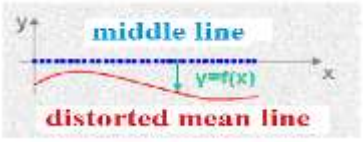

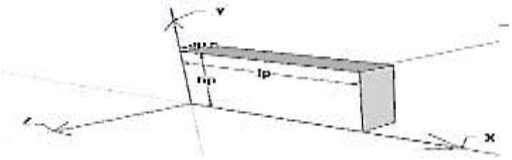

We know that the radius of curvature ρ is $\frac{1}{\rho} = \frac{\frac{d^2f(x)}{dx^2}}{\left(1+\frac{df(x)}{dx}\right)^{\frac{3}{2}}} \approx \frac{d^2f(x)}{dx^2} \approx \frac{d\varpi}{dx} = -\frac{M_z(x)}{E_P I_P(x)}$ Eq (43)

Since the bridge is parallelepiped in shape, the bending moment of inertia along the z axis of the section of this bridge is:
$I_{GSZ} = \frac{b_P\ a_P^3}{12} = Cte$ (Eq. 44)

So: $\frac{d^2(f(x))}{d(x^2)} = \frac{d\varpi}{dx} = \frac{M_z(x)}{E_P I_P(x)} \Rightarrow f(x) = -\iint \frac{M_z(x)}{E_P I_P(x)} d(x) = -12 \iint \frac{M_z(x)}{E_P b_P a_P^3} d(x)$

In the case of a beam recessed at both ends, we have a hyperstatic system.

However, we know (See works on Resistance of Materials) that at equilibrium, the sum at all points of the forces and bending moments is zero. Because of the symmetry of the system, we therefore have $R_{AZ} = R_{BZ}$ and $M_{BZ} = M_{Az}$ and the computational reasoning for the deformation equation is identical for $0 \le x \le lp / 2$ or $lp2 \le x \le lp$ so.

For the forces and reactions: $\overrightarrow{R_A} + \overrightarrow{R_A} + \overrightarrow{F_{CA}} = \overrightarrow{0} \Rightarrow +F_{CA} = 0 \Rightarrow R_{AZ} = R_{BZ} = \frac{F_{CA}}{2}$ And for bending Moments:

M_x = the bending moment at a point x <lp / 2
M_{AZ} = the bending moment in A
F_{CA} = the force of Casimir applied in lp / 2 see (81)
Mz (x) = Bending moment depending on the position x on the bridge
I_P (x) the bending moment of inertia of the bridge section

$$M_z(x) = -E_P I_P \frac{d^2z}{dx^2} = \frac{F_{CA}}{2} x - M_{AZ} \Rightarrow E_P I_P z(x) = -\left(\frac{F_{CA}}{12} x^3 - M_{AZ} \frac{x^2}{2} + C_1 x + C_2 \right)$$

$$So\ FOR\ 0 \le x \le \frac{l_P}{2} \Rightarrow z(x) = -\frac{\left(\frac{F_{CA}}{12} x^3 - M_{AZ} \frac{x^2}{2} + C_1 x + C_2 \right)}{E_P I_P}$$

However, we have the boundary conditions which impose:

$$In\ x = 0 \Rightarrow z(0)\ and\ \left(dz/dx \right)_{x=0} = 0 \Rightarrow C_{(M)1} = C_2 = 0$$

$$In\ x = \frac{l_P}{2} \Rightarrow \left(\frac{dz}{dx} \right)_{x=\frac{l_P}{2}} = 0 \Rightarrow (M_{AZ})_{x=\frac{l_P}{2}} = -\frac{F_{CA} l_P}{8}$$

$$\Rightarrow (M_{AZ})_{x=0} = -\frac{F_{CA}\ l_P}{8}$$

$$\Rightarrow z(x) = -\frac{\frac{F_{CA}\ l_P}{12} x^3 - \frac{F_{CA}\ l_P}{16} x^2}{E_P I_P} = \frac{F_{CA}\ l_P\ x^2}{16\ E_P\ I_P} \left(l_P - \frac{4x}{3} \right) for\ 0 \le x \le l_P/2$$

The maximum deflection in x = lp / 2 gives an arrow : $z_{max} = \frac{F_{CA}\ L_P^3}{192\ E_P\ I_P}$ for $x = \frac{L_P}{2}$ (Eq. 45)

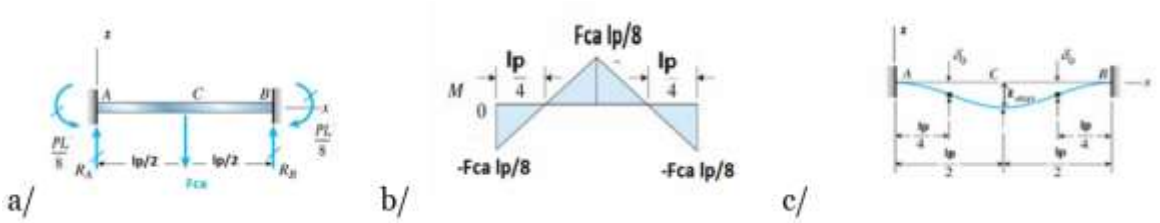

Figure 81: a / Forces, shear forces and Moments applied on the bridge. b / Variation of bending moment. c / Shape and arrow of the bridge recessed at both ends. With: δ0 = inflection points, z_{max} = arrow of the bridge

Calculation of the Resonant Frequency of the Piezoelectric Bridge

It is demonstrated (*see for example: Vibrations of continuous media Jean-Louis Guyader (Hermes)*) that the amplitude z (x, t) of the transverse displacement of a cross section of the beam is given by the partial differential equation , if one neglects the internal damping. $\frac{\delta^4 z}{\delta x^4} + \frac{\rho S}{E_P I_P} \frac{\delta^2 z}{\delta t^2} = 0$

With $k = (\rho S \omega^2 / E_p I_p)^{1/4}$,the solution of this differential equation is written in the general form:

$Z(x) = A1 \exp(k x) + A2 \exp(-k x) + A3 \exp(i k x) + A4 \exp(i k x)$ and in the more convenient form:

$$z(x) = a \sin(k x) + b \cos(k x) + c\, sh(kx) + d\, ch(kx)$$

Keeping into account the boundaries conditions: $\left[sh(k l_P)^2 - \sin(k l_P)^2 \right] - \left[ch(k l_P) - \cos(k l_P) \right]^2 \Rightarrow \cos(k l_P) = \frac{1}{ch(k l_P)}$

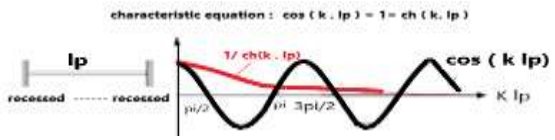

Figure 82: Numerical solution of equation 18

The numerical resolution (for example by the dichotomy method in figure 68 of this equation gives for the first 5 solutions: a1 = 4.7300; a2 = 7.8532; a3 = 10.9956; a4 = 14.1317; a5 = 17.2787

So, the first resonant frequency of the piezoelectric bridge is

$$\text{Eq(46)}\ \varpi_{P1} = (4.73)^2 \sqrt{\frac{E_P I_P}{M_S l_P^3}} \Rightarrow f_{P1} = \frac{1}{2\pi} (4.73)^2 \sqrt{\frac{E_P I_P}{M_S l_P^3}} \qquad M_{Stucture} = \rho_P a_P S_P + \rho_i a_i S_i + \rho_s a_s S_s$$

For example, for a bridge recessed at both ends with the following characteristics,

For geometries: lp=50 μ m, bp= 150 μm, ap =10 μm; Sp=1,5 10^{-9} m^2, Ip= bp.ap^3/12= 1.25 10^{-20} m^4 ;li = 10 μm ; bi=150 μm ; ai=10μm ; ls = 1000μm; bs=150 μm; as=10μm

For the material: PZT: density r = 7600 (kg/m^3), Young's modulus Ep = 6 * 10^{10} (Pa) (Kg m s^{-2})

For the section inertia: $I_p = I_{GSZ} = \frac{b_P\ a_P^3}{12} = 1.25\ 10^{-20}\ m^4$

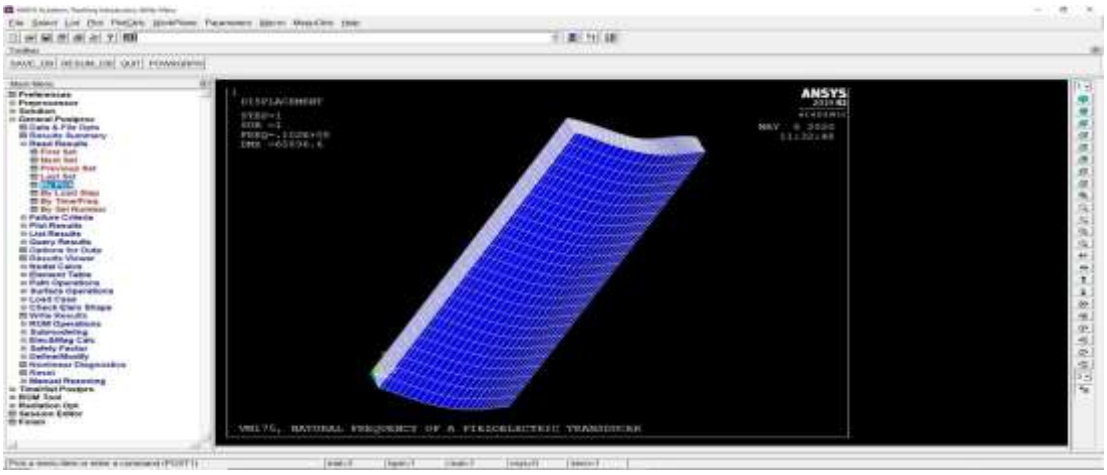

Figure 83: ANSYS simulation of the resonant frequency of the piezoelectric

Then the calculated first resonance frequency is for the PZT material: f_{p1} = 1.1553 * 10^7 hertz.

For this recessed bridge, an ANSYS simulation (figure 82) gives a resonant frequency of f1 = 1.02 . 10^7 Hz which is close to that calculated in the draft calculation presented in this report and validates the orders of magnitude obtained with the equations for these preliminary calculations.
If one carries out the calculation of the resonant frequency of the structure of figure 5 which comprises a free sole of Casimir S_{S2} parallel to a fixed surface S_{S3} and transmitting by a mechanical link finger the force of Casimir, one finds that the resonant frequency has the same form but with Ms a fixed mass applied in the middle of the bridge.

$M_{Structure}$ = the total mass of the structure. $M_{Stucture} = \rho_S a_S S_S + \rho_i a_i S_i + \rho_P a_P S_P$

ρ_p, ρ_i , ρ_S , the medium density of the piezoelectric material, of the connecting finger, of the Casimir electrode sole and S_p, S_i, S_s the longitudinal surfaces of this bridge. Indeed, the presence of the Casimir sole connected by the Casimir force transmission finger in the middle of the piezoelectric bridge, modifies the resonant frequencies of this bridge

The calculated resonance frequency then becomes for the same geometries and materials. f_{s1}=2.509 10^6 hertz. With these characteristics, an ANSYS simulation of this structure gives a close resonance frequency: f_{s1} = 2.62 10^6 Hertz.
This approach greatly simplifies these preliminary calculations because otherwise the curvature of the piezoelectric bridge makes the Casimir force strongly depend on the longitudinal and transverse positions x and z of the facing surfaces.